Aus der Medizinischen Universitätsklinik und Poliklinik

Tübingen

Abteilung Innere Medizin I

(Schwerpunkt: Gastroenterologie, Hepatologie,

Infektionskrankheiten)

Ärztlicher Direktor: Professor Dr. N. Malek

Difficult to treat cancer entities such as sarcomas and peritoneal carcinosis challenged by suicide gene-armed virotherapeutic vector systems MeV and VACV

Inaugural-Dissertation
zur Erlangung des Doktorgrades
der Medizin

der Medizinischen Fakultät
der Eberhard Karls Universität
zu Tübingen

vorgelegt von

Nora Mayer

aus

Heilbronn-Neckargartach

2014

Dekan: Professor Dr. I. B. Autenrieth

1. Berichterstatter: Professor Dr. U. M. Lauer

2. Berichterstatter: Prfessor Dr. T. Iftner

Widmung

Meiner Oma Maria†.

Outline

OUTLINE IV

1 INTRODUCTION 1

1.1 CANCER WORLDWIDE AND THERAPY OPTIONS 1

1.2 VIROTHERAPY AS A NOVEL TREATMENT OPPORTUNITY 2

1.3 VACCINIA VACCINE VIRUSES GLV-1H68 AND GLV-1H95 5

1.4 MEASLES VIRUS MEV-SCD 8

1.5 SUICIDE GENE THERAPY ENHANCES VIRAL ONCOLYTIC EFFICIENCY 10

1.6 AIM OF THIS DISSERTATION 13

2 MATERIALS AND METHODS 14

2.1 CELL CULTURE 14

2.1.1 Cell culture materials 14

2.1.2 Characteristics of the cell lines 15

2.1.3 Cell culture 17

2.1.4 Cryopreservation of cells 18

2.1.5 Thawing of cells for recultivation 18

2.1.6 Cell count determination with the Neubauer haemocytometer 19

2.2 VIRUS INFECTION 19

2.2.1 Virus infection without suicide-gene therapy 19

2.2.2 Virus infection combined with suicide-gene therapy and 5-FC 20

2.3 OVERVIEW OF CELL-VIRUS INTERACTION IN ELECTRON MICROSCOPY 21

2.4 DETECTION OF GFP BY FLUORESCENCE MICROSCOPY 22

2.5 QUANTIFICATION OF THE RELATIVE FLUORESCENCE INTENSITY 23

2.6 B-GALACTOSIDASE DETECTION BY LACZ-STAINING 23

2.6.1 Materials for lacZ-staining 23

2.6.2 Experimental procedure of lacZ-staining 24

2.7 WESTERN BLOT ANALYSIS 26
2.7.1 Materials for Western Blot analysis 26
2.7.2 Preparation of cell lysates 27
2.7.3 Bradford dye Assay 27
2.7.4 Sodium-dodecylsulfate-polyacrylamide gel electrophoresis 28
2.7.5 Western blotting 30
2.7.6 Staining of the protein bands 31

2.8 CELL MASS QUANTIFICATION USING SULFORHODAMINE-B ASSAY 32
2.8.1 Materials for Sulforhodamine-B (SRB) assay 32
2.8.2 Procedure of SRB assay 32

2.9 LDH-RELEASE ASSAY 33
2.9.1 Materials for LDH-release assay 33
2.9.2 Procedure of the LDH-release assay 33

2.10 ESTABLISHING OF A GROWTH CURVE TO PURSUE THE REPLICATION BEHAVIOUR OF THE RESPECTIVE VIRUS 36
2.10.1 Procedure of measles virus growth curve 36
2.10.2 Procedure of Vaccinia virus growth curve 39

2.11 QUANTIFICATION OF CD46-RECEPTOR EXPRESSION BY FLOW CYTOMETRY 43

3 RESULTS 45

3.1 ELECTRON MICROSCOPY OF MEV-SCD/ GLV-1H68 REPLICATION 45
3.1.1 MeV-SCD replication in A673 and BRZ sarcoma cells 45
3.1.2 GLV-1h68 replication in CC531s colon carcinoma and SKOV3ip.1 ovarian carcinoma cells 48

3.2 QUANTIFICATION OF CD46 RECEPTOR MOLECULES ON TUMOR CELLS 56

3.3 INFECTION EFFICIENCY OF MEV-EGFP AND GLV-1H68 57
3.3.1 Fluorescence monitoring shows successful infection with MeV-GFP 57
3.3.2 Expression of SCD in A673 and BRZ cells in Western blot analysis 60
3.3.3 Relative green fluorescence intensity shows successful infection with GLV-1h68 61
3.3.4 Visualization of β-galactosidase-expression by X-Gal-conversion confirms the results of successful infection with GLV-1h68 63

3.4 REPLICATION BEHAVIOUR OF MEV-SCD AND GLV-1H68 65
3.4.1 Growth curve of MeV-SCD in A673 and BRZ cells 65
3.4.2 Growth curve of GLV-1h68 in CC531s and SKOV3ip.1 cells 67

3.5 MEASUREMENT OF CYTOTOXIC EFFECTS OF VIRUS-INFECTION 69
3.5.1 Suicide gene plus 5-FC enhances the cytotoxic effect of MeV-SCD 69
3.5.2 GLV-1h68 shows a highly oncolytic potency 78

3.6 THE DISCOVERY OF PARTIALLY GLV-1H68-RESISTANT CELL-LINES 82
3.6.1 Cytotoxic effect of GLV-1h68 on SCOS-cells 82

3.7 VIROTHERAPY USING THE ARMED GLV-1H95 LED TO A STRONGER CYTOTOXIC EFFECT THAN GLV-1H68-TREATMENT ALONE 83
3.7.1 Cytotoxic effect of GLV-1h95 on SCOS cells 83
3.7.2 Comparison of GLV-1h68 and GLV-1h95 effects 84
3.7.3 Replication behaviour of GLV-1h68 in non-responding tumor cell lines 89

3.8 GLV-1H68 INFECTION OF PRIMARY HUMAN HEPATOCYTES (PHH) 90

4 DISCUSSION 93

5 SUMMARY/ZUSAMMENFASSUNG 106

6 ABBREVIATIONS 110

7 LIST OF FIGURES 113

8 LIST OF TABLES 115

9 REFERENCES 116

10 DANKSAGUNG 126

1 Introduction

1.1 Cancer worldwide and therapy options

Malignant neoplasms were declared the leading cause of death (26.6%) in developed countries followed by heart (10.3%) and cerebrovascular diseases (9.4%) in 2004 (American Cancer Society, 2011). Estimates from the International Agency for Research on Cancer (IARC) formulated a number of new cancer cases of 12.667.500 million in 2008 worldwide. The number of total worldwide cancer deaths in 2008 was 7.6 million. The two most common types of cancer in women are breast cancer and cervix uteri carcinoma, the most common cancer cases in men are lung & bronchus carcinoma and prostate cancer (Farley et al., 2010). Both women and men are also affected by another type of malignancy: colorectal cancer. Colorectal cancer is one of the three most common tumors in both women and men worldwide (American Cancer Society, 2011).

Some cancers can be detected and eradicated as precancerous lesions or early stage cancers due to successful screening methods, e.g. colorectal cancer (CRC). But in most cases an aggressive cancer therapy is the only possibility to extirpate the malignant cells. A common problem is the prevalence of metastatic lesions in case of already advanced stage disease at time of diagnosis. 15-20% of the patients suffering from CRC show metastasis at initial diagnosis, most frequently localized within the liver and secondly within the peritoneal cavity (LMU München, 2012). Peritoneal carcinosis is often combined with clinical symptoms and is likely to drastically reduce the quality of life. Moreover patients with peritoneal carcinosis were shown to often have a very short median survival (Sadeghi et al., 2000).

The three common options for cancer treatment are surgery, chemotherapy and radiotherapy, which can be applied alone or in combination (Farley et al., 2010). Besides these three modalities there are several other treatment options available like hormone-therapy, monoclonal antibodies and small molecules.

In case of peritoneal carcinosis, systemic chemotherapy and hyperthermic intraperitoneal chemotherapy (HIPEC) are the most common treatment options

(Glockzin et al., 2007) and surgery is used to treat frequent complications like stenosis or gastrointestinal bleeding. HIPEC enhances the local toxic effect while decreasing systemic toxic side effects. Peritonectomy (Sugarbaker, 2007), which is also called cytoreductive surgery (CRS), combined with intraperitoneal HIPEC enhanced the median survival of patients significantly (Esquivel et al., 1993; Verwaal et al., 2003). It could be shown that macroscopic CRS led to a significant increase in survival (Glehen et al., 2004). Nevertheless, all these therapy options still remain mostly palliative in nature.

It is well known that patients suffering from peritoneal carcinosis only benefit from a complete eradication of all tumor cells within the peritoneal cavity and not from a tumor debulking surgery (peritonectomy). The problem of incomplete tumor cell eradication also exists in other malignancies, e.g. sarcomas, which often resist first line therapy.

At this point, alternative therapy modalities have to be strongly considered. Virotherapy represents one of these alternative therapy options. This “new” treatment option lately became more and more part of preclinical and clinical research and now seems to be waiting in the wings to enter the clinic as soon as first virotherapeutics will be approved by the regulatory authorities.

1.2 Virotherapy as a novel treatment opportunity

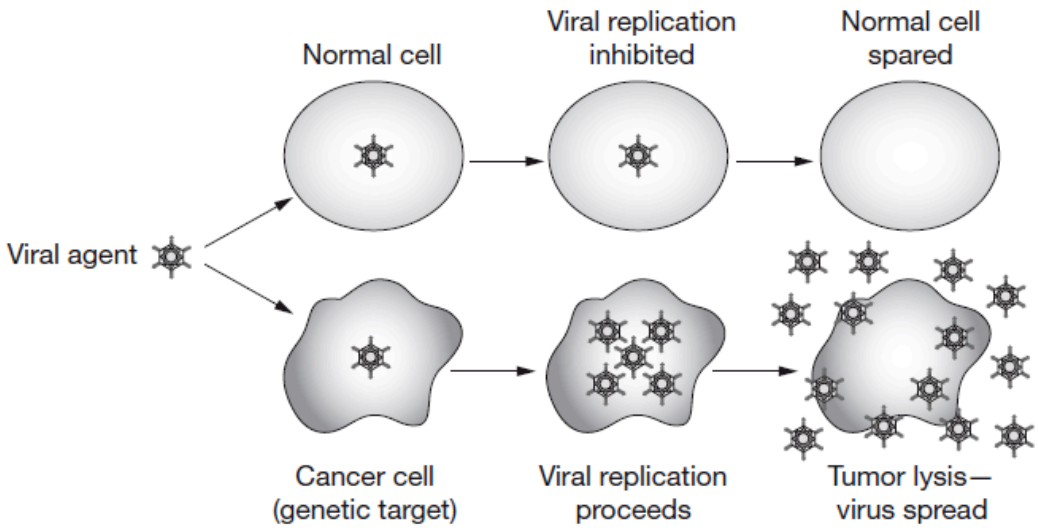

Figure 1. Oncolytic mechanism of a viral agent/virotherapeutic (Liu et al., 2004)

Virotherapy is the treatment of cancers using attenuated, replication-competent, and recombinant viral agents that selectively infect and kill cancer cells. Several mechanisms like the impact of viral replication within the cancer cells, a directly cytotoxic effect and the increasing viral load due to massive production of progeny virus particles lead to cell lysis (so-called oncolysis) and viral spread. Normal cells and healthy tissues around tumorous lesions are only marginally affected by viral cell killing.

The first experiences with viruses showing oncolytic potency and tumor regression were noted in early case reports from the beginning of the 20th century. Tumor regression was observed after natural infection (Bluming et al., 1971; Pasquinucci, 1971; Taqi et al.,1981) or was caused by viral vaccines (Greentree, 1983; Hansen et al., 1978).

In the middle of the 20th century, cancer treatment with oncolytic wild type or vaccine viruses started and was directly followed by the treatment of cancer with engineered viruses showing a high selectivity for cancer cells. Finally, engineered armed viruses were used for treatment (Liu et al., 2004). Several of these oncolytic viruses have already entered clinical trials (Arakawa et al., 1987; Hamid et al., 2003; Nemunaitis et al., 2011). In a further step, virotherapy was combined in a widespread manner with chemotherapeutics such as 5-FU (Gnant et al., 1999) and radiotherapy (Ottolino-Perry et al., 2010). First promising results using combination therapies were published: The combination of chemotherapy and the oncolytic adenovirus ONYX-015 (Khuri et al., 2000), the combination of the vaccinia vector GLV-1h68 and cisplatin/gemcitabine (Yu et al., 2009) and the combination treatment with chemotherapeutics and an oncolytic HSV-agent (Kanai et al., 2010) have already shown quite encouraging results.

The most important key data concerning virotherapy are safety and oncolytic efficiency, which are directly related to the modes of application, distribution, shedding and immune system-mediated elimination of the viral agent. In our studies we chose two viral vector systems which have an outstanding safety profile (Enders et al., 1954; Yu et al., 2009), provide several application modalities (Grote et al., 2011; Mastrangelo et al., 2000; Peng et al., 2002;) and

have already been successfully applied for the treatment of solid tumors in human xenograft animal models (Grote et al., 2001; Yu et al., 2007). One of these vectors is the 3rd generation vaccinia virus GLV-1h68, the other one is the recombinant measles virus MeV-SCD. To buy into Ivaylo Gentschev et al.: ”Virotherapy using oncolytic vaccinia virus strains is one of the most promising new strategies for cancer therapy” oncolytic vaccinia virus strains is one of the most promising new strategies for cancer therapy.” (Gentschev et al., 2010). The understanding of vaccinia virus behaviour in humans due to the eradication of smallpox argues for the future clinical use of vaccinia virus-based viro-therapeutics. Therefore, JX-594 (Jennerex Biotherapeutics), a targeted oncolytic poxvirus, was one of the first viral agents to be tested in preclinical and clinical trials (Kim et al., 2006; Park et al., 2008). MeV-SCD, a measles virus vaccine-based virotherapeutic vector, is the other promising tool derived from Edmonston B strain. This strain was used as an anti-measles vaccine in many parts of the world. The vaccine strains derived from the Edmonston B strain are known as Mérieux, Rouvax, Moraten, Lirugen, Morbilvax, Attenuvax, Mevilin, and Rimevax. The measles vaccines supplied through the World Health Organization's program on Immunization in the Americas are prepared from seeds derived from Edmonston B (EPI Newsletter, 1980).

Several viruses like vesicular stomatitis virus (VSV) (Stojdl et al., 2000), Newcastle Disease virus (NDV) (Lorence et al., 1988), human reovirus (Coffey et al., 1998), recombinant adenovirus (Toth et al., 2010), recombinant Herpes simplex virus (HSV) (Yoon et al., 2000), recombinant vaccinia virus (VACV), recombinant measles virus (MeV) and some more viruses have already been tested positive with regard to their oncolytic potential.

Now that virotherapeutics have entered clinical trials, it has to be investigated which viral vector is the most suitable oncolytic agent in which kind of cancer. The ultimate goal would be to treat cancer patients in the future with “customized” virotherapeutics, which specifically address patient individual tumor biologies. This can be achieved due to the fact that virotherapeutics are of recombinant nature thus allowing a straightforward encoding of “customized” functional transgenes on each and every vector modification.

1.3 Vaccinia vaccine viruses GLV-1h68 and GLV-1h95

In the 18th century Edward Jenner carried out the first vaccinations in humans using a cowpox virus called 'vaccinia' in England. In 1958, the World Health Organisation started a vaccination campaign with VACV to eradicate smallpox (variola) worldwide. In 1979, smallpox was declared eradicated throughout the globe (Fenner, 1993). A molecular biological investigation revealed that the used VACV was not identical with the virus Jenner had used. Researchers suspect that the vaccinia virus, which was held for a cowpox virus, is in fact an already extinct animal pox virus. So the origin of this specific virus remains unclear.

Variola and VACV belong to the genus *Orthopoxvirinae* in the biological family *Chordopoxvirinae.* The poxvirus is the largest known virus and the particles can reach a diameter of 100-300 nm and have a clearly structured surface.

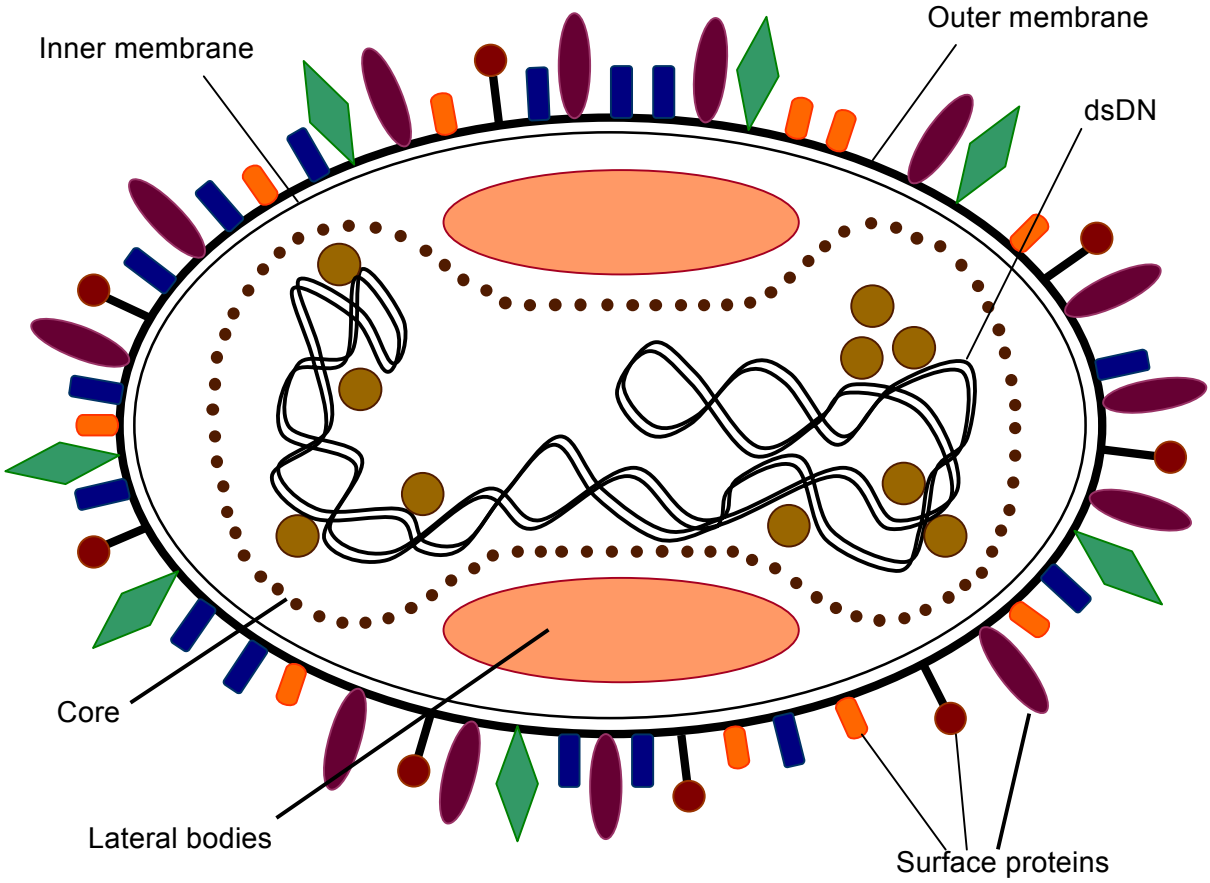

Figure 2. Schematic representation of VACV
The intracellular form of a VACV particle is shown (IMV = intracellular mature virus). The extracellular form is surrounded by a lipoprotein envelope containing several viral surface

proteins. The dsDNA is associated with different viral enzymes and regulatory proteins which stabilize the supercoiled structure of the s-shaped dsDNA. The biconcave core consists of viral proteins and surrounds the dsDNA. Both lateral bodies lie next to the concavity of the core, their function is unknown.

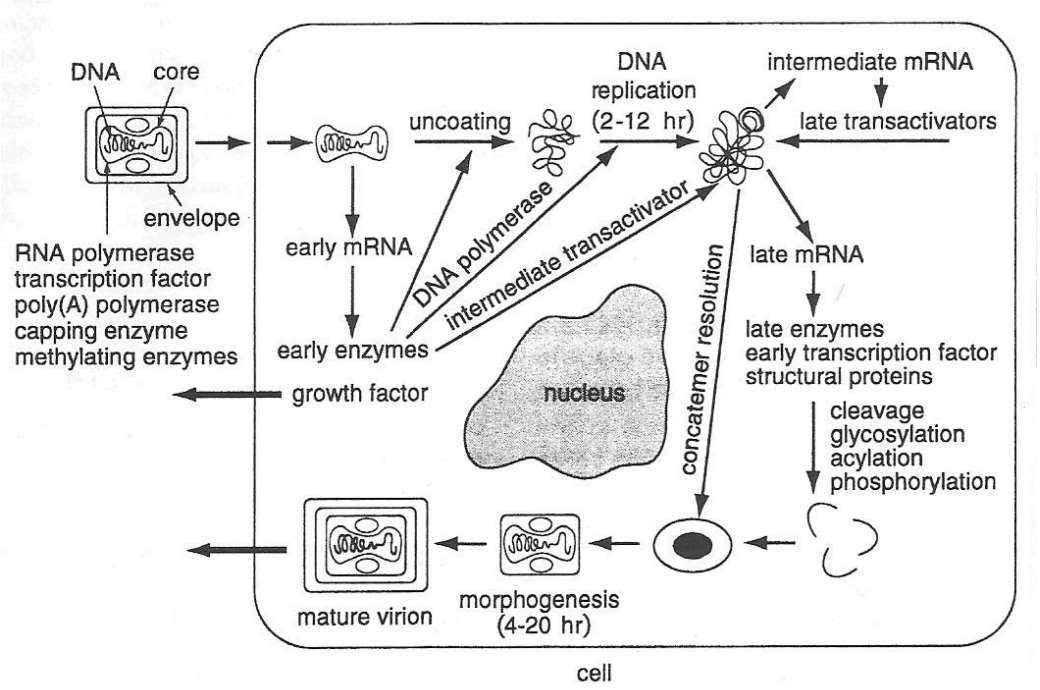

Figure 3. Replication cycle of VACV
VACV enters the cell via membrane fusion. The virion is released into the cytoplasm. VACV replicates in the cytoplasm and does not enter the nucleus. Early genes are expressed first, leading to the formation of the early enzymes. These enzymes lead to the next steps e.g. secretion of several proteins, uncoating of the virion, synthesis of DNA polymerases and to the activation of transcriptional transactivators of the intermediate class of genes. DNA replication lasts about 2-12 hours. Intermediate mRNAs encode late transactivators which activate the transcription of late mRNAs resulting in the expression of late enzymes, early transcription factors and structural proteins. Virus assembly of new virions takes another 4-20 hours until the mature virion exits the cell via the cell membrane (Moss et al., 1998).

As already described in the previous paragraph, there is a wide range of potential oncolytic agents. So why is VACV such a suitable oncolytic agent?
One reason is related to its short and well-characterized life cycle. First, viral particles are released 8 hours post infection (hpi) and infected cells disintegrate already at 48 to 72 hpi according to data being provided in this dissertation and published data (Kirn et al. 2009). Furthermore, VACV is able to infect and lyse a large amount of different tumor tissues because of its ability to enter tumor cells without the use of a distinct receptor but by membrane fusion (Moss, 2006). It replicates within the cytoplasm without penetrating into the nucleus and integrating into the host genome. A further safety aspect is the lack of airborne

spread of vaccinia species. The VACV genome is genetically very stable and provides a large insertion capacity (of up to 25 kb) for transgenes (Chen et al., 2009). It does not cause any known disease in humans (Roizman et al., 1994) and because of its use as smallpox vaccine, viral side effects are well-documented and there is the chance to react to them with vaccinia specific therapeutics (Cono et al., 2003). Because of its enveloped forms containing complement control factors of the host's immune system (EEV = extracellular enveloped virion), VACV is able to escape the immune system and spread through the host's bloodstream (Vanderplasschen et al., 1998). Therefore, the fight against distant metastases has become a realizable aim of virotherapy after systemic or intratumoral administration of VACV.

The virus used in this dissertation is VACV-based virotherapeutic vector GLV-1h68. GLV-1h68 was derived from the LIVP strain (Lister strain from the Institute for Research on Viral Preparations, Moscow, Russia) which itself originated from the Lister strain (Al'tshteĭn et al., 1985). The construction of the GLV-1h68 virus has been described in detail before (Zhang et al., 2007). The GLV-1h68 genome includes four expression cassettes encoding the Renilla luciferase-*Aequorea* green fluorescent protein (*ruc-gfp*) in the F14.5L locus, a reverse inserted human transferrin receptor (*rtfr*), *β*-galactosidase (l*acZ*) in the J2R (thymidine kinase) locus and *β*-glucuronidase (*gusA*) in the A56R (hemagglutinin/ HA) locus of the viral genome.

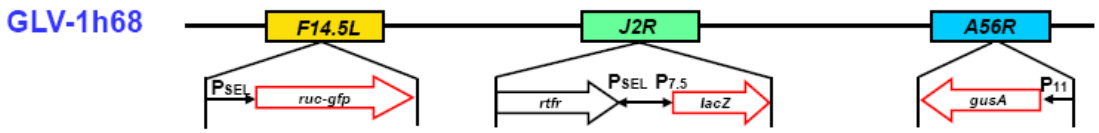

Figure 4. Genome of the GLV-1h68 virus derived from LIVP (Zhang et al., 2007)
GLV-1h68 is a genetically stable, replication competent, recombinant, attenuated (Buller et al., 1985) VACV that selectively infects cancer cells and was tested harmless to healthy tissues and organs (Zhang et al., 2007). The contribution of inactivated F14.5L to the attenuation of GLV-1h68 was examined by comparing the virulence of GLV-1h68 with *F14.5L*-null and revertant viruses Zhang et al., 2009). The attenuation of GLV-1h68 was confirmed in several tumor models and was lately shown in a clinical study in the Royal Marsden Hospital (data not published yet).

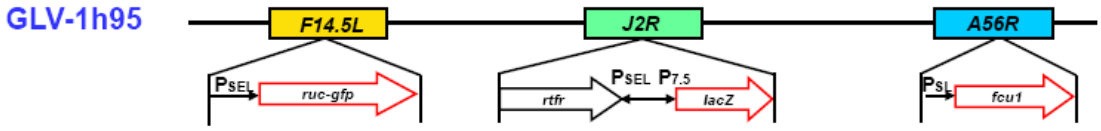

Figure 5. Genome of the GLV-1h95 variant derived from GLV-1h68
VACV GLV-1h95 is based on the GLV-1h68 virus containing the additional transgene FCU1 (yeast FCY1/FUR1 fusion gene) (Erbs et al., 2000) in the A56R locus. For inserting FCU1, *gusA* had to be taken out of A56R. The FCU1 parental plasmid was provided by Transgene. The transgene was amplified by Jochen Stritzker (Würzburg) and inserted downstream of a VACV synthetic late promoter P_{SL}. FUC1 encodes the enzymes Cytosine Deaminase (FCY1) and uracil phosphoribosyltransferase (FUR1) which convert the prodrug 5-fluorocytosine into the chemotherapeutic 5-fluorouracil. So GLV-1h95 was armed with a suicide gene to enhance the cytotoxicity in comparison to the non-armed GLV-1h68.

1.4 Measles virus MeV-SCD

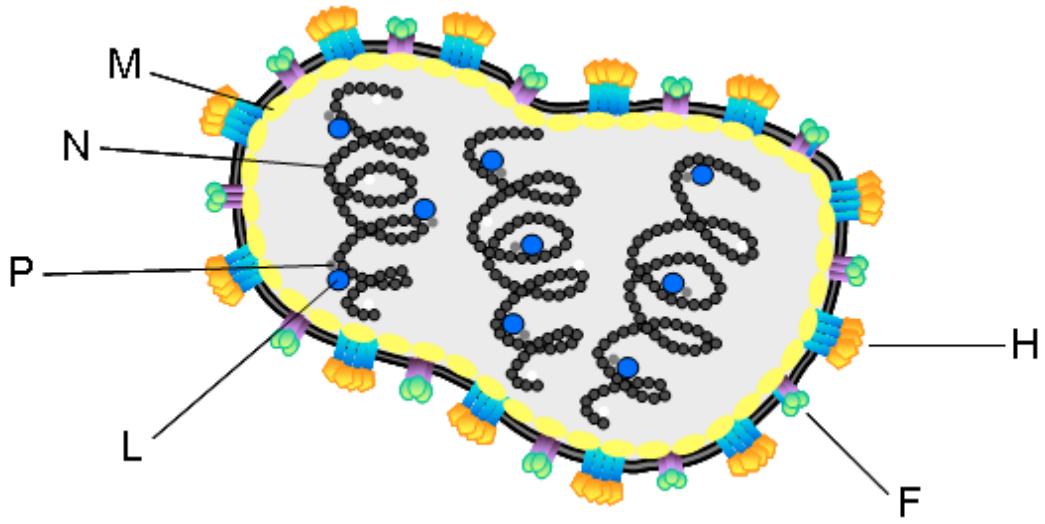

Figure 6. Measles virus (MeV) including six structural proteins and the negative strand RNA (Guy Ungerechts, NCT Heidelberg)

MeV belongs to the family *Paramyxoviridae* genus *Morbillivirus*. Wild type MeV is an enveloped virus with a nucleocapsid core. The negative strand RNA genome encodes six structural proteins **N** (*nucleocapsid protein*), **P** (*phosphoprotein associated with RNP in polymerase complex*), **M** (*matrix protein*), **F** (*fusion glycoprotein*), **H** (*haemagglutinin*) and **L** (*large protein*). The expression of the six structural proteins follows a transcriptional gradient which means that the most upstream gene (N) is transcribed most abundantly. The

negative strand RNA serves as a template for the positive antigenome strand, which vice versa serves as a template for further negative strand RNA.

Paramyxoviridae replicate within the cytoplasm. The H-protein located on the viral surface binds to the cellular receptor. The F-protein is the second surface protein on the viral lipid envelope. It is required for the fusion of the viral and the cellular membrane. The P-, N- and L-protein initiate replication whereas the M-protein serves as a structural protein within the virus.

Replication starts with the transcription of viral RNA into mRNA by RdRP (RNA-dependent RNA polymerase, consisting of P- and L-protein) from the 3' end to the 5' end of the genome. Due to the genome structure (**Figure 7**), the RdRP complex has to reinitiate transcription at each gene start signal encoding for a structural protein. As RdRP may drop off the template, the above-mentioned gradient in mRNA synthesis arises. Having translated enough N-protein, the RdRP starts to generate full-length antigenomic transcripts, which then serve as templates for the production of genomic RNAs. Both genomes and antigenomes can be packaged into virions. The lipid bilayer envelope around the new virions is derived from the host cell membrane.

In 1954, a MeV was isolated from the eleven-year old David Edmonston and was attenuated in several passages in cell culture (Griffin et al., 1996). This so-called attenuated Edmonston-B-strain was used for measles vaccination by the WHO as described previously.

For infection trials in cell culture a vector derived from the Edmonston-B-strain called MeV-GFP was used carrying the marker gene GFP in the leader position.

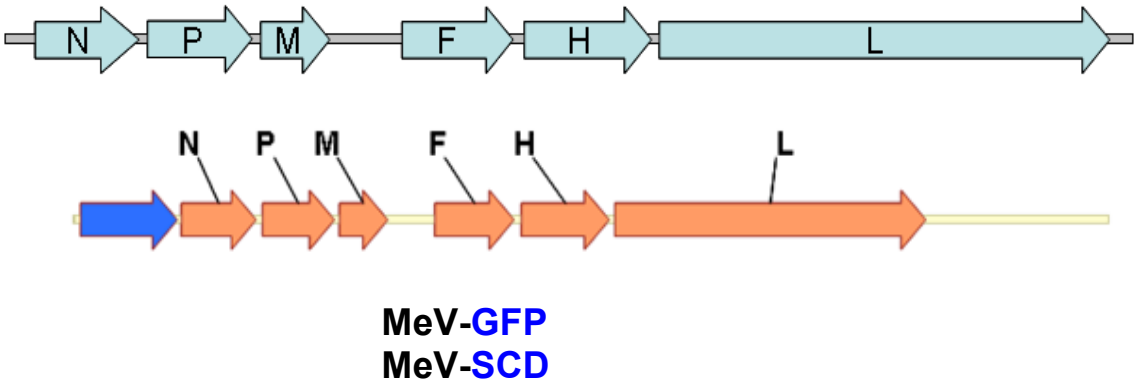

Figure 7. Wild type MeV genome (light blue) and MeV-SCD/GFP genome (orange)
Wild type MeV genome (light blue) consists of six regions coding for structural proteins N (nucleocapsid protein), P (phosphoprotein), M (matrix protein), F (fusion glycoprotein), H (haemagglutinin) and L (large protein). SCD (dark blue) was inserted into the leader position of the attenuated Edmonston-B-strain. The arrow sizes correspond to the size of the respective genes.

To enhance the oncolytic potential MeV was armed by inserting the SCD gene. SCD encodes a fusion protein consisting of yeast cytosine deaminase and yeast uracil phosphoribosyltransferase (see below). The SCD gene was positioned in the leader position to ensure sufficient production of SCD-enzyme (gradient). The insertion of SCD into the leader position did not result in an inhibition of viral replication. The vector sequence of MeV-SCD is 100% identical to the vaccine strain Schwarz (Mérieux) and was cloned by Sascha Bossow (NCT Heidelberg).

1.5 Suicide gene therapy enhances viral oncolytic efficiency

To enhance the cytotoxicity of MeV and VACV on tumor cells, both viruses were armed with the suicide gene Super Cytosine Deaminase (SCD).

The Cytosine Deaminase (CD)/ 5-fluorocytosine (5-FC) suicide gene system was introduced in 1982 (Nishiyama et al., 1982). The enzyme CD catalyzes the deamination of cytosine to uracil in fungi (Erbs et al., 1997) and bacteria (de Haan et al., 1972), but is not existent in mammalian cells. Furthermore CD is able to convert 5-fluorocytosine to 5-fluorouracil. 5-FC is a common antifungal (Tassel et al., 1968) drug but was tested harmless to healthy mammalian cells (Akbulut et al., 2003). Despite the successful usage of the *Escherichia coli* CD (Kuriyama et al., 1999), the yeast CD extracted of *Saccharomyces cerevisiae*

species was considered more effective than the typically used bacterial CD (Hamstra et al., 1999). Moreover it is hypothesized that the combination of the YUPRT and the YCD enhances tumor cell sensitivity to 5-FU. So, Graepler et al. again generated the bifunctional Super Cytosine Deaminase (SCD) fusion gene consisting of YUPRT, which converts 5-FU into 5-FUMP, and YCD (Akbulut et al., 2003). Hence, a MeV vector carrying the SCD gene in the leader position was cloned by Neubert et al., MPI of Biochemistry, Martinsried. First investigations confirming the functionality and the oncolytic success in vitro of this engineered MeV-SCD and first in vivo studies were completed recently (Lampe et al., manuscript submitted).

In case of VACV, GLV-1h95 was derived from GLV-1h68 by replacing the *gusA* gene by the yeast FCU1 (FCY1/FUR1) fusion gene. The FCU1-gene also combines the enzymatic activities of the FCY1- (Saccharomyces cerevisiae cytosine deaminase) and the FUR1-gene products (uracil phosphoribosyltransferase) and was established because the suicide gene therapy with the FCY1-gene and the FUR1-gene alone or in combination was ineffective in vitro (Fogar et al., 2007).

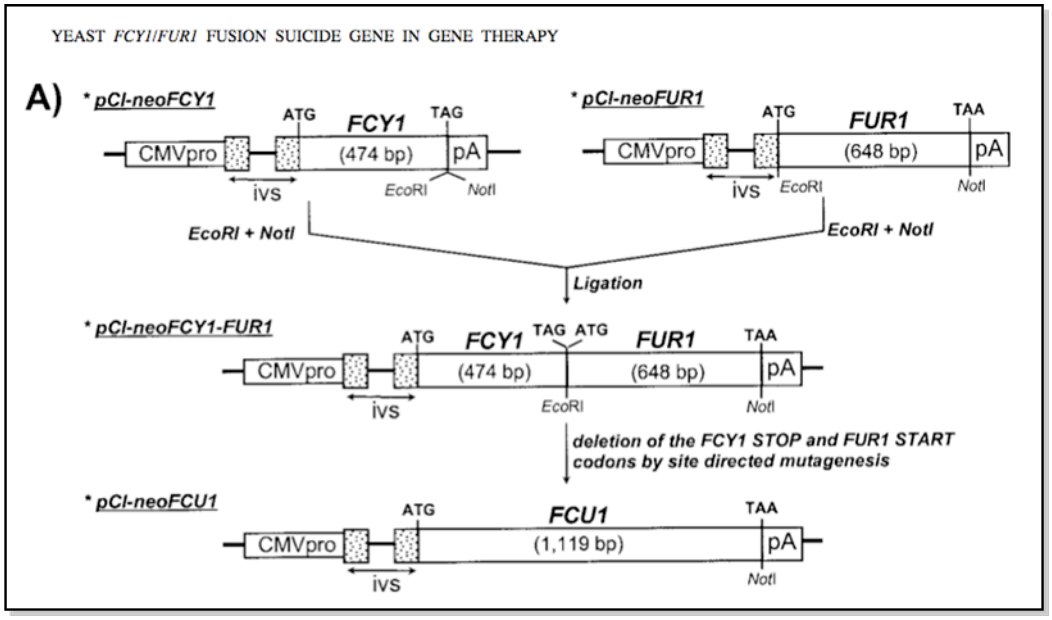

Figure 8. Yeast FCY1/FUR1 (FCU1) fusion gene (Erbs et al., 2000)

The great advantage of the Super-CD/ 5-FC system was that the systemically administered prodrug 5-FC showed no cytotoxic side effects outside the tumor tissue. The tumor cells were transfected with SCD using MeV-SCD or VACV as

a vehicle. So, SCD was only expressed in tumor cells and not in non-transformed mammalian cells, which led to selective conversion of the non-toxic prodrug 5-FC into the highly cytotoxic compound 5-FU within the tumor. 5-FC can be applied systemically. As 5-FU is a highly diffusible molecule (Kuriyama et al., 1998), it provides an effective bystander effect meaning that it also kills primarily non-infected neighbouring cells. 5-FU is a very common clinical chemotherapeutic for diverse tumor-entities (Hofer et al., 1998; Kuriyama et al., 1999).

The mechanism leading to cell death consists of two different pathways which can be seen in **Figure 9**. 5-FC first is deaminated into 5-FU by the CD. The YUPRT converts 5-FU into 5-FUMP. Both RNA and DNA synthesis can be inhibited by 5-FU in the following ways: When 5-FUMP is phosphorylated to 5-FUDP and 5-FUTP, 5-FUTP is incorporated into RNA which leads to a stop of protein synthesis. 5-FUDP can also be reduced to 5-FdUDP and hydrolyzed to 5-FdUMP which is a competitive inhibitor of thymidylate synthetase (TS), which catalyzes the indispensable conversion of dUMP to dTMP. dTMP is phosphorylated to the nucleotide dTTP, which is one of the four necessary components for the de novo synthesis of DNA. 5-FdUDP can also be phosphorylated to 5-FdUTP which is incorporated into DNA.

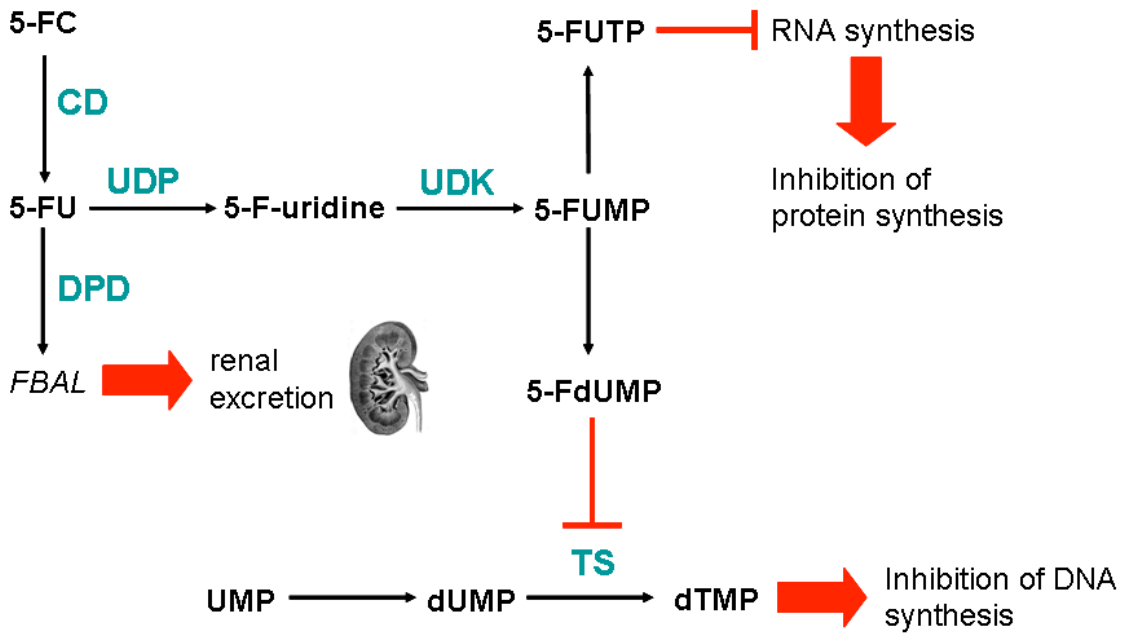

Figure 9. Suicide gene therapy using the Super-CD/ 5-FC system

5-FC is converted into 5-FU by Cytosine Deaminase (CD). One part of the 5-FU is renally excreted as FBAL. UDP converts 5-FU to 5-F-uridine which is transformed into the key metabolite 5-FUMP. 5-FUMP is incorporated into RNA after its phosphorylation to 5-FUTP. 5-FUMP can also be reduced to 5-FdUMP which inhibits TS. The inhibition of dTMP synthesis stops the incorporation of dTTP (activated dTMP) into the DNA resulting in an inhibition of DNA synthesis. 5-FC–5-fluorocytosine, 5-FU-5-fluoruracil, FBAL- α-fluoro-β-alanin, 5-F-uridine-5-fluorouridine, 5-FUMP- 5-fluorouridine monophosphate, 5-FUTP-5-fluorouridine triphosphate, 5-FdUMP-5-fluorodeoxyuridine monophosphate, CD-cytosine deaminase, UDP-uridine phosphorylase, DPD-dihydropyrimidine dehydrogenase, UDK-uridine kinase, TS-thymidylate synthetase. (Chung-Faye et al.)

1.6 Aim of this dissertation

The treatment of solid tumors being resistant to first line therapies like surgery, chemotherapy and radiation displays a huge problem in today´s cancer therapy. Therefore, alternative therapy options are shortlisted for additional treatment of cancer. One of these alternative treatment options is the use of therapeutic oncolytic viruses called virotherapy. For each cancer species the most “appropriate” and promising viral vector must be found, especially for first line therapy resistant tumors.

This dissertation was destined to characterize two genetically engineered, attenuated, replication competent viral vector systems, VACV and MeV, with regard to their basic infection efficacy, their replication behaviour within tumor cells and their oncolytic potential in vitro. The antitumor efficacy of both virotherapeutic systems should be investigated in a non-armed (2nd generation) and in an armed (3rd generation) version of each of the tow vector systems. The armed vectors express the suicide gene SCD which is able to toxify the non-toxic prodrug 5-FC.

First of all, we set out to investigate if there is a difference in the oncolytic potency between the MeV system and the VACV system. Secondly, our experiments should make clear if there are differences in the oncolytic potential between the armed and non-armed versions of the respective vectors. Moreover, it then was needed to demonstrate that virotherapy using these potentially oncolytic agents does not harm healthy tissue in the tumor environment but indeed selectively kills the tumor cells.

2 Materials and methods

2.1 Cell culture

2.1.1 Cell culture materials

Cell culture materials	
DMEM with stable L-glutamine with 4.5 g/l glucose	Biochrom AG
OPTI-MEM®	Gibco/ Invitrogen
RPMI	PAA Laboratories GmbH
William´s E + GlutaMAX^{TM} –I	Gibco/ Invitrogen
Fetal bovine serum (FBS)	PAA Laboratories GmbH
HEPES buffer, 1M in 0.85% NaCl	Lonza, AppliChem GmbH
phosphate buffered saline (PBS) without Ca^{2+} and Mg^{2+}	PAA Laboratories GmbH
Trypsin/ EDTA 0.05%	PAA Laboratories GmbH
L-glutamine	Biochrom AG
NEAA (non essential amino acids)	PAA Laboratories GmbH
D-(+)-glucose 45%	Sigma
4% paraformaldehyde (PFA)	Otto Fischar GmbH
Penicillin Streptomycin	Bio Whittaker®, Lonza
Gentamycin	CAMBREX
Trypan Blue solution 0.4%	Sigma
Triton-X-100	Roth
ddH_2O	MilliQ Synthesis System

All media, antibiotics, PBS, Trypsin/EDTA 0.05%, L-glutamine and D-(+)-glucose were stored at 4°C during the time of use. Trypsin/EDTA 0.05% and FBS were stored at -20°C before use. The FBS was heat-inactivated at 56°C for 30 minutes.

2.1.2 Characteristics of the cell lines

Name	Origin	Species	Culture medium	Morphology
Tumor cell lines				
A673	extraosseus Ewing´s sarcoma	human	DMEM-10	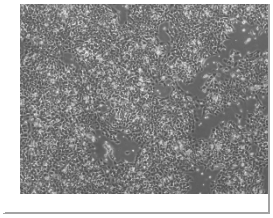
BRZ	alveolar rhabdomyosarcoma	human	DMEM-10	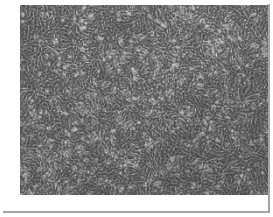
SRH	sclerosing rhabdomyosarcoma resistant to first line chemotherapy	human, primary	DMEM-10	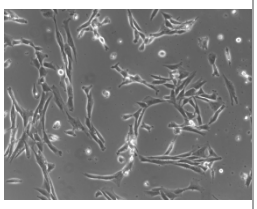
SCOS	osteosarcoma resistant to first line chemotherapy	human, primary	DMEM-10	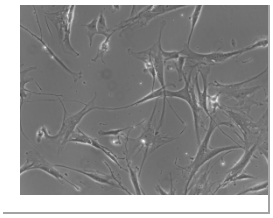
PLC/PRF/5	hepatoma	human	DMEM-10	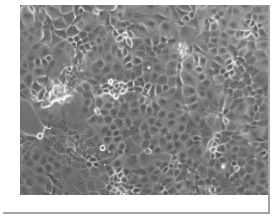
CC531s	colorectal adenocarcinoma	rat	DMEM-10 supplemented with 1 mM HEPES buffer	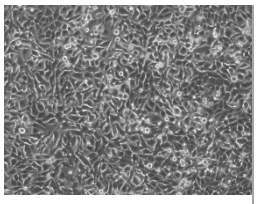

SKOV3ip.1	ovarian adenocarcinoma	murine	DMEM-10	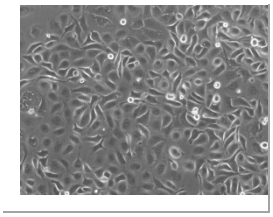
HT-29	colorectal carcinoma	human	DMEM-10	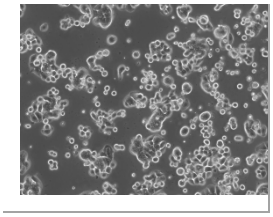
SiHa	cervical squamous cell carcinoma	human	DMEM-10 containing 1% NEAA	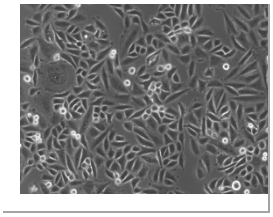
NCI-H1299	breast adenocarcinoma	human	DMEM-10 containing 10 mM HEPES	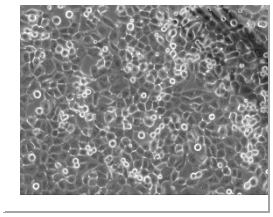
Non-tumor cell lines				
PHH	primary human hepatocytes	human	500 ml DMEM supplemented with 21 µl insulin (10 U), 188 µl hydrocortisone and 5 ml penicillin/streptomycin (100.000 U/ ml)	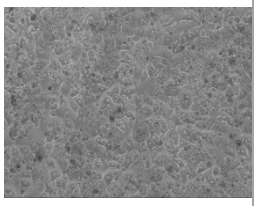
Vero	African green monkey kidney epithelial cells	simian	DMEM-10	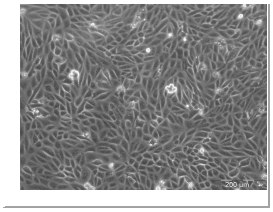
CV-1	African green monkey kidney fibroblasts	simian	DMEM-10	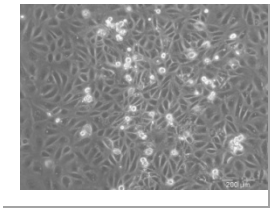

2.1.3 Cell culture

The cell lines described in the previous paragraph were cultivated as permanent cell cultures and were maintained as adherent monolayer. All cell lines except the PHHs were grown in Dulbecco's modified Eagle medium (DMEM) containing 10% heat-inactivated fetal bovine serum (FBS) (DMEM-10) at 37°C in a humidified atmosphere of 5% CO_2 in plastic culture flasks. No antibiotic or fungicide was added in the media except in the medium of primary human tissue which was supplemented with penicillin/ streptomycin. All cultures were tested to be free of mycoplasma.
When cells grew confluent, they were passaged every two to three days to avoid a lack of nutrients. All media and buffers were warmed to 37°C before use.

To passage the confluent cell lines, they were washed once with PBS to eliminate dead cells and the rest of the FBS in the culture flask. Afterwards, trypsin/ EDTA 0.05% was added. To optimize the activity of the protease trypsin, the culture flask was placed into the incubator at 37°C for two to eight minutes. The supplemented EDTA exerted an additional effect: it acidulated the cell solution and led to a maximum effect of the trypsin. Under the treatment with trypsin/ EDTA 0.05%, cells detached from the plastic ground of the culture flask. Fresh culture medium was added to stop the activity of the trypsin. Cells were centrifuged in a 50 ml Falcon tube at 1200 rpm for five minutes at room temperature (RT) and the cell pellet was resuspended in fresh medium. One fifth to one tenth of the cell solution was cultivated in fresh medium again. The split ratios of the different cell lines were empirically determined.

Kind of vessel	Growth area [cm^2]	Media volume [ml]	Trypsin/EDTA [ml]
Multi-well plate			
96-well	0.32-0.6	0.2	-
48-well	1	0.4	-
24-well	2	0.5	-
6-well	9.5	2	0.5
Petri-dish			
60x15mm	-	9	-
Culture flask			
750 ml	175	25	5
300 ml	75	15	2.5

Table 1. Growth area and volumes used in various culture vessels

2.1.4 Cryopreservation of cells

To create a standby of cells, cells were expanded in 75 cm^2 culture flasks and were frozen at -180°C in cryovials. Therefore, cells which were in the exponential growth stage were trypsinized and centrifuged as described in 3.1.3. The cell pellet was resuspended in DMEM containing 10% dimethylsulfoxide (DMSO) and 20% FBS. Aliquots of 1 ml volume each were immediately frozen at -80°C and transferred to -180°C for long time storage one day later.

2.1.5 Thawing of cells for recultivation

One aliquot of the respective cell line was quickly thawed in the water bath at 37°C. Cells were immediately added to 9 ml prewarmed culture medium and centrifuged at 1200 rpm for five minutes at RT. The cell pellet was resuspended in 10 ml fresh culture medium and transferred into a culture flask.

2.1.6 Cell count determination with the Neubauer haemocytometer

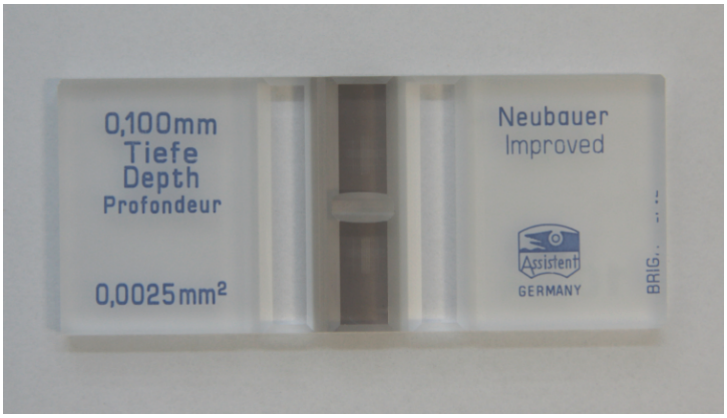

Figure 10. Neubauer haemocytometer

Before seeding cells, exact cell count was determined. Cells were trypsinized and centrifuged as described in 3.1.3. Cells were resuspended in DMEM-10 and 10 µl of the cell suspension were added to 90 µl trypan blue (0.4% w/v, Sigma). Trypan blue served to differentiate between dead and healthy cells. 10 µl cell suspension were pipetted into the chamber between the hemocytometer and a glass cover. Healthy cells appeared white under the microscope in front of the blue background. Cells in the four quadrants of the Neubauer hemocytometer were counted and the mean was calculated. The mean was multiplied with 10^4 because each quadrant measures 10^{-4} cm^2 and the result was multiplied with the factor 10 because of the 1:10 dilution in trypan blue.

$$\frac{cells}{ml} = \frac{counted\ cells}{quadrants} \times 10^5$$

2.2 Virus infection

2.2.1 Virus infection without suicide-gene therapy

One day before infection, cells were seeded out in culture medium in cell culture plates or in petri dishes. The next day, virus stock was diluted to the necessary titer in OPTI-MEM®. Infection took place in OPTI-MEM®, using different multiplicities of infection (MOI). **MOI** means the number of infectious virus particles per cell at the time point of infection. After the infection the plates were

placed into the incubator at 37°C. Plates were gently moved every 15 minutes to facilitate equal infection. 3 hpi (MeV)/ 1 hpi (VACV), the inoculum was aspirated and replaced by fresh culture medium.

For the production of growth curves of GLV-1h68 in CC531s- and SKOV3ip.1-cells, virus stock solution was diluted in DMEM supplemented with 2% FBS (DMEM-2) and cells were infected as described previously.

Plate/ dish	Culture medium/ well	Inoculum/ well
6-well plate	2 ml	1 ml
24-well plate	500 µl	250 µl
60x15mm petri dish	9 ml	4 ml

Table 2. Volumes used for culture medium and inoculum in different cell cultures

2.2.2 Virus infection combined with suicide-gene therapy and 5-FC

As MeV-SCD and GLV-1h95 express the suicide genes SCD and FCU1, the inoculum was replaced by fresh culture medium supplemented with different concentrations of the prodrug 5-fluorocytosine (5-FC). 5-FC is normally used as an antifungal nucleoside analogue in clinical approach as it showed antifungal effects and provided no toxic effect to humans. The SCD/ FCU1 gene products expressed in infected cells convert 5-FC into the highly diffusible toxic metabolite 5-fluorouracil (5-FU), which leads to RNA miscoding followed by incorrect protein synthesis and inhibits DNA synthesis. 5-FU is a common chemotherapeutic in clinical use. 5-FC was used at 1 mM, 10^{-1} mM, 10^{-2}, 10^{-3} and 10^{-4} mM. 3 hpi (MeV-eGFP) or 1 hpi (GLV-1h95), the inoculum was removed and the cells were treated with the before prepared 5-FC solutions in quadruplicates ab initio (**Figure 11**). To lengthen the process of viral replication, 5-FC was alternatively added 48 hpi because the toxic metabolite 5-FU is likely to inhibit *viral replication* as well as the host DNA replication (McCart et al., 2000).

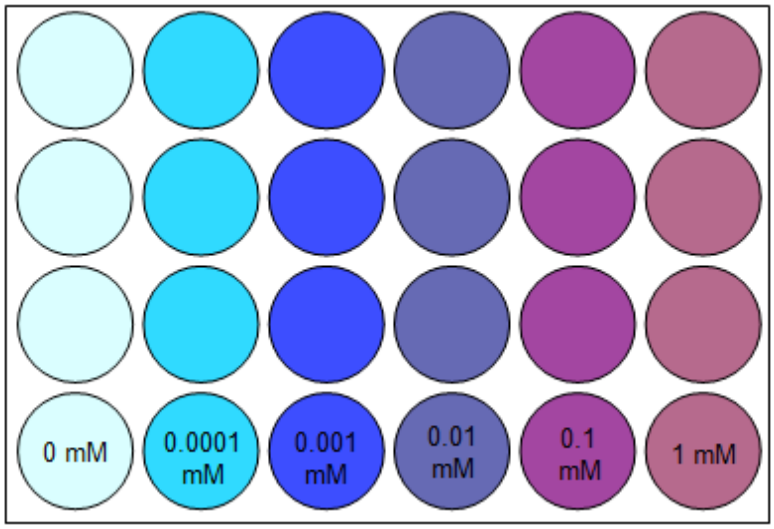

Figure 11. 5-FC concentrations in a 24-well plate
5-FC was added to the 24-well plate in increasing concentration steps from 0.0001 mM to 1 mM in quadruplicates. Four wells were treated with 0 mM 5-FC and DMEM-10 solely. Same colour means same 5-FC-concentration.

2.3 Overview of cell-virus interaction in electron microscopy

To visualize the behaviour of GLV-1h68 in the infected cell lines CC531s and SKOV3ip.1 and the behaviour of MeV-SCD in the infected cell lines A673 and BRZ, electron microscopy was performed with the help of B. Fehrenbacher, Dermatology, University Hospital Tübingen.

$2x10^6$ cells were seeded out per 10 cm petri dish in 9 ml DMEM-10. The next day, one dish of each cell line remained mock infected and three dishes were infected with GLV-1h68 at the MOI of 0.1 and with MeV-SCD at the MOI of 1 as described in 3.3.1.

24, 48, 72 and 96 hpi the cells from one petri dish of each cell line were trypsinized and centrifuged as described before. The cell pellet was fixed in 500 µl Karnovsky fixing solution for one hour at RT and subsequently stored at 4 °C. The Karnovsky fixing solution is composed of two separate solutions. Solution A consists of 30 ml 0.2 M natrium-cacodylate, 40 ml 7.5% paraformaldehyde and 50 mg $CaCl_2$ dissolved in triple distilled H_2O. Solution B consists of 30 ml 12% glutaraldehyde dissolved in triple distilled H_2O. Both solutions were frozen in separate cryovials. The solutions should be defrosted and mixed immediately before use.

The mock-infected cells were fixed 48 hpi because of high confluence at this time point. Electron microscopy was done by B. Fehrenbacher, Dermatology, University Hospital Tübingen.

2.4 Detection of GFP by fluorescence microscopy

Cells were infected as described before. Fluorescence microscopy was done at different time points post infection using the *OLYMPUS IX50* microscope and the associated *OLYMPUS U-RFL-T* function for the fluorescence photos, which were taken with the *F-View Soft Imaging System* and the corresponding *anaLYSIS* software.

Phase contrast photos were taken at 4x lens magnification using the *PhL* ocular or at 10x lens magnification using the *Ph1/ PhC* ocular. Fluorescence photos were taken of the same detail as the phase contrast photos using the fluorescence light filter. Phase contrast and fluorescence photos were finally overlaid.

2.5 Quantification of the relative fluorescence intensity

$5x10^4$ cells per well were seeded in one half of a 24-well plate, which is exemplarily shown in **Figure 12**. On the following day, cells were either mock-infected or infected with GLV-1h68 at MOI 0.1 and 1 in quadruplicates. The inoculum was replaced by DMEM-10 1 hpi. Fluorescence intensity was measured 24, 48, 72 and 96 hpi using the *Multiplate Elisa Reader Tecan GENios Plus* and the software *XFluor4*. Fluorescence intensity was measured in random circle points in each well.

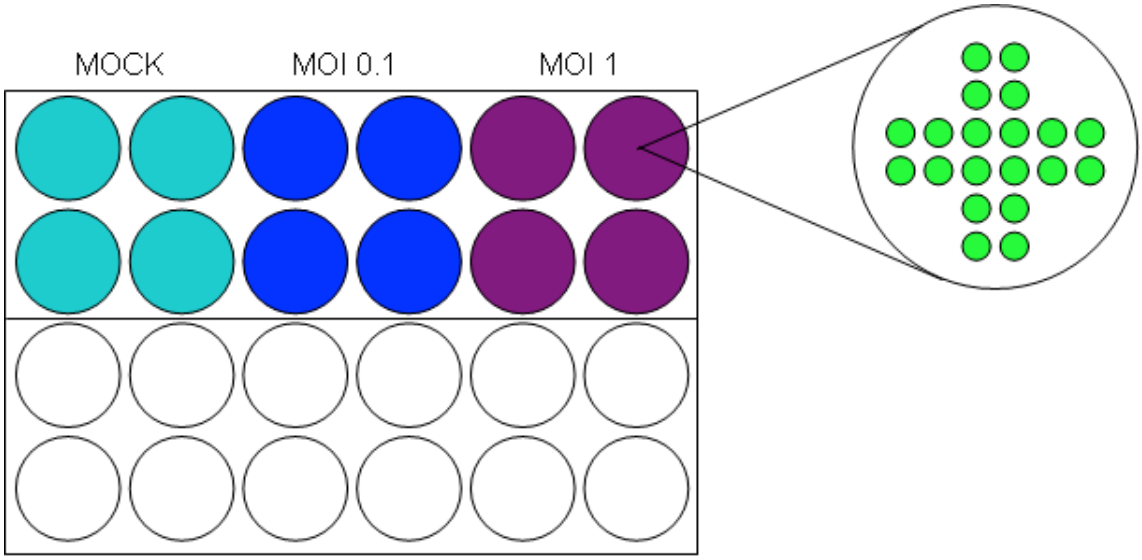

Figure 12. Green fluorescence intensity measurement
The upper half of the 24-well plate was used for green fluorescence measurement in the Tecan GENios Multiplate Elisa Reader. Four wells (same colour) formed a group of mock-infected cells or cells infected at MOI 0.1 and 1. The detail on the right shows the random circle points of green fluorescence measurement in one well.

2.6 β-galactosidase detection by lacZ-staining

2.6.1 Materials for lacZ-staining

X-Gal staining was first performed using `*The Senescence Cells Histochemical Staining Kit´* from Sigma. The staining kit was replaced by an alternative X-gal staining method.

Senescence Cells Histochemical Staining Kit (Sigma-Aldrich)

Contents of the staining kit:

X-Gal solution, staining solution, reagent B, reagent C, PBS 10x, fixation solution 10x

Alternative X-Gal staining method	
PBS 1x	PAA Laboratories GmbH
Paraformaldehyde (PFA) 4.0%	Otto Fischar GmbH
Glutaraldehyde 25%	Roth
$K_2[Fe(CN_6)]$	Sigma
$K_3[Fe(CN_6)]$	Sigma
$MgCl_2$ 1M (1.017g $MgCl_2$ in 5 ml ddH_2O)	-
X-Gal	Carl Roth GmbH

2.6.2 Experimental procedure of lacZ-staining

The lacZ staining assay is an established method to show the presence of *β*–galactosidase, an enzyme which is encoded by the lacZ-gene within the GLV-1h68 genome.

The intracellular *β*-galactosidase activity can be detected by the colour change of the colourless substrate *X-Gal* (5-brom-4-chlor-3-indoxyl-*β*-D-galactopyranosid) into blue (indigoid dye: 5,5'-dibrom-4,4'-dichlor-indigo) after getting converted by the *β*-galactosidase enzyme. Our purpose was to reveal the ability of GLV-1h68 to infect the analyzed cell lines. As it has already been tested successfully, we used the Senescence Cells Histochemical Staining Kit from Sigma for this assay but changed to a low priced variant of self-preparing the required contents.

$1x10^6$ cells were seeded out in 500µl DMEM-10 per well onto a 24-well plate and were infected with GLV-1h68 in quadruplicates at the MOI of 0.1 and 1 or remained mock-infected 24 hours later.

At the time point of interest, the cells were washed twice with 500 µl 1x PBS per well. The fixation solution was prepared by combining 4.92 ml PBS 1x, 0.08 ml 25% glutaraldehyde and 5 ml 4% paraformaldehyde. Afterwards, cells were fixed using 700 µl of the fixation solution per well for a minimum of six minutes at RT. The staining solution consisted of PBS, $K_2[Fe(CN_6)]$-solution,

$K_3[Fe(CN_6)]$-solution, $MgCl_2$ and X-Gal, which was heated up to 37°C to avoid precipitation. The staining solution was filtered through a 0.2 µm filter to eliminate potential aggregates which would disturb the staining result. The exact assembly of the fixing and the staining solution is reported in **Table 3**. 10 ml of each the fixing and the staining solution were prepared.

	Content	Concentration
Fixing solution	PBS	1x
	PFA	4% in PBS
	glutaraldehyde	25%
Staining solution	PBS	1x
	$K_2[Fe(CN_6)]$	50 mM in DMSO
	$K_3[Fe(CN_6)]$	50 mM in PBS
	$MgCl_2$	1 M in ddH_2O
	X-Gal	400 mg in 10 ml DMSO

Table 3. Fixation and staining solution for *β*-galactosidase-staining using X-Gal

For 10 ml fixing solution 4.92 ml PBS, 5 ml PFA and 0.08 ml glutaraldehyde were used, for 10 ml staining solution 7.73 ml PBS, 1 ml $K_2[Fe(CN_6)]$, 1 ml $K_3[Fe(CN_6)]$, 0.02 ml $MgCl_2$ and 0.25 ml X-Gal were pipetted together.
Subsequently cells were washed three times with PBS again before staining the cells with 750 µl of the staining solution per well. Plates were sealed with parafilm and stored at 37°C in a CO_2-free atmosphere. After at least two hours infected cells appeared blue visible to the naked eye and by using the brightfield microscopy. Photos were taken using the OLYMPUS IX50 microscope, the F-View Soft Imaging System and the analySIS program.

2.7 Western Blot analysis

2.7.1 Materials for Western Blot analysis

Tris-buffered saline (TBS) (pH 7.4)	NaCl 150 mM Tris 50 mM adjust pH with HCl (37%)
Tris-buffered saline-Tween	TBS (pH 7.4) 0.02% Tween-20
Tris-buffered saline-Triton (TBS-T)	TBS (pH 7.4) 0.02% Triton-100
1x Wet-Transfer-buffer	Tris 48 mM Glycine 39 mM MeOH 20%
PAGE 5x Running-buffer (pH 8.3)	125 mM Tris 950 mM glycine 0.5% w/v SDS adjust pH with HCl (37%)
Tris-HCl (pH 8.8)	1.5 M, adjust pH with HCl (37%)
Tris-HCl (pH 6.8)	1 M, adjust pH with HCl (37%)
Sodiumdodecyl-sulfate (SDS)	10% w/v ddH_2O
ammonium persulfate (APS)	10% w/v in ddH_2O
TEMED $C_6H_{12}N_2$	-

Table 4. Chemicals for Western Blot analysis

Primary antibodies			
Target structure	Species/ name	Dilution in Roti-Block	Firm/ origin
Vinculin (human)	Mouse/ V9131	1:10.000	Sigma-Aldrich
SCD	-	1:1.000	Transgene S.A.

Table 5. Primary antibodies for Western Blot

Secondary antibodies			
Target structure	**Species/ name**	**Dilution in Roti-Block**	**Firm/ origin**
Rat IgG (SCD)	HRP-labelled, goat anti-rat	1:20.000	Biorad
Mouse IgG (Vinculin)	HRP-labelled, goat anti-mouse	1:30.000	Biorad

Table 6. Secondary antibodies for Western Blot analysis

2.7.2 Preparation of cell lysates

$2x10^6$ cells were seeded out in 8 ml DMEM-10 per 10 cm diameter petri dish. The next day, cells were washed once with 8 ml PBS per petri dish and afterwards infected at MOI 0.1 in 4 ml OPTI-MEM® or mock infected as described in 3.3.1. 48 hpi cells were washed once with 8 ml PBS and were subsequently lysed in 500 µl NP40 lysis buffer (50 mM Tris-HCl (pH 7.6), 150 mM NaCl, 1% NP40). Cells were scraped off the bottom of the petri dish and transferred into a 1.5 ml reaction tube. Three freeze-thaw-cycles followed. Cells were first shock-frozen in liquid nitrogen and subsequently thawed again in the heating block at 37°C. Afterwards, the samples were centrifuged at full speed at 4°C for five minutes and supernatants were transferred to fresh reaction tubes.

2.7.3 Bradford dye Assay

The Bradford dye assay (Bradford 1976) is based on the equilibrium between two forms of Coomassie Brilliant Blue G-250 dye. Under strongly acid conditions, the dye is most stable as a doubly-protonated red form. Upon binding to protein (especially to basic and aromatic amino acids) it is most stable as an unprotonated form. This leads to a shift of the absorption peak from 465 to 595 nm and the G-250 dye appears blue. The higher the protein concentration the higher is the absorption at 595 nm.

Bradford dye assay was performed to determine the content of protein in the cell lysates, which were prepared for Western blot analysis. The BIO-RAD

protein assay kit (Bio-Rad Laboratories GmbH) was used for protein content examinations.

To generate a standard curve a stock solution of bovine serum albumin (BSA) (10 mg/ ml) was diluted to the final concentrations 0.5, 0.25, 0.1 and 0.05 mg/ ml in ddH_2O.

The Bradford dye reagent was diluted 1:5 in ddH_2O and the cell lysates were diluted 1:50 and 1:100 in ddH_2O.

10 µl of each dilution and of the standards were transferred in duplicate to a 96 well plate. ddH_2O was used as a blank. 200 µl Bradford dye were added to each well. The optical density (OD) of all samples was measured in the Multiplate Elisa Reader using the *magellan software*. The OD of the BSA standard served to generate a standard curve which was used as a reference to calculate the protein content of the samples.

2.7.4 Sodium-dodecylsulfate-polyacrylamide gel electrophoresis

Proteins can be separated according to their molecular weight by the **S**odium-**d**odecyl**s**ulfate-(SDS) **p**oly**a**crylamide **g**el **e**lectrophoresis (PAGE) (Laemmli et al., 1970). The addition of β-mercaptoethanol leads to the breakup of the disulphide bridges and to the unfolding of the proteins. The attachment of SDS to the exposed proteins afterwards leads to a net charge of the protein according to its mass.

First of all the buffer tank, the gel chamber, the stacking and the separating gel for the SDS-PAGE were prepared. The composition of the two gels is shown in **Table 7**. The polyacrylamide concentration of the separating and the stacking gel defined the pore size of the gels.

Content	Separating gel (12%)	Stacking gel (5%)
ddH_2O	3.3 ml	1.4 ml
30% acrylamide	4.0 ml	0.33 ml
1.5 M Tris (pH 8.8)	2.5 ml	-
1 M Tris (pH 6.8)	-	0.25 ml
10% SDS	0.1 ml	0.02 ml
10% APS	0.1 ml	0.02 ml
TEMED	0.004 ml	0.002 ml

Table 7. Composition of the stacking and the separating gel

ddH_2O, 30% acrylamide, Tris and 10% SDS were mixed in a 15 ml tube. APS and TEMED were added to the separating gel, APS served as a radical and TEMED was the initiator of the polymerisation reaction. They both started the polymerisation, so the separating gel had to be filled into the gel cassette immediately. The gel was overlaid with some isopropanol to create a flat surface on which the stacking gel could be filled. Polymerisation took about 30 minutes. Then the isopropanol was removed from the polymerized gel and the surface of the gel was washed once with ddH_2O.

APS and TEMED were added to the stacking gel and the stacking gel was immediately filled over the separating gel. The comb (which formed 10 slots) was inserted straight afterwards. Polymerisation took about 15 minutes.

Then the gel cassette was placed into the buffer tank which was afterwards filled to the rim with the buffer solution. The slot-forming comb was carefully removed and the integrity of the slots was checked.

75 µg of cell lysate per lane were loaded onto the gel. Before loading, one fifth of the sample volume of 6 x SDS loading buffer was added and samples were boiled for 5 minutes at 95°C. A positive control and a molecular weight marker (Full range rainbow protein marker, Amersham Biosciences) were added in one slot in addition. The molecular weight marker helped to identify the band of protein we were searching for.

2.7.5 Western blotting

After separation by SDS-PAGE proteins were electrophoretically transferred to a polyvinylidene difluoride- (PVDF) membrane (Amersham Hybond P, GE Healthcare). Western blot analysis was done to proof the expression of Super Cytosine Deaminase (SCD) in the before infected cell lines. The enzyme SCD served as the evidence of MeV-SCD infection.

The PVDF-membrane was wetted with methanol and was afterwards embedded between gel, Whatman papers and sponges as shown in **Figure 13**.

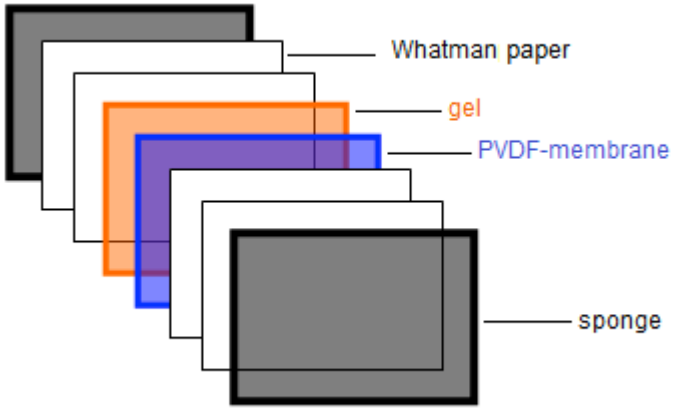

Figure 13. The correct order of the blotting membranes from back to front
sponge - 2 Whatman paper - gel - PVDF membrane - 2 Whatman paper – sponge. All layers were fixed and placed into the wet transfer buffer for blotting.

All layers in this exact arrangement were prepared in a box with 1x wet transfer buffer (3.8.1) and were clamped in a special device to keep the gel close to the PVDF-membrane. It was very important to avoid air bladders between the gel and the Amersham Hybond P membrane because they would inhibit transfer. To control successful blotting the membrane was stained for two minutes with Ponceau-S solution (0.1% w/v Ponceau-S in 5% acetic acid). The staining solution was removed and the membrane was washed with ddH_2O until the removed solution was almost free of Ponceau-S dye.

2.7.6 Staining of the protein bands

To avoid the non-specific binding of the antibody, the membrane was blocked with 5% milk powder in TBS-Tween. The membrane was washed twice in TBS/ Triton and subsequently cut in two parts at 70 kDa, separating the 116 kDa Vinculin band from the 35 kDa SCD band. The primary anti-SCD antibody was diluted in 1x Roti-Block and the “SCD-part” of the membrane was incubated in this solution, the primary anti-Vinculin antibody was diluted in 1x Roti-Block and the “Vinculin-part” of the membrane was incubated in this separate solution at 4°C on the shaker overnight.

Antibody solutions were removed the next day and stored at 4°C for reuse after the addition of 0.05% sodium-acid.

Afterwards both membranes were washed three times with TBS/ Triton for five minutes.

The secondary horseradish peroxidase (HRP) labelled goat anti-rat antibody (SCD) was diluted 1:20.000 in Roti-Block, the secondary HRP labelled goat anti-mouse antibody (Vinculin) was diluted 1:30.000 in Roti-Block. Incubation within the antibody-solutions occurred on the shaker for one hour at RT. Afterwards both membranes were washed three times with TBS/ Triton for ten minutes.

Proteins were visualized by enhanced chemiluminescence (ECL). Equal amounts of both components of the detection reagent were mixed and the two parts of the membrane were incubated in 1 ml ECL solution for three minutes. Afterwards, both membranes were fixed in a plastic foil in a Dr. GOOS Suprema UNIVERSAL 100 photo cassette (Dr.GOOS Suprema GmbH). The membranes were exposed to the high performance chemiluminescence film Amersham Hyperfilm™ ECL (GE Healthcare Limited).

2.8 Cell mass quantification using Sulforhodamine-B assay

2.8.1 Materials for Sulforhodamine-B (SRB) assay

Materials for SRB assay	
Tecan GENios Microplate Elisa Reader	MTX lab systems
24-well microplate	TPP
96–well microplate	Costar
phosphate buffered saline (PBS)	PAA Laboratories GmbH
Trichloroacetic acid (TCA, 10% w/v)	Roth
Sulforhodamine B	Sigma
SRB staining solution (0.4% w/v in 1% acetic acid)	Sigma
Acetic acid (1%)	Merck (100%)
Tris-base solution (TBS) (10 mM)	Sigma

Table 8. Materials for SRB assay

2.8.2 Procedure of SRB assay

The SRB-assay (Skehan et al., 1990) provides the ability to quantify the drug- or virus-induced cytotoxicity in adherent cell culture (reduction of cell mass) because the measured optical density (OD) is correlated directly positive to the remaining number of cells in the respective sample. For this reason the SRB assay is often indispensable in cancer research to determine the drug-caused cytotoxicity and proliferation stop (Skehan et al., 1990).

The SRB-dye is an anionic protein dye which binds to basic amino acids in TCA-fixed cells. After solubilising the SRB-dye, remaining protein mass can be determined by measuring the OD. In comparison to the measured OD in wells containing mock-infected cells, the change in protein mass (and indirect cell count) can be examined.

$4x10^4$ cells per well were seeded in 24-well plates in 500 µl DMEM-10. On the following day cells were infected with different MOIs as it was described before.

At the respective time point cells were carefully washed twice with 500 µl ice cold PBS per well and were subsequently fixed with 250µl cold 10% trichloracetic acid (TCA). Plates were stored for 30 min at 4°C.

After fixation, cells were washed three times with tap water. Plates were dried at 40°C overnight and could be stored limitless at RT.

To stain cells, 250 µl of the SRB-staining-solution were added to each well for ten minutes. The staining solution was removed and the wells were washed four times with 1% acetic acid to remove the not cell bound dye. Plates were dried for a minimum of 3-6 hours or overnight and measurement took place within the next 48 hours. To make cell mass measurable, the cell-associated dye was solubilised in 1 ml 10 mM tris base solution per well. To assure complete solution, plates were shaken some times and the tris base solution incubated for 10 minutes. Measurement took place in the Microplate Elisa Reader in a transparent flat-bottomed 96-well plate. 80 µl of each sample were transferred to the 96-well plate in duplicate. The OD was measured at 550 nm wavelength.

2.9 LDH-release assay

2.9.1 Materials for LDH-release assay

Materials for LDH-release assay	
Tecan genios Microplate Elisa Reader	MTX lab systems
LDH-P mono Kit	Analyticon Biotechnologies AG
Triton X-100	Roth
PBS	PAA Laboratories GmbH

Table 9. Materials for LDH-release assay

2.9.2 Procedure of the LDH-release assay

Lactate dehydrogenase (LDH) is the enzyme which catalyzes the interconversion of pyruvate and lactate in glycolysis under hypoxic conditions while the important oxidation of NADH into NAD^+ is simultaneous.

$$pyruvate + NADH + H^+ \xleftrightarrow{LDH} lactate + NAD^+$$

At the instance of cell death, LDH is released. By detecting the amount of LDH released into the culture medium, cell death can be quantified in vitro. Measurement was performed in the Multiplate Elisa Reader with the program

magellan. LDH catalyzes the oxidation of NADH to NAD^+. The conversion between the two coenzymes NADH and NAD^+ can be easily detected because of the different ultraviolet (UV) absorption spectra between the oxidized and the reduced form. While NAD^+ has a peak in absorption at the wavelength of 259 nm, NADH has a peak at 339 nm in addition to its peak at 259 nm (**Figure 14**). By measuring the decrease of molecules showing a peak at 339 nm, the program can draw a conclusion to the released amount of LDH and the dimension of cell death.

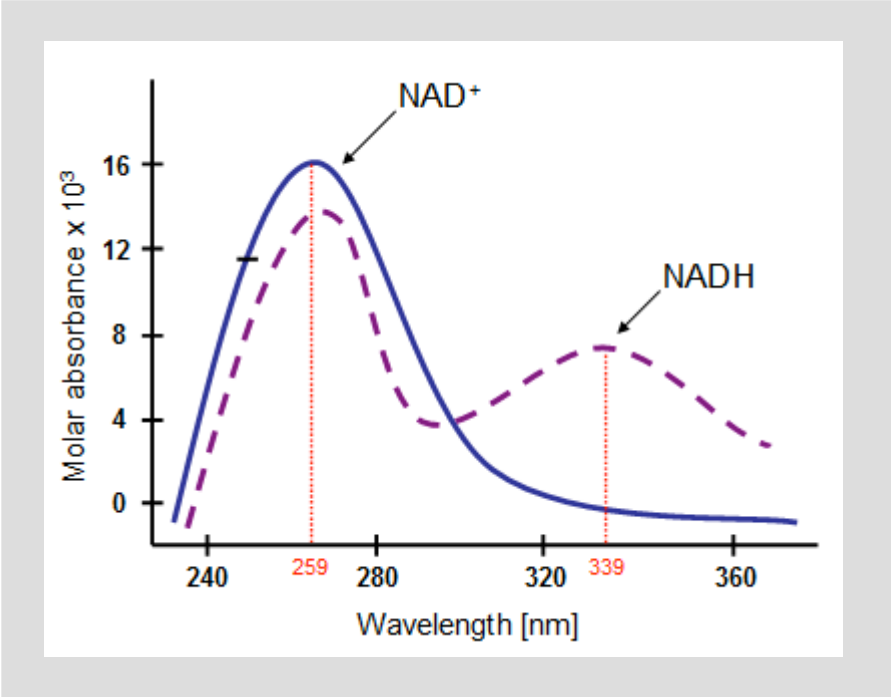

Figure 14. The oxidation of NADH to NAD^+ is catalyzed by the enzyme lactate dehydrogenase
The diagram shows the wavelength of the maximum absorption of UV-light of NAD^+ at 259 nm wavelength and of NADH at 259 nm as well and the second peak at 339 nm wavelength.

$4x10^4$ cells per well were seeded in a 24-well plate. 24 hours later, the cells were infected with different MOIs as described in 3.3.1.

LDH substrate was prepared according to the manufacturer´s protocol. To measure LDH activity, the supernatant of the cells was transferred into a 48-well plate. Cells were lysed with 500 µl - 1 ml PBS containing 0.1% Triton per well. To ensure complete lysis, cells were incubated at 37°C for ten minutes. Complete cell lysis was controlled under the phase contrast microscope.

10 µl of each supernatant sample and 10 µl - 20 µl of each lysis sample depending on the amount of LDH in the respective cell line were transferred to a flat bottomed 96-well plate in duplicate. Before the NADH-solution was added the program *magellan* and the Microplate Elisa Reader were prepared ready. Afterwards 200 µl solubilised NADH-solution were added to each well of the 96-well plate using the multichannel pipette. The plate was placed instantly into the Multiplate Elisa Reader. Received data was checked the moment straight after measuring if the amount of LDH was too high, these samples had to be diluted in some more medium containing 5% FBS and had to be measured again. Results were represented in diagrams performed with the program GraphPadPrism4.0.

To present the percentage of LDH-release, 0.1% Triton/ PBS was used as a 100% LDH release control and result values were calculated with the *Microsoft Excel* program as follows:

$$\%\ LDH\ release = \frac{LDH_{supernatant} - LDH_{background}}{LDH_{lysed\ cell\ layer} + \left(LDH_{supernatant} - LDH_{background}\right)}$$

2.10 Establishing of a growth curve to pursue the replication behaviour of the respective virus

2.10.1 Procedure of measles virus growth curve

2.10.1.1 Materials for the establishment of a measles virus growth curve

Materials for the establishment of a measles virus growth curve	
Dulbecco´s modified Eagle´s medium	Biochrom AG
Fetal bovine serum (FBS)	PAA Laboratories GmbH
PFA 4%	Otto Fischar GmbH
Goat anti-mouse Alexa 546	Molecular Probes
Anti-MeV-NP	Clone 120, ECACC (No.95040312)
TBS-Tween 0.02%	Tween: Promega

Table 10. Materials for the establishment of a measles virus growth curve

2.10.1.2 Production of the virus infected samples

$1x10^5$ cells per well were seeded in a 6-well plate in 2 ml DMEM-5. The next day cells were infected with MeV ld-SCD at the MOI of 0.03 in 1 ml OPTI-MEM® per well. 3 hpi the infection medium was removed. Cells were washed three times with PBS and 1 ml DMEM-5 was added. At the time points 3, 24, 48, 72 and 96 hpi the supernatant of one well was aspirated and assembled in one reaction tube, the remaining cell monolayer was scraped off in 1 ml OPTI-MEM® using a cell scraper and assembled in a separate reaction tube. Samples were frozen immediately at -80°C.

2.10.1.3 Titration and the 50% end point dilution assay ($TCID_{50}$ = tissue culture infectious dose 50)

After assembling and freezing the 96 hpi sample, all samples were unfrozen again, vortexed and centrifuged for two minutes at 3000 rpm to separate cells from virus particles. Supernatants were transferred to fresh reaction tubes without dissolving the pellet. The transferred samples were diluted in a seven times 1:10 dilution series in DMEM-5 using a 96-well plate.

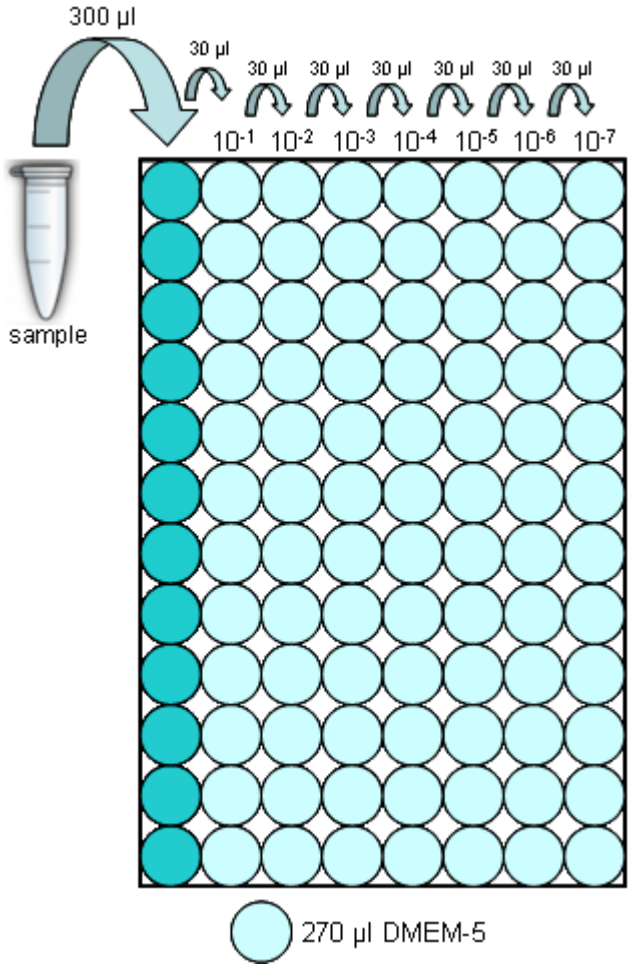

Figure 15. Sample dilution for virus titration in DMEM-5
Samples were diluted in a 96 well plate. 300 µl per sample were transferred to the first line of the plate. 270 µl DMEM-5 were added to the rest of the wells. 30 µl of each sample were diluted tenfold in 270 µl with the multichannel pipette, new pipette tips were used for each dilution step (Rabenau et al., 2005).

Titrations were performed on Vero cells which were seeded out some hours before in 96-well plates in DMEM-5. 50 µl of each sample dilution was transferred fourfold to the Vero-cells.

96 hours later, cells were washed once with 150 µl PBS per well and were subsequently fixed with 50 µl PBS containing 4% PFA per well for ten min at RT.

Infected cells were detected with virus-specific immunofluorescence-staining.

Before staining, cells were washed twice with 200 µl PBS per well and underwent a 30 min blocking step in TBS-Tween containing 1% FBS to diminish nonspecific staining. Cells were stained with anti-MeV-NP antibody (anti-MeV-NP, diluted 1:1000 in TBS-Tween, 50 µl per well). After 30 min cells were

washed three times with TBS-Tween. Incubation with the secondary antibody (goat anti-mouse, Alexa 546, Molecular Probes, diluted 1:1000 in TBS-Tween) was performed for 30 min in the dark. Afterwards cells were washed three times with 200 µl TBS-Tween per well. For fluorescence microscope observation, 100 µl PBS was added to each well. Infected wells were detected microscopically, whereas each well with at least one infected cell was declared infected.

Viral titer determination was done using the $TCID_{50}$-formula. Viral titers were calculated and presented as [PFU/ml]. The growth curve was finally done using GraphPadPrism4.0.

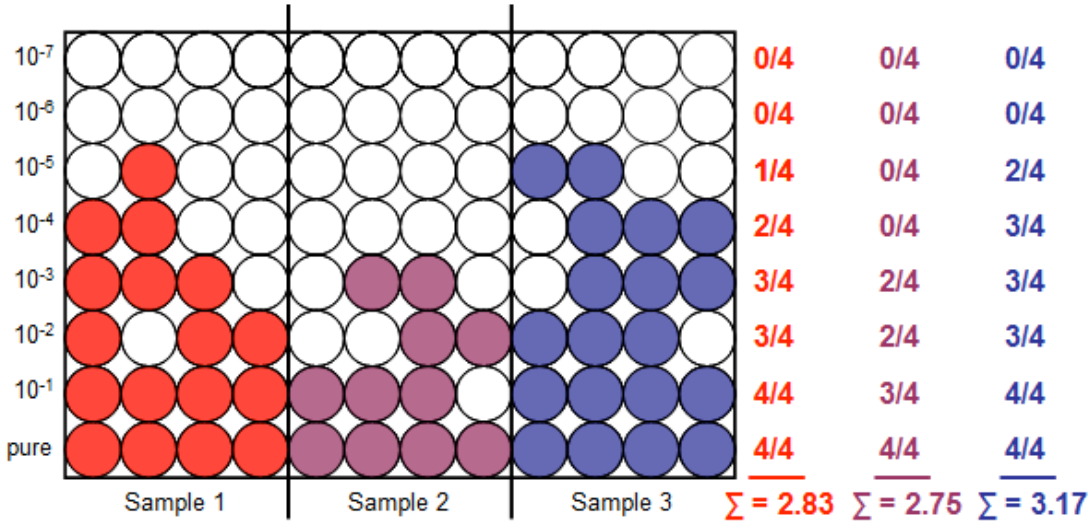

Figure 16. $TCID_{50}$-titration for viral growth curve of MeV ld-TRK
Dilution of virus samples (10^0 - 10^{-7}) were transferred fourfold to Vero-cells in a 96 well plate. 96 hpi cells were fixed and stained with anti-MeV-NP-antibody. Infected cells appeared red (shown here as red, lavender and blue) and the amount of wells containing infected cells per dilution were quantified in fluorescence microscopy. TCID50/ml concentration was calculated with the formula by Kärber and Spearman (**Figure 17**).

$$TCID_{50}/ml \quad \frac{viral\ particles}{ml} = \frac{10^{1+\sum \inf ected\ wells - 0.5\times\log 10}}{0.03\ ml\ inserted\ viral\ solution}$$

Figure 17. $TCID_{50}$-formula by Spearman (1908) and Kärber (1931)

2.10.2 Procedure of Vaccinia virus growth curve

2.10.2.1 Materials for the establishment of a vaccinia virus growth curve

Virus plaquing overlay medium (1.5% carboxymethylcellulose)	
500 ml glass bottle containing a stir bar	
Dulbecco´s modified Eagle´s medium	Biochrom AG
PEN/STREP/Amphotericin B	BioWhittaker®, Lonza
Fetal bovine serum (FBS)	PAA Laboratories GmbH
Carboxymethylcellulose sodium salt (CMC)	Sigma Aldrich

Table 11. Materials for the preparation of virus plaquing overlay medium CMC

7.5 g CMC were added to the 500 ml glass bottle. The bottle was autoclaved with the stir bar inside. Afterwards 500 ml DMEM were added under the hood. The CMC on the bottom of the bottle was dislodged with a 10 ml pipette and the bottle was placed on the stirrer overnight until all of the CMC was completely dissolved.

The next day 25 ml FBS (5%) and 5 ml antibiotic-antimycotic-solution (1%) were added and the overlay medium was placed on the stirrer for 15 minutes again. The overlay medium was stored at 4°C. Right before use, it was warmed to RT.

Crystal violet stain	
500 ml glass bottle containing stir bar	
Crystal violet	Fluka Chemie AG
37% formaldehyde	Roth
Ethanol	Merck

Table 12. Materials for crystal violet stain

0.65 g crystal violet was added to the 500 ml glass bottle containing a stir bar. 25 ml ethanol was added additionally and the solution was stirred for about one hour. Afterwards 150 ml of 37% formaldehyde was added and the bottle was filled to the 500 ml mark with ddH_2O. The staining solution was stirred overnight and then stored at RT.

2.10.2.2 Extraction of the virus infected samples

$5x10^5$ cells per well were seeded out in 2 ml DMEM-10 in one and a half 6-well plates (9 wells). The next day cell count was determined as described in 3.1.6 using three wells. The quantity of virus needed for infection was calculated according to the cell number.

GLV-1h68 was thawed from -80°C and sonicated for 30 seconds. Right afterwards the infection solution was prepared for one 6-well plate requiring 500 µl DMEM-2 per well plus a reserve; 3.5 ml. GLV-1h68 was immediately placed on ice until freezing again at -80°C.

Cells were infected as described in 3.3.1. One hour later, the inoculum was removed and the plate was carefully washed two times with 2 ml PBS per well. 2 ml DMEM-10 were added thereafter and the plate was placed into the incubator at 37°C.

The rest of the inoculum was frozen at -80°C for the titration of the inoculum.

Virus harvest took place 1, 24, 48, 72 and 96 hpi. One well of the 6-well plate was used for one time point. Cells were detached with a sterile cell scraper in 2 ml DMEM-10 and were filled into a fresh Eppendorf cup. Each sample was frozen immediately after harvesting in -80°C until virus titration.

2.10.2.3 Titrations and Crystal violet staining

One day before titration, $2x10^5$ CV-1 cells per well were seeded out in a 24-well plate in 500 µl DMEM-10. Alternatively, $1x10^5$ cells per well in 500 µl DMEM-10 were seeded out two days before titration. The titration of one cell line required 48 wells (2x 24-well plate) containing confluent CV-1 cells.

Before starting the dilution series, the samples underwent a three times freeze-thaw process. They were thawed in the 37°C heating block and were frozen in liquid nitrogen in turns. Dilution series was performed in a 48-well plate, diluting the respective sample in 1:10 dilution steps to the necessary dilution levels (**Table 13**). Useful levels of dilution were identified in a previous trial.

Harvest time point [hpi]	Levels of dilution series
inoculum	pure; 10^{-1}; 10^{-2} ; 10^{-3}
1	pure; 10^{-1}; 10^{-2}; 10^{-3}
24	10^{-1}; 10^{-2}; 10^{-3}; 10^{-4}
48	10^{-3}; 10^{-4}; $5x10^{-4}$; 10^{-5}
72	10^{-4}; $5x10^{-4}$; 10^{-5}; 10^{-6}
96	10^{-4}; $5x10^{-4}$; 10^{-5}; 10^{-6}

Table 13. Viral dilution series for virus titration on CV-1 cells

After having finished the dilution series, DMEM-10 was removed from the CV-1-cells in the 24-well plates and replaced by 200 µl of each prepared dilution in duplicates. Incubation was performed for one hour at 37°C in 5% CO_2 while plates were gently moved every 20 minutes. Afterwards cells were covered with 1 ml DMEM-5 overlay medium containing 1.5% carboxymethylcellulose (CMC) per well to avoid virus spreading and incubated at 37°C for another 48 hours.
Crystal violet stain was performed 48 later. 1 ml crystal violet was added carefully on top of the overlay medium per well. Plates were incubated for 3 to 6 hours or overnight at RT. Afterwards the crystal violet and the overlay medium were removed from the wells under the hood and the plates were washed with sterile water until the washing solution remained almost clear. The high concentrated formaldehyde washing solution was disposed of as hazardous waste. To dry the plates after the washing steps, they were gently tapped on a towel and left on a fresh towel with the openings down for some minutes at RT.

2.10.2.4 Analysis of Plaque assay results

Plaque counting took place when the plates were dry. The unstained plaques could be detected in the violet stained cell layer of CV-1 cells with the naked eye. Plaques were only counted in those wells containing 10-80 plaques. One plaque was caused by one virus particle, so the viral titer in the respective sample could be directly calculated by the plaque count per well by the following formula:

$$viral\ titer\left[pfu/ml\right] = average\ plaque\ count\left(per\ dilution\right) \times 5 \times inverse\ of\ dilution$$

cell line	time point	dilution	well 1	well 2	av.	PFU/ml	Inverse of dilution	Viral titer [PFU/ml]	average viral titer
CC531s	96 hpi	1E-04	89	92	90.5	452.5	1E+04	4.53E+06	7.91E+06
		5E-04	39	36	37.5	187.5	5E+04	9.38E+06	
		1E-05	13	18	15.5	77.5	1E+05	7.75+E06	
		1E-06	1	3	2	10	1E+06	1.00E+07	

Table 14. From plaque assay count to viral titer
Plaques of the four dilutions of the 96 hpi-sample were counted, mean was multiplied with factor 5 and with inverse of dilution. Mean of viral titers was 7.91E+06.

Mean of plaque count in well 1 and 2 was multiplied with the factor 5 to obtain a total volume of 1 ml (cells were infected in 200 µl DMEM-2). The result was multiplied with the inverse of dilution. Viral titer was indicated in [pfu/ml].

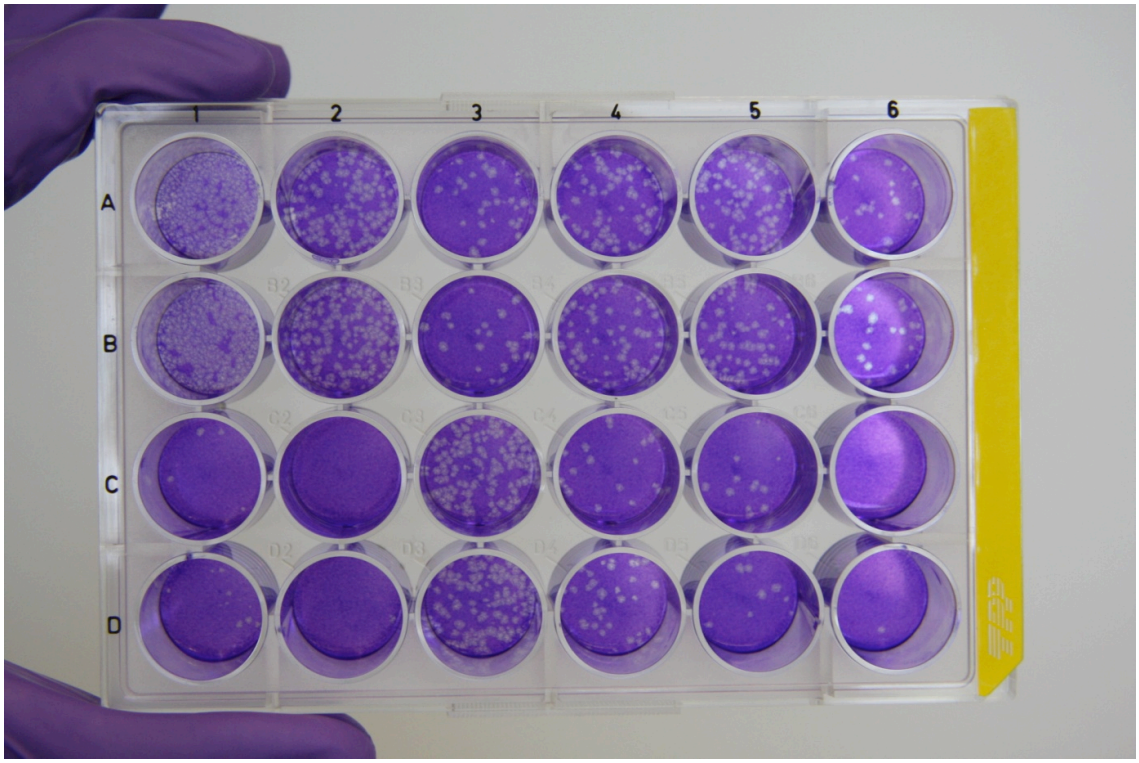

Figure 18. 24-well plate after crystal violet staining showing varying numbers of plaques
Plaques were counted in all wells except A1, B1, C2, D2, C6 and D6. These wells were irrelevant for viral titer determination because of either too high or too little plaque count.

2.11 Quantification of CD46-receptor expression by flow cytometry

Materials for flow cytometry	
Accutase	PAA Laboratories
FACS-buffer (PBS with 10% FCS)	-
Fc-blocking solution Gamunex	-
sotype control	eBioscience Inc.
Anti-CD46-PE (Phycoerythrin)	eBioscience Inc.
Flow cytometer	Becton Dickinson FACSCalibur

Table 15. Materials for flow cytometry

In tumor cells, CD46, a complement regulatory molecule, is often over-expressed to protect the cells from complement mediated cell lysis. This is one reason for the high level of infection of tumor cells by many established measles virus vaccine strains which use CD46 as an entrance to the cell. To detect and quantify the amount of CD46 on tumor cell surface, cells were marked with anti-CD46-antibodies and the fraction of $CD46^+$-cells was detected using the flow cytometer.Flow cytometry is a method for quantitative detection of cell surface and intracellular proteins, DNA and peptides. Only few molecules emit intrinsic fluorescence, so most of the molecules like ours must be labelled with a special dye or fluorescence labelled antibodies. The labelled molecules separately pass the flow cell of the flow cytometer where they become activated by a laser beam. The photomultiplier detects the emitted fluorescence light and the light diffusion. The amount of light diffusion directly correlates with the size and the complexity of a cell. In our experiment, cluster of differentiation (CD) molecules were detected at the basis of an antigen-antibody-reaction.

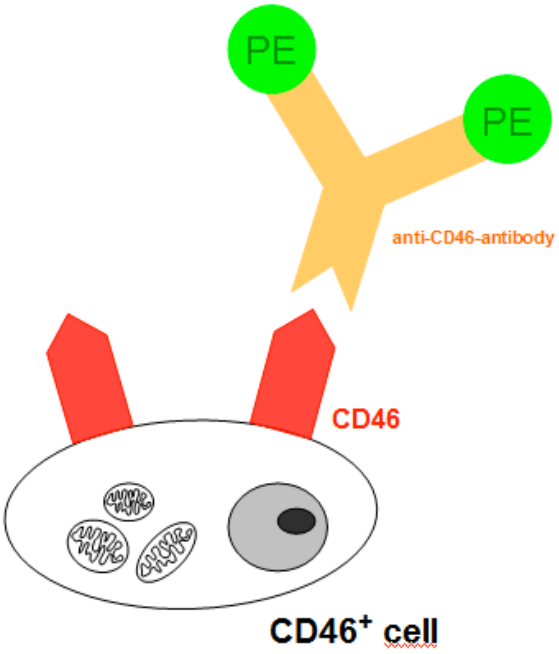

Figure 19. Labelling of a CD46$^+$ cell with anti-CD46-antibody and Phycoerythrin (PE)

For **f**luorescence **a**ctivated **c**ell **s**orting (FACS)-staining cells were detached with accutase. 6x10^5 cells were used and resuspended in 50 µl FACS buffer. To block F_c receptors 10 µl Gamunex was added. After 5 min incubation on ice, cells were stained with Phycoerythrin (PE) conjugated anti-CD46-antibody or the corresponding isotype control. PE is one of the most common antibody-labelling-dye for FACS analysis. One PE molecule is likely to binding one antibody molecule. After 30 min incubation on ice 3 ml PBS were added and the tubes were centrifuged as before. The cell pellet was resuspended in 500 µl FACS buffer. Until measurement, samples were stored on ice or when measurement took place the next day cells were fixed with 1.3% PFA. Measurement was done using the flow cytometer and the program *CellQuest*. Analysis was done with the software *WinMDI* and results were presented in a histogram (4.2).

3 Results

3.1 Electron microscopy of MeV-SCD/ GLV-1h68 replication

3.1.1 MeV-SCD replication in A673 and BRZ sarcoma cells

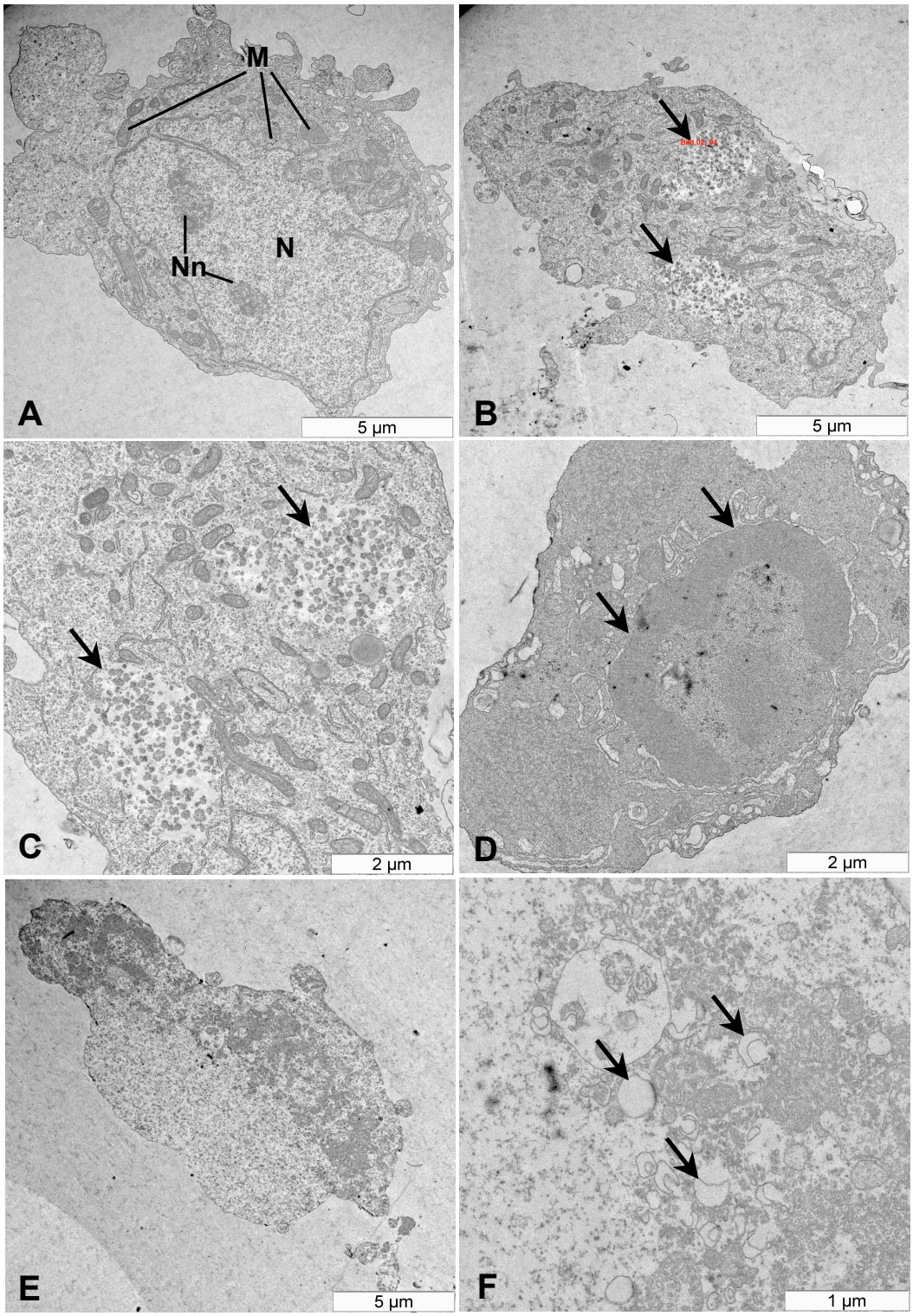

Figure 20. Electron microscopy of MeV-SCD infected A673 cells

A673 cells were infected with MeV-SCD at MOI 1 or remained uninfected. The normal cell structure of a mock-infected A673 cell with intact cell membrane, mitochondria (**M**), rough endoplasmic reticulum and the nucleus (**N**), including two nucleoli (**Nn**), is shown (**A**). Two aggregates of viral inclusion bodies within the cell 24 hpi with MeV-SCD at MOI 1 are shown in a lower (**B**) and a higher magnification (**C**). 48 hpi the chromatin condensation in A673 cell nuclei (**D**, arrows) was the first sign of apoptosis in the infected cells. In another cell, the process of disintegration has already started and the inner cell morphology seems to be completely out of order (**E**). Another sign of disintegration is the presence of several autophagosomes (**arrows**) in **F**.

A673 cells were infected with MeV-SCD (**3.3.1**) at a multiplicity of infection (MOI) of 1 or remained uninfected. Virus infection and production of new viral bodies had already started 24 hours post infection (hpi) (**B**). Signs of viral infection were aggregates of viral inclusion bodies (**B**, **C**) and signs of cell death were chromatin condensation (**D**), disintegrating cells (**E**) and the formation of autophagosomes (**F**). Cell death in A673 cells appeared first 48 hpi.

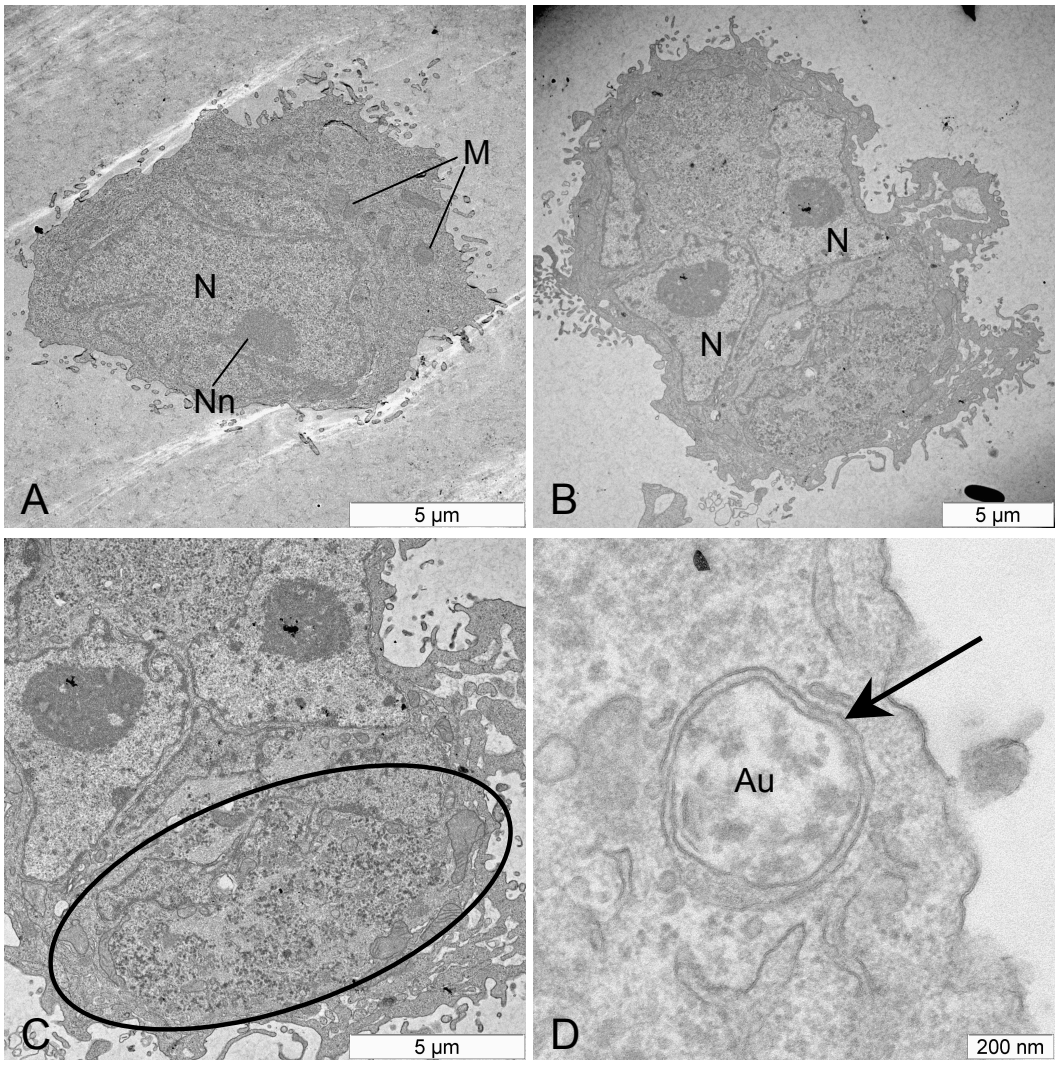

Figure 21. MeV-SCD infection in BRZ cells

BRZ cells were infected with MeV-SCD at MOI 1 or remained uninfected. In **A**, a mock-infected normal cell structure is shown including mitochondria (**M**), an intact plasma membrane and a nucleus (**N**) with nucleolus (**Nn**). 24 hpi no viral inclusion bodies were detectable (data not shown). 48 hpi, BRZ cells showed typical syncytia formation (**B**, one cell with two nuclei (**N**)) and distributed viral inclusion bodies (**C,** rounded by a circle). Signs of both necrosis and apoptosis such as autophagosomes (**Au**) became visible (**D**).

BRZ cells stayed uninfected (**A**) or were infected with MeV-SCD at MOI 1 or remained mock-infected. Viral infection first appeared 48 hpi when viral inclusion bodies (**C**) and typical syncytia formation (**B**) were observed at first sight. Autophagosomes indicated cell death 48 hpi (**D**).

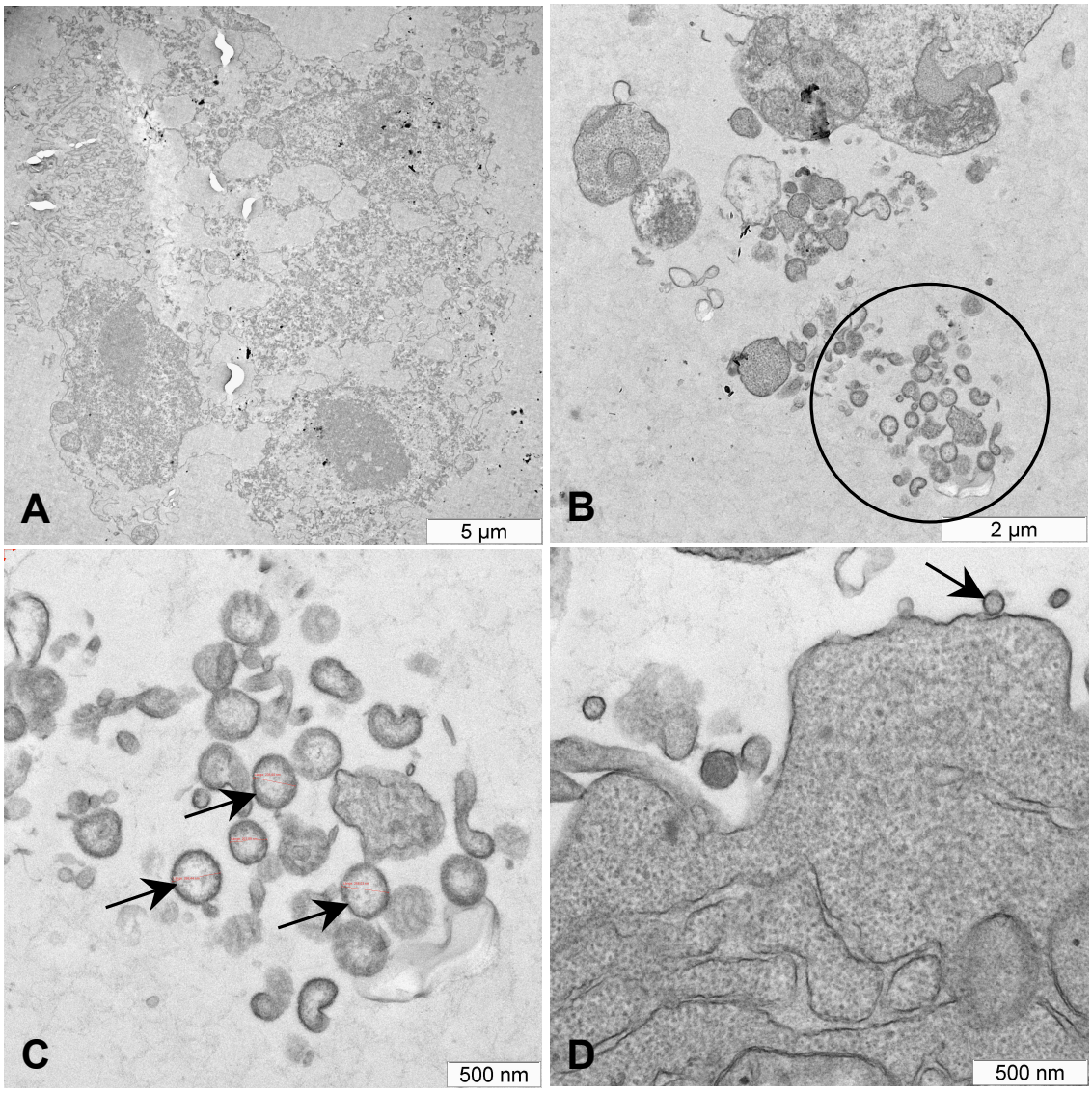

Figure 22. MeV-SCD infection in BRZ cells
In **A**, a disintegrated cell which has lost its plasma membrane is shown. In **B** and **C**, the debris of an apoptotic cell is shown, surrounded by completely assembled viral particles (circle in **B**, arrows in **C**). One viral particle is instantaneously budding off a BRZ cell in **D** (arrow).

Disintegration of BRZ cells (**A**) appeared together with the discovery of intact new viral particles shown in two different magnifications in **B** (circle) and **C** (arrows). The moment of one virus particle budding off one BRZ cell was fixed in **D**.

3.1.2 GLV-1h68 replication in CC531s colon carcinoma and SKOV3ip.1 ovarian carcinoma cells

3.1.2.1 GLV-1h68 replication in SKOV3ip.1 cells

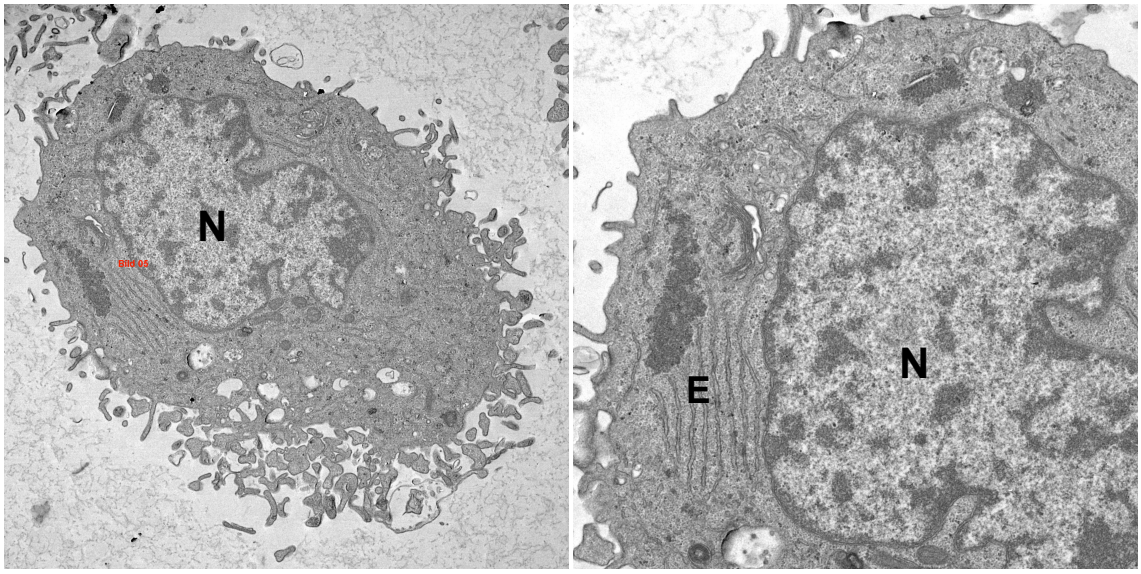

Figure 23. Electron microscopy photos of a SKOV3ip.1 cancer cell
SKOV3ip.1 cells were infected with GLV-1h68 at MOI 0.1 or remained mock-infected. Electron microscopy photos were taken 24, 48 and 72 hpi. An intact SKOV3ip.1 cell with nucleus (**N**) and endoplasmatic reticulum (**ER**) is shown.

A SKOV3ip.1 cell with intact plasma membrane, uniform cytoplasm, nucleus (**N**), different stadia of chromatin condensation and endoplasmatic reticulum (**ER**) is shown in a lower (left panel) and a higher (right panel) magnification. Photos were taken for comparing studies between non-infected and infected cells.

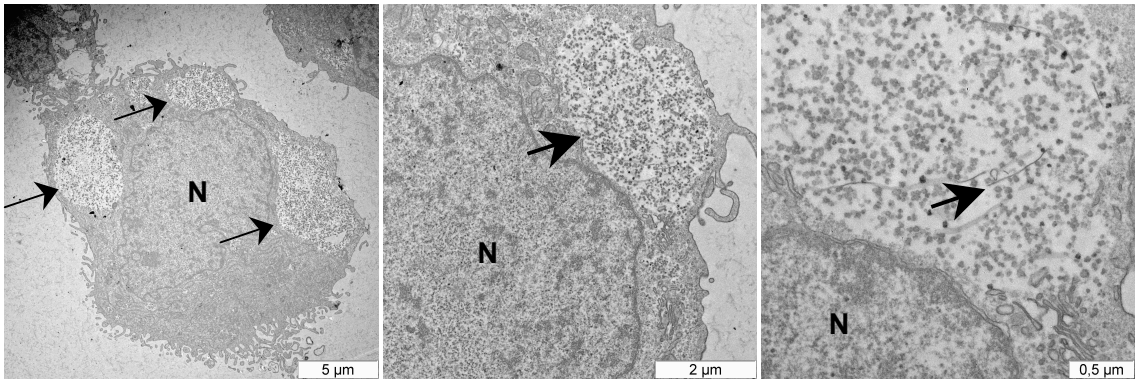

Figure 24. GLV-1h68 infected SKOV3ip.1 cell 24 hpi
This SKOV3ip.1 cell, infected with MOI 0.1, shows the presence of three morphologic separated viral fabrics called “Guarnierische inclusion bodies” within the cytoplasm (arrows). Three viral fabrics in increasing magnification from left to right are presented.

Viral inclusion bodies were first observed 24 hpi. Three viral fabrics besides the nucleus in the cytoplasm of the SKOV3ip.1 cell are shown (**arrows**). Often, more than one viral fabric was located in one cell as shown representatively in **Figure 24.**

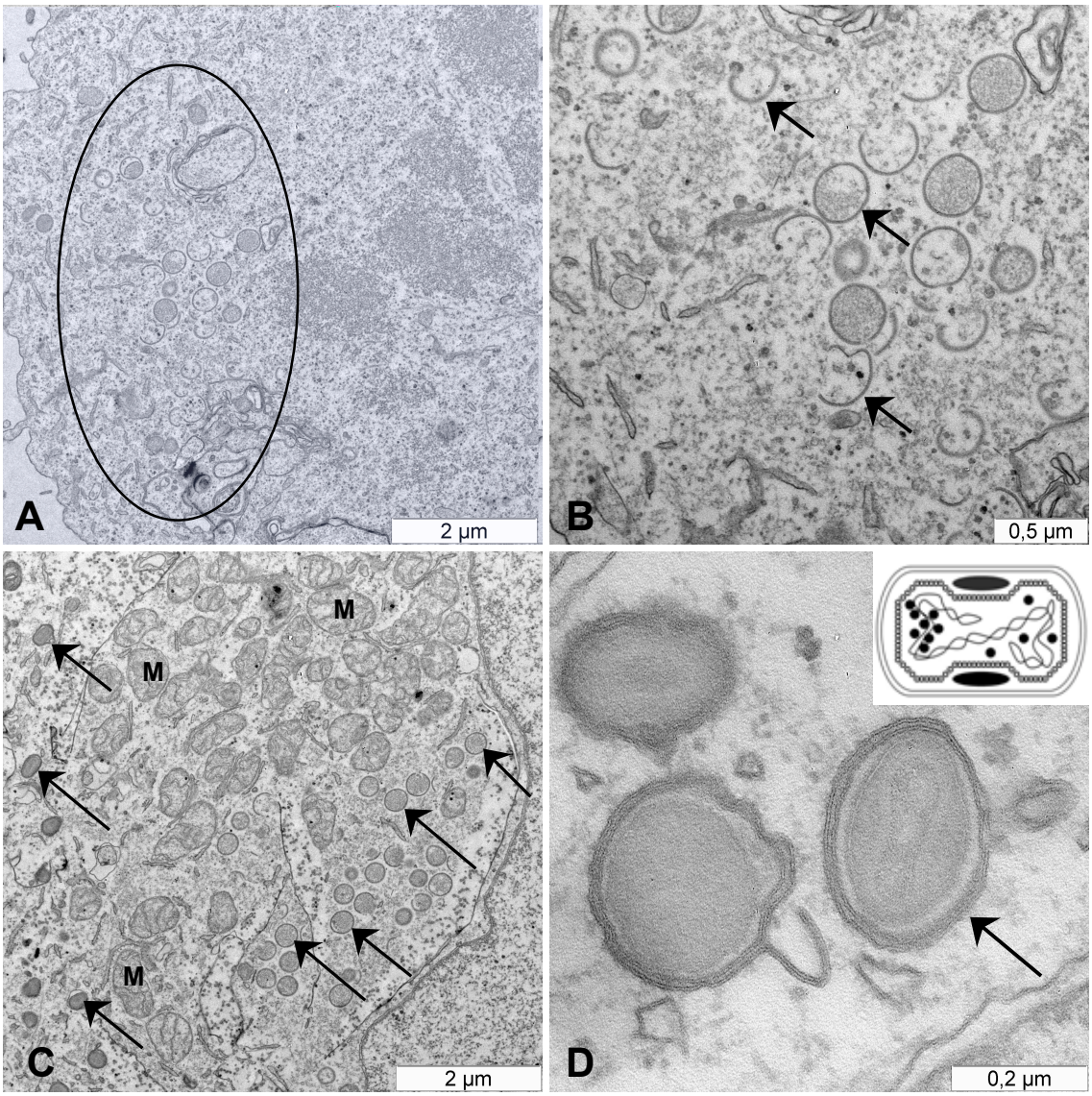

Figure 25. Viral replication in a SKOV3ip.1 cell 48 hpi with GLV-1h68 at MOI 0.1
Different assembly stages of viral particles in an infected SKOV3ip.1 cell were observed 48 hpi (**A**). Virus assembly starts with a semilunar membrane fragment which grows to a globular baby-virus (**B**). Afterwards, the electron dense nucleoprotein-complex which was produced before is incorporated into the semilunar membrane. The resulting particle is now called **IEV** = intracellular enveloped virion. In **C**, both IEVs (on the right) and further developed forms called **IMV** = intracellular mature virion of GLV-1h68 (left) are shown (arrows). In between the two viral particle stadia, mitochondria (**M**) are shown.
Image **D** shows three enlarged IMVs. One of those particles (arrow) already shows the typical biconcave core structure and the lateral bodies as it is seen in the schematic drawing of VACV (right upper corner).

48 hpi early and late stadia of virus assembly in SKOV3ip.1 cells could be observed (**A, B, C**). Three of the last stadium viral particles are shown in **D** at a high magnitude. The detail (**D**) shows the schematic configuration of an IMV virus particle.

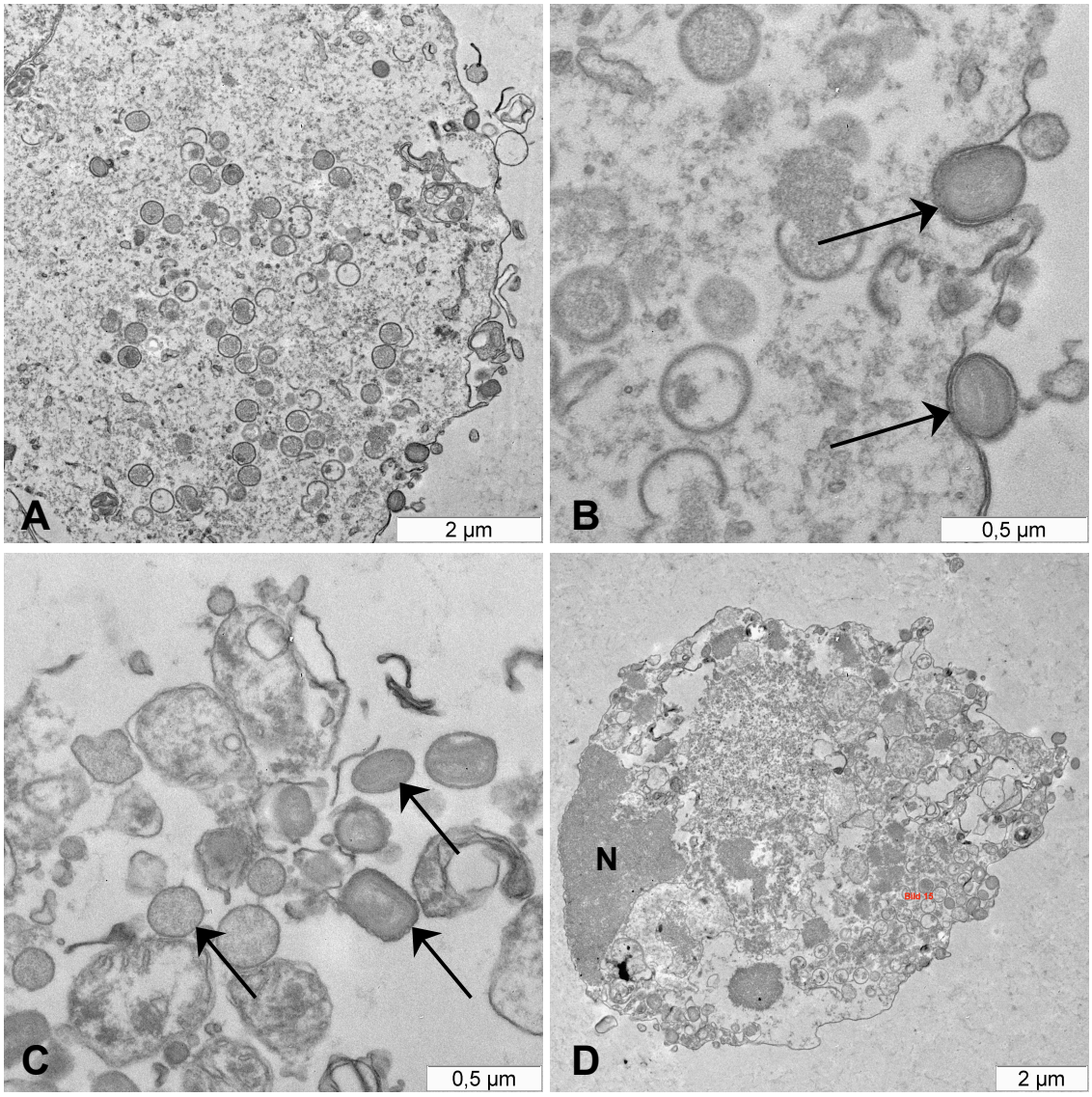

Figure 26. Virus-production in a GLV-1h68 infected SKOV3ip.1 cell at MOI 0.1 72 hpi
In **A** lots of pre-stage GLV-1h68 virions in the cytoplasm are shown. Next to the plasma membrane there are some IMVs (intracellular mature virions) which bud off the cell. Such a budding scene was magnified in **B**, where two IMVs bud off the infected cell. Released viral particles at different stages of development were observed (**C**). One IEV lies next to a typical brick-shaped virion and a not yet brick-shaped form (arrows). Due to virus infection a SKOV3ip.1 cell totally lost its original organization and integration. The nucleus (**N**) shows condensate chromatin and cell cytoplasm appears irregular and lost its uniformity (**D**).

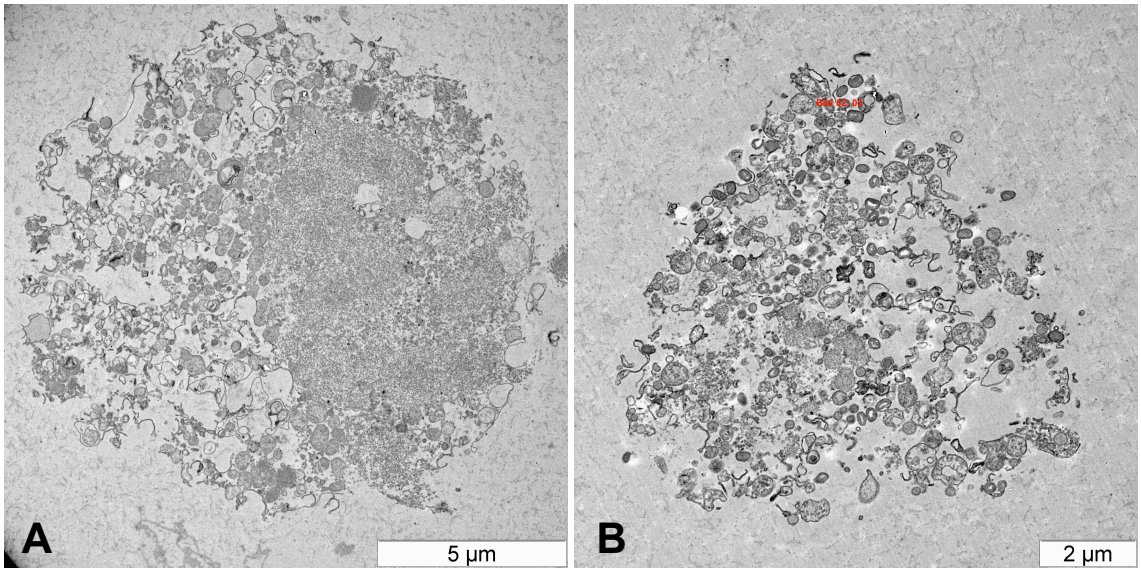

Figure 27. Apoptotic SKOV3ip.1 cells after virus production
SKOV3ip.1 cells collapsed 48 hpi (**A**) and 72 hpi (**B**) after successful release of the progeny virions.

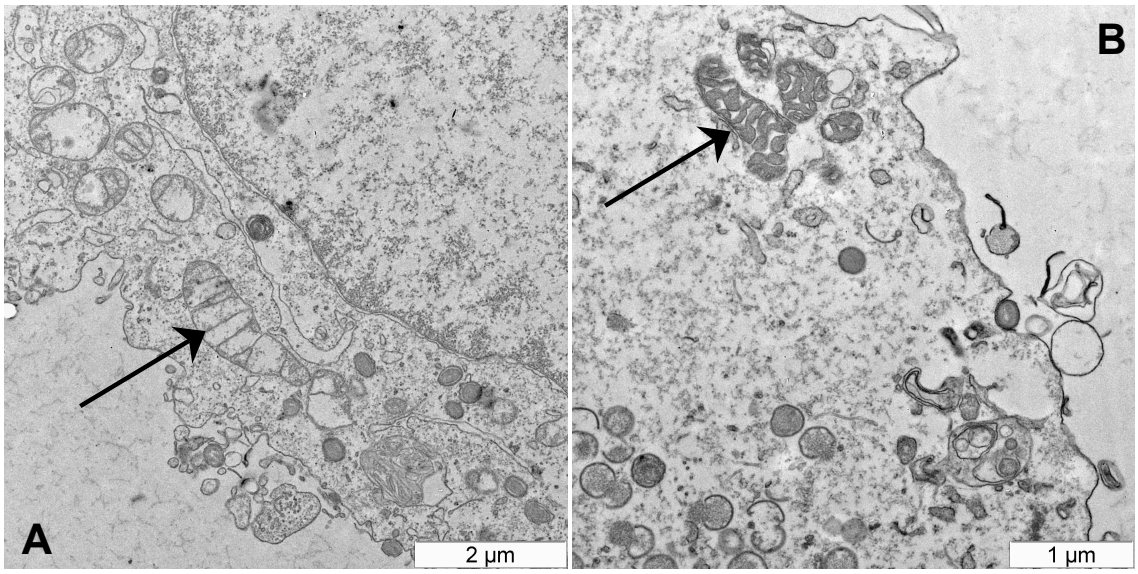

Figure 28. Apoptosis in virus infected SKOV3ip.1 cells
In infected cells, mitochondria show typical signs of apoptosis. Two different morphologic manifestations are shown (arrows).

3.1.2.2 GLV-1h68 replication in CC531s cells

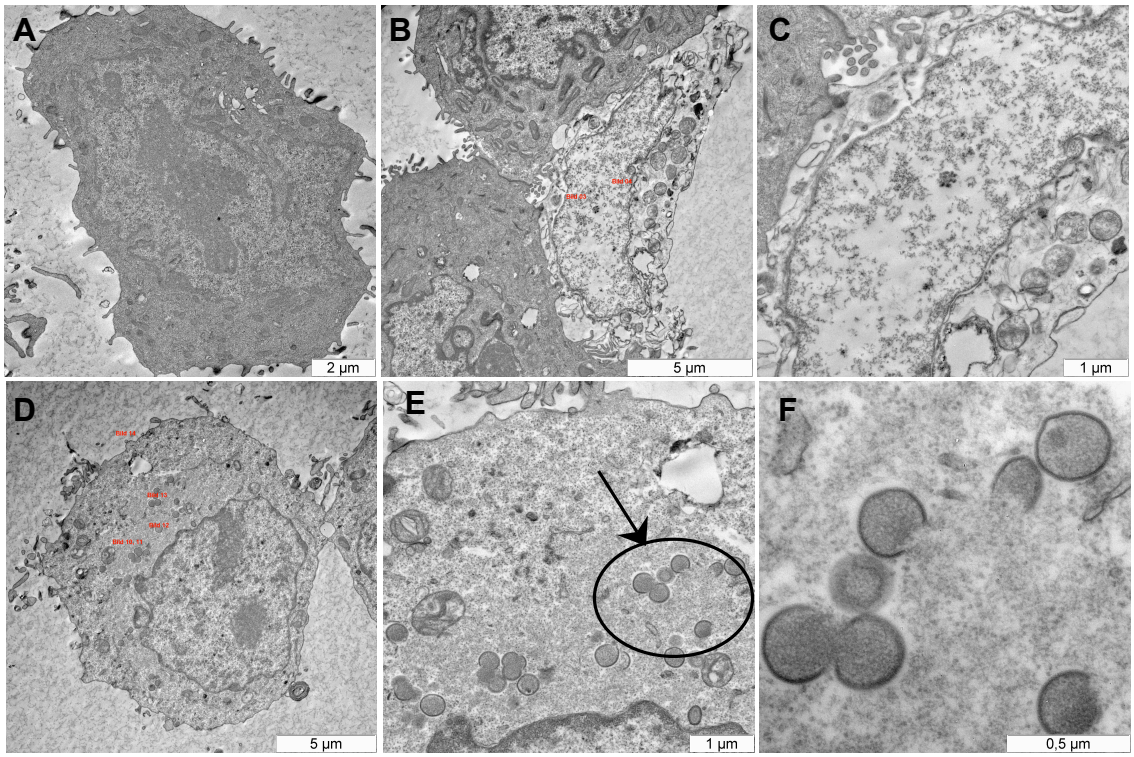

Figure 29. Virus production in CC531s cells infected with GLV-1h68 at MOI 0.1
CC531s cells were infected with GLV-1h68 at MOI 0.1 or remained uninfected. **A** shows a healthy mock infected CC531s cell. In **B**, 24 hpi a "virus fabric" containing viral proteins is shown on the right (arrow) and is magnified in **C**. Different assembly levels of virus particles are shown 24 hpi (**D, E** and **F**). The IEVs in **E** (arrow) are magnified in **F**.

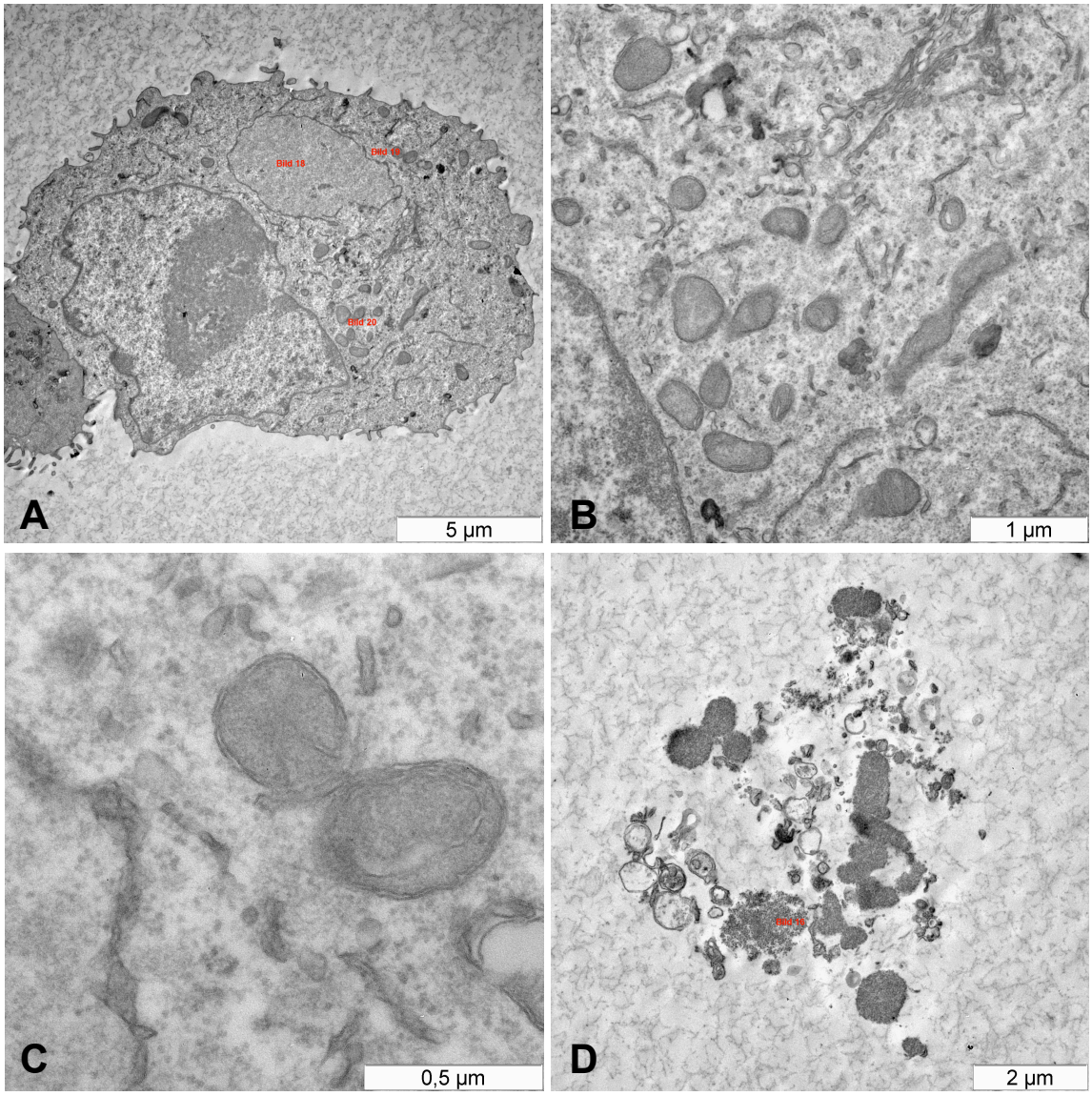

Figure 30. Virus-production in CC531s cells infected with GLV-1h68 at MOI 0.1 24 hpi
A, B and **C** show accumulations of mostly IMV-particles within the cytoplasm. The CC531s cell in **D** disintegrated after infection and viral production.

In order to find out more about morphologic steps of both MeV-SCD and GLV-1h68 replication behaviour, electron microscopy was performed. MeV-SCD replication was monitored in A673 and BRZ cells (**3.1.1**). GLV-1h68 replication was monitored in SKOV3ip.1 (**3.1.2.1**) and CC531s cells (**3.1.2.2**). We observed that GLV-1h68 and MeV-SCD differ a lot in morphology and size due to the difference in virus species (**1.3**, **1.4**). In case of GLV-1h68 specifically viral development stadia (**Figure 25** and **26**) became visible in contrast to MeV-SCD where simply viral fabrics (**Figure 20**) and mature virions (**Figure 22**) were observed.

Another reason we performed electron microscopy was to find out the reaction of infected cells to viral burden. All cell lines showed signs of cell death post infection. A673 cells showed clear signs of apoptosis such as chromatin condensation and autophagosomes (**Figure 20**). BRZ cells showed apoptotic characteristics like autophagosomes as well and we additionally observed syncytia formation as a typical reaction of cells infected with MeV-SCD (**Figure 21**). In SKOV3ip.1 cells, disintegration (**Figure 27**) and two types of apoptotic mitochondria were found 72 hpi with GLV-1h68 (**Figure 28**). CC531s cells had already lost their integrity 24 hpi (**Figure 30**).

Summing up, MeV-SCD and GLV-1h68 replication was successful in all cell lines and led to morphologically intact viral yield. CC531s cells died first 24 hpi with GLV-1h68 followed by A673, BRZ 72 hpi with MeV-SCD and SKOV3ip.1 cells 72 hpi with GLV-1h68. Classic apoptotic cell alterations were observed in all cell lines except CC531s.

3.2 Quantification of CD46 receptor molecules on tumor cells

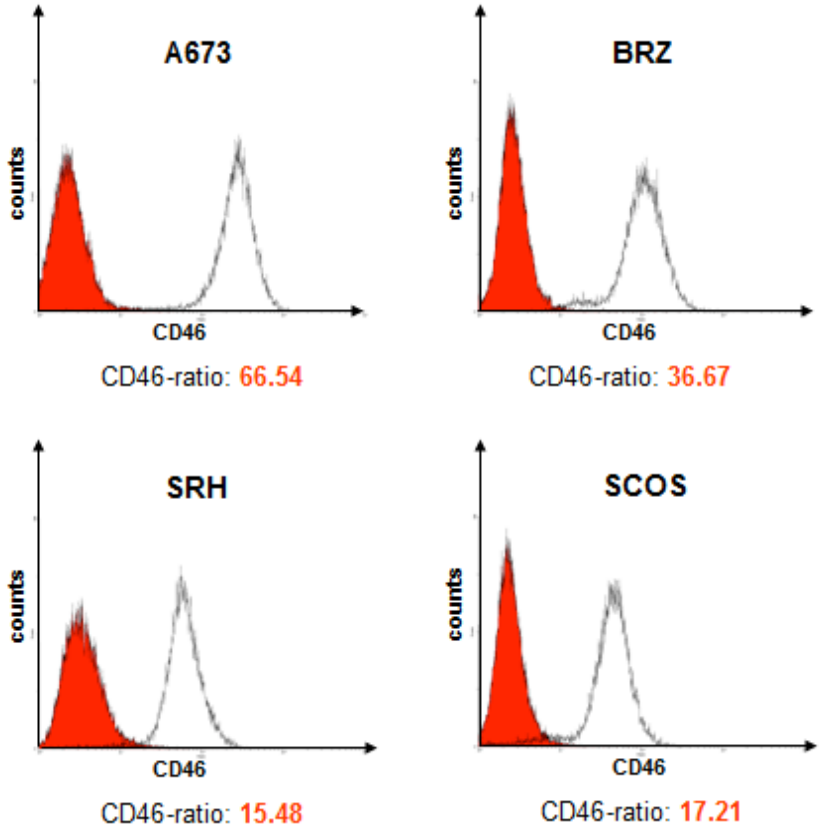

Figure 31. Flow-cytometric quantification of CD46 density on tumor cell surfaces
Cells were labeled with anti-CD46-PE antibody (**white** histogram) or incubated with an isotype control (**red** histogram) and were analyzed by flow cytometry. The ratio of the arithmetic mean fluorescence index of the white histogram: red histogram was calculated and indicated the CD46 expression level on cell surfaces. An arithmetic mean under 20 is considered as marginal CD46 expression on the cell surface. Analysis was done using ***winMDI*** software.

In order to determine the quantities of CD46 receptors on surfaces of tumor cell lines specifically addressed in this dissertation we performed cell cytometry. Tumor cells were labelled with a PE-linked anti-CD46-antibody or were incubated with an isotype control. Fluorescence exerted by PE (Phycoerythrin) was measured in flow cytometry (**3.12)**. Cell count of the isotype control is shown in the red histogram; anti-CD46-labeled cells are represented in the white histogram (**Figure 31**).

CD46 expression was detected on all tested cell lines but expression levels differed a lot. The ratio of the arithmetic mean of anti-CD46-stained cells/isotype control was calculated to quantify the CD46 expression level on cell surfaces. A673 cells had the highest CD46-receptor-density (ratio: **66.54**) followed by the BRZ cells (ratio: **36.67**). Of note, SRH cells (ratio: **15.48**) and SCOS cells (ratio: **17.21**) showed a ratio of under **20**, which was declared a sign of marginal CD46 expression.

3.3 Infection efficiency of MeV-GFP and GLV-1h68

3.3.1 Fluorescence monitoring shows successful infection with MeV-GFP

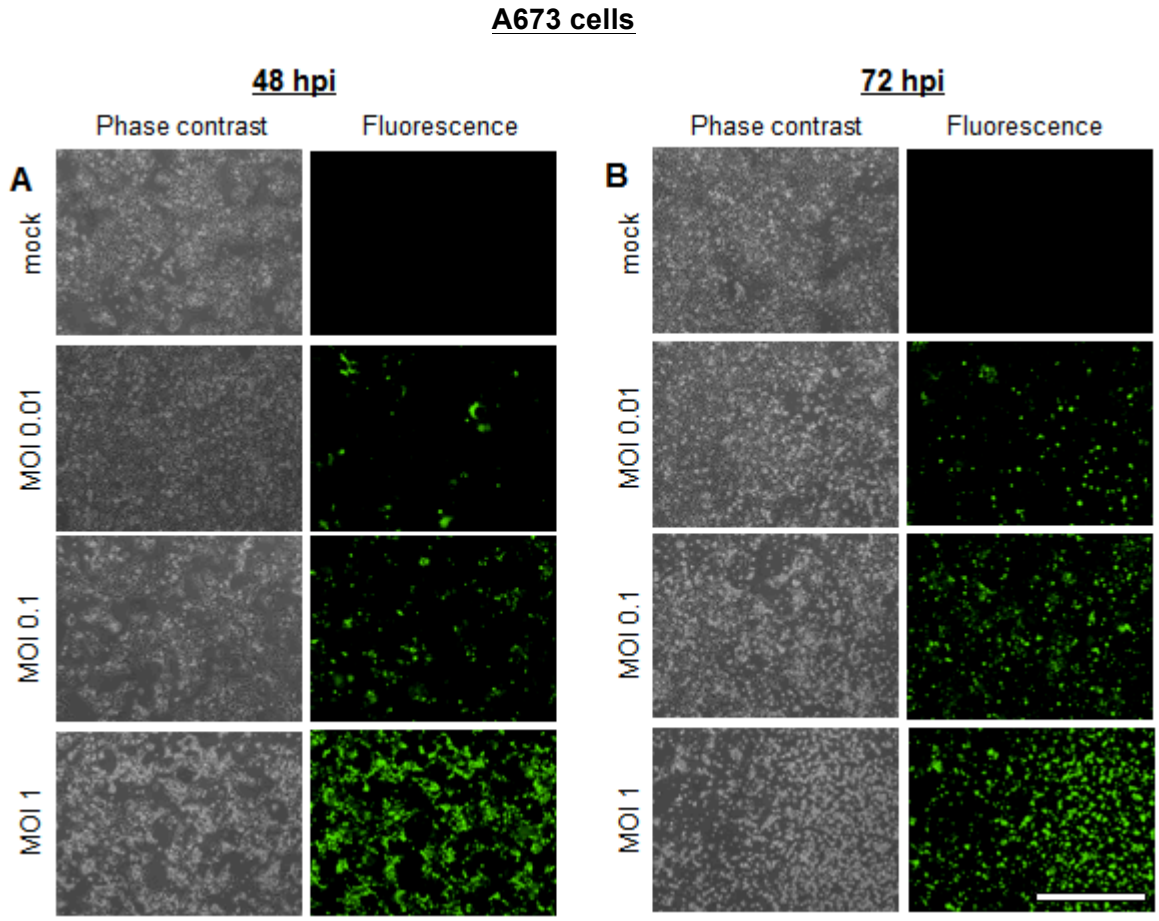

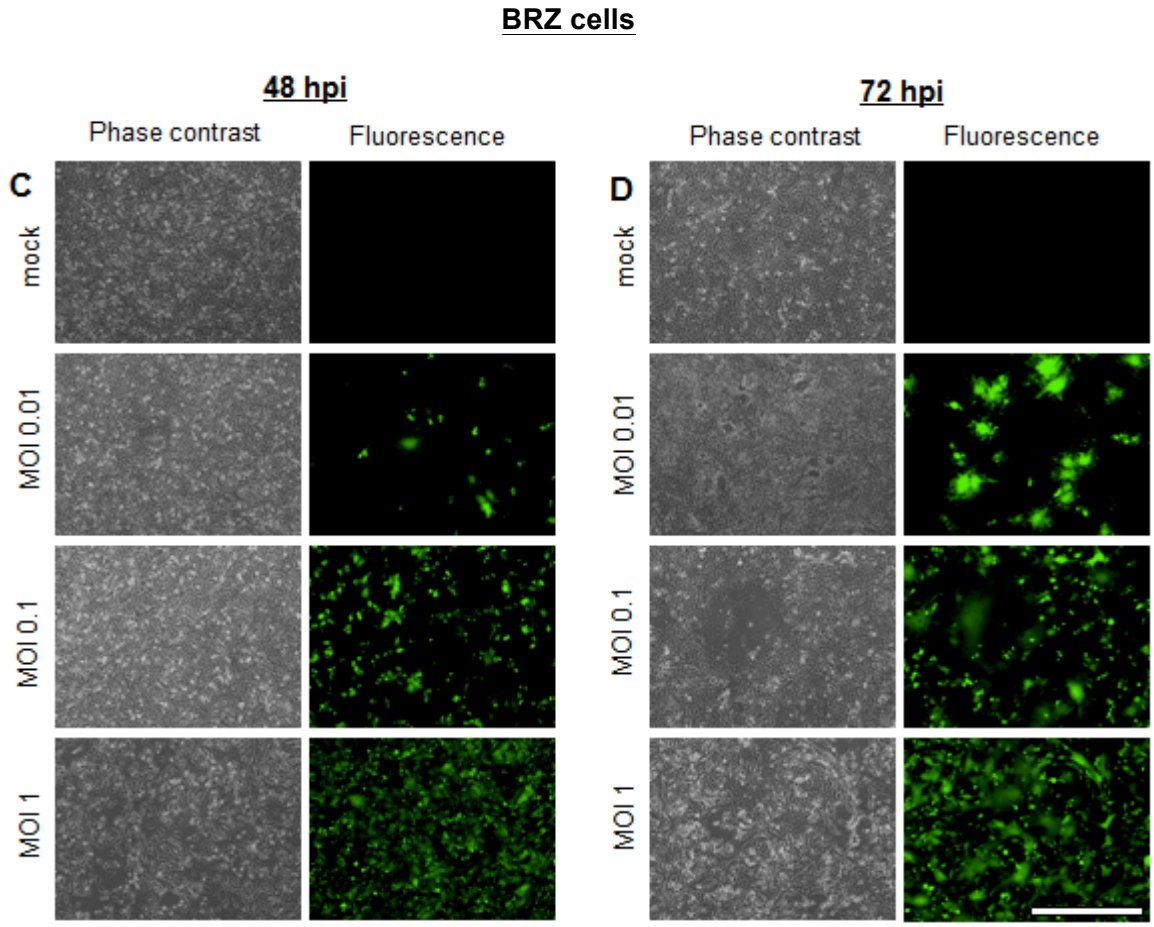

Figure 32. Monitoring of MeV-GFP-infection by fluorescence microscopy
A673 (**A, B**) and BRZ cells (**C, D**) were infected at MOI 0.01, 0.1 and 1 or were mock-infected. Serial phase contrast and corresponding fluorescence photos were taken 48 and 72 hpi at the same magnification. Measuring carriage (white) in the right lower corner represents 1000 µm. Mock-infected cells showed no green fluorescence whereas virus-infected cells showed increasing fluorescence intensity depending on the MOI. Both A673 and BRZ cells formed syncytia 48 hpi (**A, C**) and BRZ cells showed large syncytia formation 72 hpi (**D**).

To monitor infection of tumor cells, A673 and BRZ cells were infected with MeV-GFP which encodes the marker gene for green fluorescent protein (GFP).

In A673 cells (**Figure 32 A, B**) there was almost no fluorescence 48 hpi at MOI 0.01 and low fluorescence at MOI 0.1. At MOI 1, most cells were infected by MeV-GFP and emitted green fluorescence. Small syncytia formations were visible. At 72 hpi, most cells already had detached and showed the typical globular shape of dead cells. All cells showed green fluorescence.

In BRZ cells (**C, D**) only a small amount of cells was infected at MOI 0.01. More cells showed green fluorescence at MOI 0.1 and almost every cell was infected at MOI 1.

72 hpi, all fluorescence photos were dominated by large multinuclear syncytia formations. Some scattered syncytia formations were visible at MOI 0.01, but most of the BRZ cells had not been infected yet. Syncytia formation was increased at MOI 0.1. In the corresponding phase contrast photo one large syncytium can be seen in the middle of the photo. The highest syncytia count occurred in cells infected with the highest MOI (MOI 1).

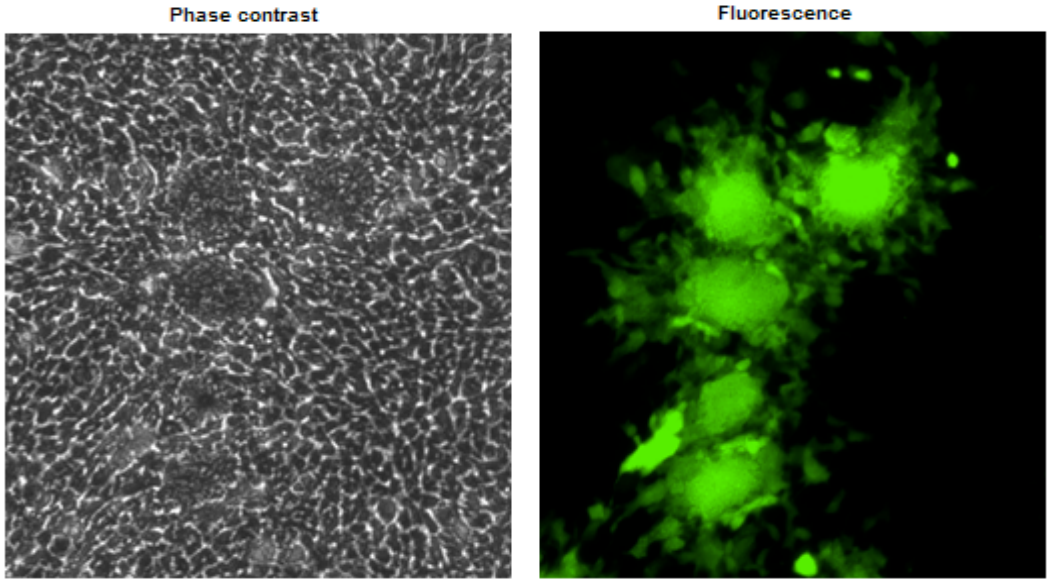

Figure 33. Large syncytia-formation of BRZ cells after MeV-SCD-infection
BRZ cells were infected with MeV-SCD at MOI 0.01. At 72 hpi phase contrast and fluorescence photos were taken. The photos are presented in a high magnification. In the middle of the photos five large syncytia are shown.

3.3.2 Expression of SCD in A673 and BRZ cells in Western blot analysis

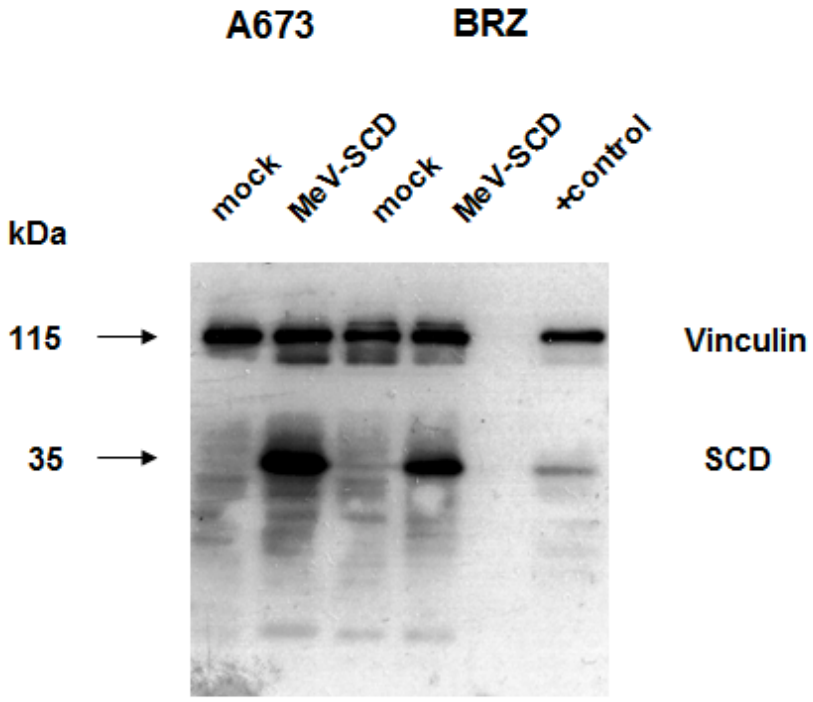

Figure 34. Western blot analysis of SCD expression in A673 and BRZ cell lysates
Tumor cells were either infected with MeV-SCD at MOI 0.1 or mock-infected. 75 µg protein (established in Bradford dye assay) of each sample were separated by 12% SDS-PAGE. Western blot analysis was done using antibodies raised against SCD and Vinculin. The stably transfected hepatoma cell line **MH-SCD** was used as a positive control (**+ control**). The Vinculin-band was detected at the molecular size of 115 kDa; the SCD band was detected at 35 kDa. Both A673 and BRZ cells were infected by MeV-SCD and were found to express the virus encoded transgenic protein SCD. The SCD-band of A673 cells showed a higher amount of SCD expression. No SCD-band was detected in the samples of the mock-infected A673 and BRZ cells (negative controls).

Western Blot analysis was done with both A673 and BRZ cells uninfected and infected with MeV-SCD. The stably transfected hepatoma cell line MH-SCD was used as a positive control. In the mock-infected samples of A673 and BRZ cells, no SCD band was detected. Both MeV-SCD infected samples of A673 and BRZ cells showed a clearly detectable SCD-specific band at 35 kDa. The SCD-band of infected A673 cells was more pronounced than the SCD-band in infected BRZ cells. In summary, firstly SCD was expressed in both examined tumor cell lines and secondly expression of SCD in infected A673 cells was higher than in BRZ cells, which was due to the higher SCD expression in A673 cells than in BRZ cells.

3.3.3 Relative green fluorescence intensity shows successful infection with GLV-1h68

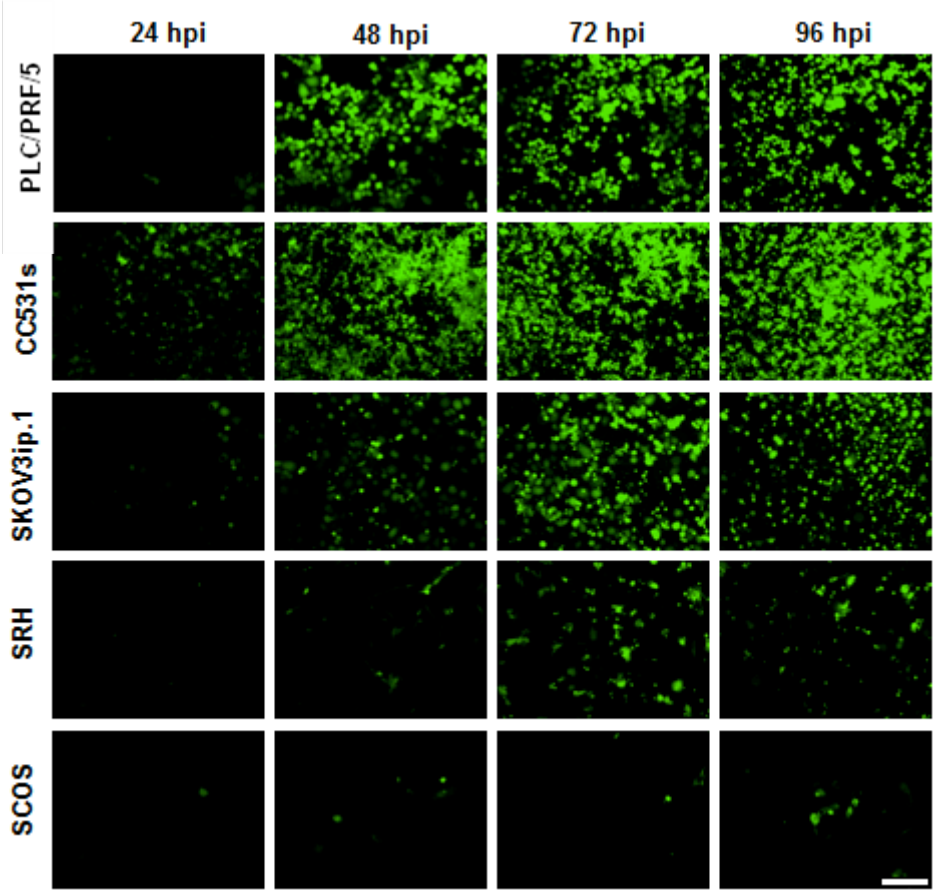

Figure 35. GFP-monitoring of fluorescence intensity in GLV-1h68 infected cell lines
PLC/PRF/5, CC531s, SKOV3ip.1, SRH and SCOS tumor cells were infected with GLV-1h68 at MOI 0.1. GFP-expression was monitored over 96 hpi. All photos were taken at the same magnification. The measuring carriage (white) in the lower right corner represents 200 µm. All cell lines showed green fluorescence of different extent as a sign of infection by GLV-1h68.

The tumor cell lines were infected with GLV-1h68 as described in **3.3.1**. To monitor the process of infection, a series of fluorescence photos was taken 24, 48, 72 and 96 hpi. It is obvious that all the tested cell lines, PLC/PRF/5, CC531s, SKOV3ip.1, SRH and SCOS were infected by GLV-1h68 and expressed the green fluorescent reporter protein. 24 hpi, there was almost no green fluorescence except in CC531s cells. 48 hpi PLC/PRF/5, CC531s and SKOV3ip.1 cells showed high intensities of green fluorescence throughout the infected wells. SRH and SCOS were also infected but only little green fluorescence was visible. Green fluorescence in SKOV3ip.1 and SRH cells increased 72 hpi. 96 hpi all cell lines emitted green fluorescence in different

intensities. CC531s cells expressed most GFP followed by SKOV3ip.1 and PLC/PRF/5 cells. SRH and SCOS expressed less GFP than the other tumor cell lines which can be explained by the lower cell division rate which was monitored in phase contrast microscopy (data not shown). Summing up, infection with GLV-1h68 and subsequent GFP expression was successful in all tested tumor cell lines.

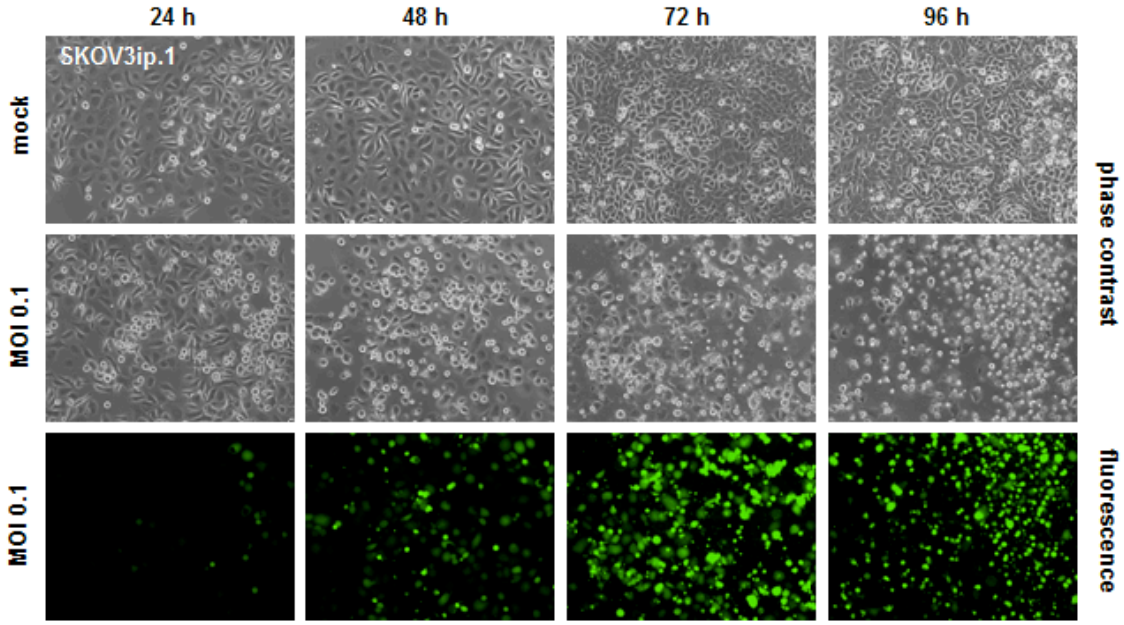

Figure 36. Measurement of infection kinetics in GLV-1h68 infected SKOV3ip.1 cells
SKOV3ip.1 cells were infected with GLV-1h68 at MOI 0.1 or remained uninfected. Both phase contrast and fluorescence photos were taken at different time points at the same magnification. The mock-infected cells grew to confluence (phase contrast) whereas the GLV-1h68 infected cells died and detached. The fluorescence photos show successful infection of SKOV3ip.1 cells already visible at 24 hpi as green fluorescence.

To visualize the progression of infection in SKOV3ip.1, cells were monitored in corresponding phase contrast and fluorescence photos (**Figure 36**). While the uninfected SKOV3ip.1 cells grew more and more confluent, an increasing number of the cells infected at MOI 0.1 died and detached from the bottom of the wells. Green fluorescence intensity and the amount of infected cells rose during the first 72 hpi. 96 hpi most of the cells had detached (as indicated by their globular shape) but still emitted green fluorescence. To differentiate between dead and vital cells we took advantage of the fact that dead cells have a dark colour whereas vital cells are light-coloured in phase contrast microscopy.

3.3.4 Visualization of β-galactosidase-expression by X-Gal-conversion confirms the results of successful infection with GLV-1h68

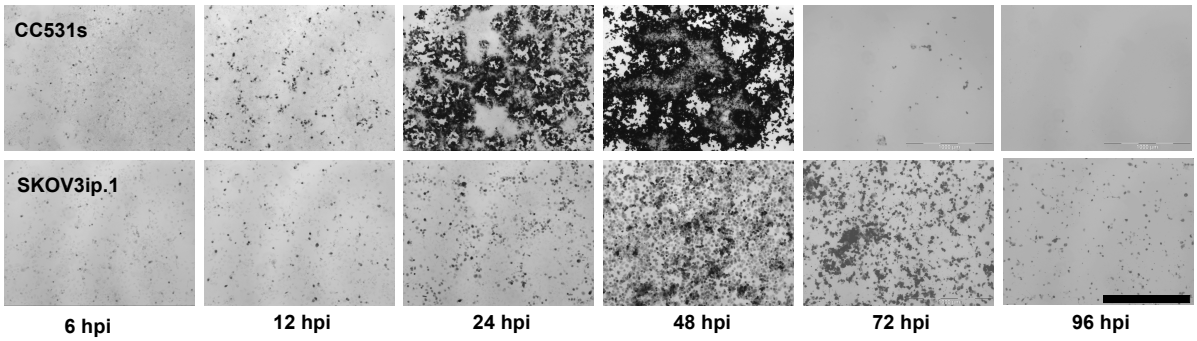

Figure 37. X-Gal-staining of GLV-1h68 infected cells
CC531s and SKOV3ip.1 cells were infected with GLV-1h68 at MOI 0.1. Brightfield photos were taken 6, 12, 24, 48, 72 and 96 hpi. All photos were taken in the same magnification; the measuring carriage (black) in the right lower corner represents 1000 µm. Both cell lines showed increasing marker gene expression as a sign of successful infection. In CC531s cells, *β*-galactosidase (*β*-gal) activity was detectable earlier than in SKOV3ip.1 cells and ended 72 hpi. *β*-gal-expression in SKOV3ip.1 cells also peaked 48 hpi but lasted until 96 hpi.

In

Figure 37 brightfield photos of X-Gal stained GLV-1h68 infected CC531s and SKOV3ip.1 are shown. 6 hpi, there is only little *β*-galactosidase (*β*-gal) activity. 12 hpi, some more cells already expressed the marker gene *β*-gal and consequently appeared in the typical indigoid blue dye. During the next 12 hpi there was a different development in terms of color intensity between the two cell lines. 24 and 48 hpi the blue dye spread “explosively” within the CC531s cells, which were still adherent to the respective well. The color-appearance of the SKOV3ip.1 cells had hardly changed until 24 hpi. Widespread *β*-gal-expression had started 48 hpi resulting in a strong blue staining. 72 hpi CC531s cells had completely detached whereas SKOV3ip.1 cells still expressed *β*-gal and were stained blue until 96 hpi, when most of the SKOV3ip.1 cells had also detached and color intensity declined to a minimum. Summing up, GLV-1h68 infection was successful in both CC531s and SKOV3ip.1 cells monitored by the marker-gene expression using X-Gal staining.

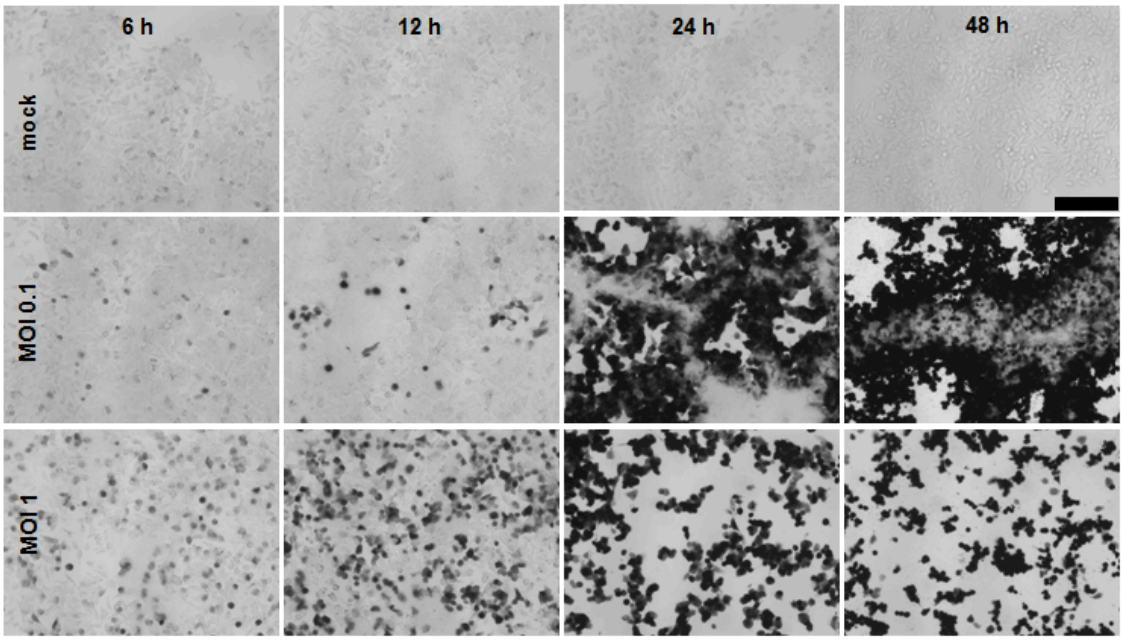

Figure 38. *β*-galactosidase expression of GLV-1h68-infected CC531s cells
CC531s cells were infected with GLV-1h68 at MOI 0.1 and 1 or remained uninfected. The brightfield photos were taken at the same magnification; measuring carriage (black) in the right upper corner represents 200 µm. Mock-infected cells showed marginal blue color due to background activity. *β*-gal expression in cells infected with MOI 0.1 increased explosively 24 hpi, so most of the cells were stained blue at this time point. The cells which had been infected at MOI 1 also showed increasing marker gene expression which decreased again 48 hpi because of cell death.

To obtain a comparison between the treatment with MOI 0.1 and MOI 1, CC531s cells were infected with both MOI 0.1 and 1. Then, X-Gal-staining was performed 6, 12, 24 and 48 hpi. 12 hpi, infection had widely spread within the CC531s cells infected with MOI 1 visible by the blue-stained cells. 24 hpi the rest of the still viable cell layer expressed *β*-gal and was stained blue. Further washing and staining steps led to a decreased number of cells which were stained blue at 48 hpi. This observation can be explained by the fact that blue staining was due to *β*-gal activity which is equivalent to effective viral infection and cell death leading to cell detachment as a consequence.

In cells infected with MOI 0.1, *β*-gal expression was marginal at 12 hpi but increased to a high expression level at 24 and 48 hpi. There were a high number of infected cells which expressed *β*-gal and were consequently stained blue. Cells still clung to the bottom of the plate at this time point. Infection with GLV-1h68 at MOI 1 led to an earlier cell death of CC531s cells which became apparent in the higher intensity of X-Gal staining in cells infected with MOI 0.1.

We observed that a lower MOI 0.1 led to an effective viral spread and less direct cell death until 48 hpi whereas higher MOI 1 obviously infected and killed cells before they were able to spread. *β*-gal expression was observed earlier and GLV-1h68 spreading was self-limited because most of the cells had died at 48 hpi.

3.4 Replication behaviour of MeV-SCD and GLV-1h68

3.4.1 Growth curve of MeV-SCD in A673 and BRZ cells

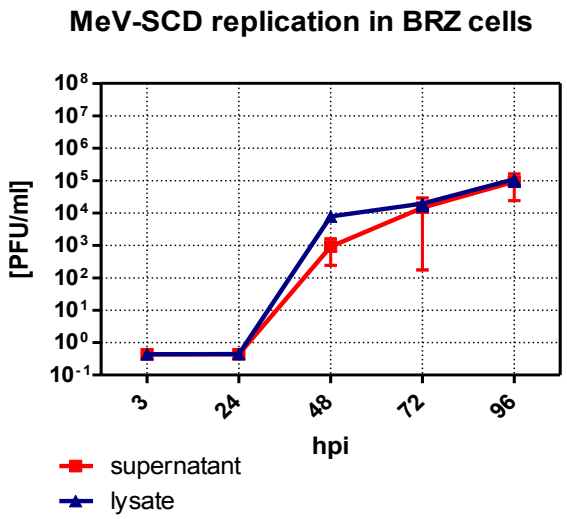

supernatant	
hpi	titer
3	4.41E-01
24	4.41E-01
48	9.21E+02
72	1.46E+04
96	9.20E+04

lysate	
hpi	titer
3	4.41E-01
24	4.42E-01
48	7.88E+03
72	1.95E+04
96	1.10E+05

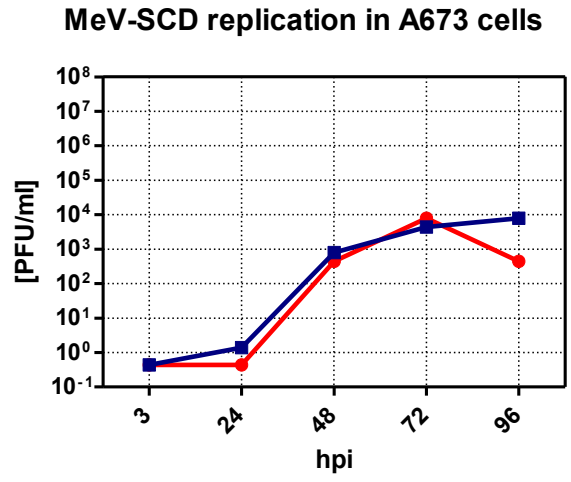

supernatant	
hpi	titer
3	4.40E-01
24	4.40E-01
48	4.40E+02
72	7.90E+03
96	4.40E+02

lysate	
hpi	titer
3	4.40E-01
24	1.40E+00
48	7.90E+02
72	4.40E+03
96	7.90E+03

Figure 39. MeV-SCD replication in A673 and BRZ cells
A673 and BRZ tumor cells were infected with MeV-SCD at MOI 0.03. Supernatants and lysates were harvested 3, 24, 48, 72 and 96 hpi and the amount of resulting viral yield was detected by standard titration in Vero cells. Data show one representative experiment of MeV-SCD replication in A673 and the mean of two independent experiments in BRZ cells. Error bars show SD. Viral titers are represented in the tables on the right.

In order to quantify viral replication in A673 and BRZ cells we performed growth curves of MeV-SCD. Replication behaviour was measured over a time span of 96 hpi. During the first 24 hpi there was hardly an increase in viral count. Between 24 and 48 hpi the number of viral particles increased by a factor of 10^3 in both cell lysates and supernatants. Thereafter, the virus replication in both cell lines nearly stagnated but reached a maximum viral yield of almost 10^4 PFU/ml in lysate 96 hpi and in supernatant 72 hpi in A673 cells. In BRZ cells, viral titers increased up to a maximum of about 10^5 PFU/ml in both supernatant and lysate. This was a tenfold higher production of viral particles in supernatant and a 100-fold higher virus production detected in cell-lysates in BRZ cells than in A673 cells 96 hpi. Viral replication in both cell lines led to a straight viral titer increase to 10^7 PFU/ml in case of A673 cells and to approximately $2x10^5$ PFU/ml in BRZ cells (cell-supernatant and cell-lysate in addition).

3.4.2 Growth curve of GLV-1h68 in CC531s and SKOV3ip.1 cells

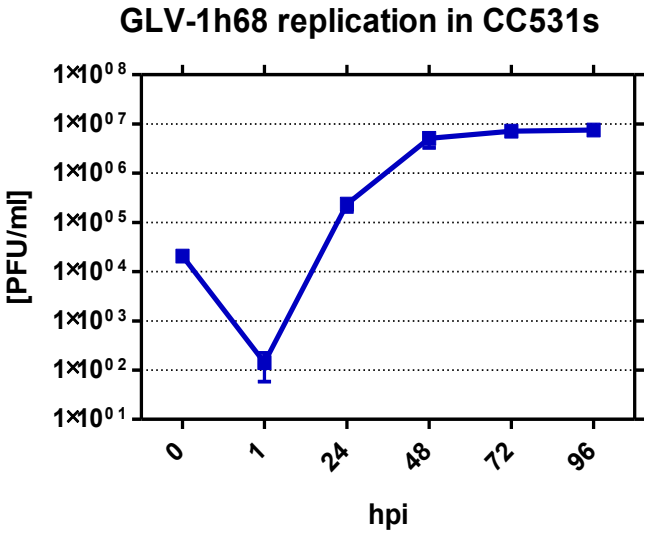

hpi	titer [PFU/ml]
0	2.08E+04
1	1.42E+02
24	2.37E+05
48	5.08E+06
72	7.18E+06
96	7.58E+06

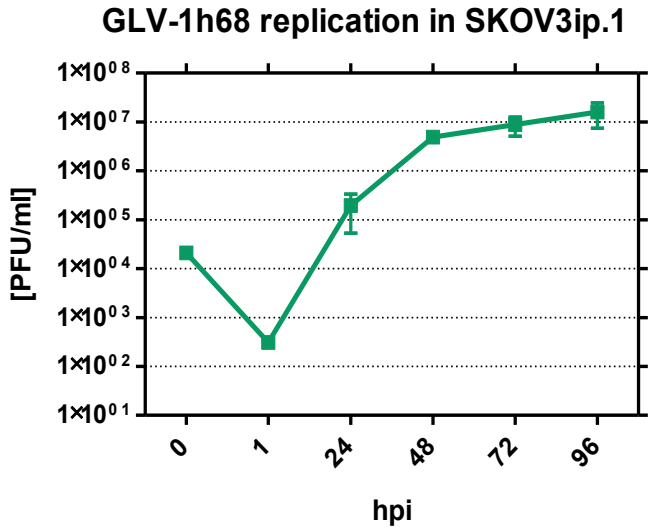

hpi	titer [PFU/ml]
0	2.09E+04
1	3.10E+02
24	1.94E+05
48	4.93E+06
72	8.82E+06
96	1.59E+07

Figure 40. Replication behaviour of GLV-1h68 in CC531s and SKOV3ip.1 cells
CC531s and SKOV3ip.1 cells were infected with GLV-1h68 at MOI 0.1. The rest of the inoculum was frozen immediately post infection at -80°C and the cells containing the viral yield were harvested and frozen 1, 24, 48, 72 and 96 hpi. All samples underwent three freeze-thaw-cycles and virus titration was performed on CV-1 cells. Diagrams show the mean of three independent experiments, error bars represent SD. Exact viral titers are shown in the corresponding tables on the right.

As previously done with MeV-SCD replication behaviour of GLV-1h68 was analyzed in growth curves. Viral replication started immediately post infection (1 hpi) and increased by the factor 10^3 within the first 24 hpi in CC531s cells. 48 hpi, a viral titer of 5.08E+06 PFU/ml was detected by viral plaque count. Viral

replication nearly reached a plateau and a maximal viral titer was measured 96 hpi as 7.58E+06 PFU/ml.

GLV-1h68 replication behaviour in SKOV3ip.1 cells was similar. The number of viral particles increased most strikingly during the first 24 hpi to a titer of 1.94E+05 pfu/ml. As it was seen in CC531 cells, virus production continued to increase tenfold during the next 24 hours and almost stagnated during the last 48 hpi. The highest titer of 1.59E+07 PFU/ml in SKOV3ip.1 cells was detected 96 hpi. Summing up we could observe that viral replication started without delay immediately post infection and resulted in high titer-increase which is quite typical for vaccinia virus infections.

3.5 Measurement of cytotoxic effects of virus-infection

3.5.1 Suicide gene plus 5-FC enhances the cytotoxic effect of MeV-SCD

3.5.1.1 A673 and BRZ cells were susceptible to 5-FU treatment

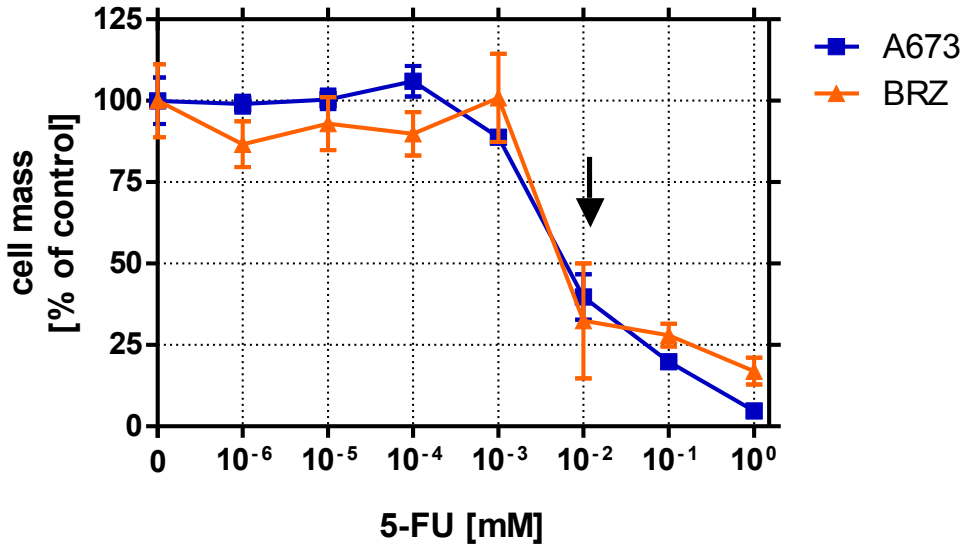

Figure 41. 5-FU treatment of tumor cell lines to ensure susceptibility
5-FU treatment of A673 and BRZ cells was performed to detect the susceptibility to the common chemotherapeutic 5-FU. Cells were treated with increasing concentrations of 5-FU and cell mass in % of control was measured 72 hpi by SRB assay. One representative of three independent experiments performed in triplicates is shown. Error bars represent SD. Both A673 and BRZ cells were sensitive to 5-FU and cell mass started visible decrease at the 5-FU-concentration of 10^{-2} mM (**arrow**).

Before starting the suicide gene therapy with MeV-SCD combined with the prodrug 5-FC, the cell lines A673 and BRZ were tested for susceptibility to 5-FU, the toxic metabolite of the harmless prodrug 5-FC. Susceptibility to 5-FU was considered a precondition for suicide gene and 5-FC treatment. Approximately all A673 cells survived the treatment with increasing concentrations of 10^{-6}-10^{-3} mM 5-FU and cell mass had hardly decreased. Treatment with 10^{-2} mM 5-FU reduced the cell mass to about 35% and the highest concentration of 1 mM 5-FU led to a remaining cell mass of about 5% of control.

BRZ cells showed the same phenomenon under the treatment at the lower concentrations 10^{-6}-10^{-3} mM 5-FU. Cell mass decreased from 100% to 30% of control after treatment with 10^{-2} mM 5-FU. Increasing concentrations of 10^{-1} and

1 mM 5-FU led to a remaining cell mass of only 15% of control. Thus both A673 and BRZ cells were susceptible to 5-FU. The minimal effective dose of 5-FU was at a concentration of 10^{-2} mM 5-FU.

3.5.1.2 Examination of MeV-SCD cytotoxicity in A673 and BRZ cells

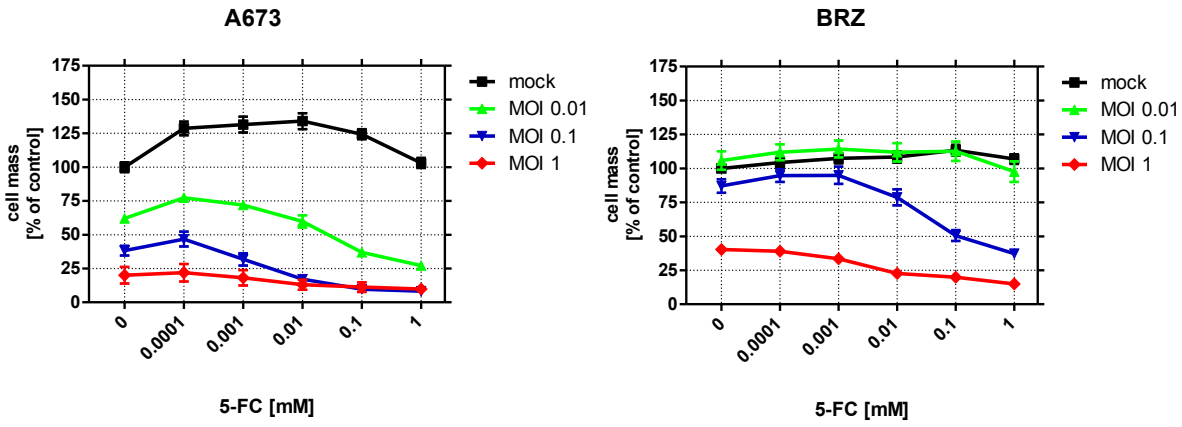

Figure 42. Measurement of A673 and BRZ cell mass decrease after MeV-SCD infection
SRB-assay was performed to assess cell viability of A673 and BRZ cells after infection with MeV-SCD combined with 5-FC treatment. Values are presented as percentages of uninfected controls, which represent 100% cell viability. Mean of three independent experiments performed in quadruplicates with both A673 and BRZ cells are shown, error bars display SEM. A673 cells died under the combination treatment with all three MOIs. BRZ cells died to a significant lower extent and cells treated with MOI 1 were only reduced to 20% of control by the combination with the highest concentration of 1 mM 5-FC.

As it was shown in the previous experiment, A673 and BRZ cells were susceptible to 5-FU. Cell viability post MeV-SCD infection was measured using SRB-assay (

Figure 42).

The sole treatment with 5-FC neither had an effect on A673 cells nor on BRZ cells (100% cell mass remaining). The sole treatment with MeV-SCD showed little response at MOI 0.01 and 0.1 in BRZ cells whereas the highest MOI 1 led to massive cell mass reduction. A673 cell mass was more affected by MeV-SCD treatment alone. With MOI 0.01, almost half of the cells were killed, the use of MOI 0.1 led to a reduction of cell mass of about 60% of control and MeV-SCD at the highest MOI 1 killed almost 80% of the cells without utilizing the suicide gene function.

The addition of increasing concentrations of 5-FC resulted in a visible improvement of cell-killing except for MeV-SCD at MOI 0.01 in BRZ cells and MeV-SCD at MOI 1 in A673 cells. BRZ cell mass treated with MOI 0.01 was not affected by the dose escalation of 5-FC and stayed the same as in the untreated control. At MOI 1 A673 cell mass was strongly reduced by MeV-SCD alone and the addition of 5-FC had only marginal effect.
1 mM 5-FC led to a successful cell-mass-reduction in combination with MeV-SCD treatment at MOI 1 in BRZ cells and at all MOIs in A673 cells.

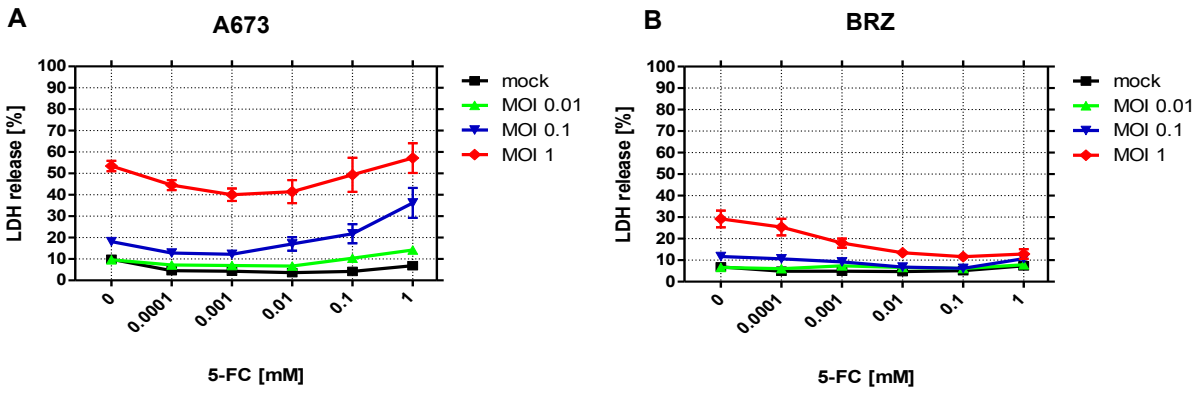

Figure 43. Cytotoxic effect of MeV-SCD and 5-FC on A673 and BRZ cells in vitro
LDH assay was performed to show the cell lysis caused by MeV-SCD in combination with the prodrug 5-FC. Measurement took place 96 hpi using LDH-release as a cell death marker. Results were calculated as indicated in **3.10.2**. Data represent mean of three (**A**) and four (**B**) independent experiments performed in quadruplicates. Error bars represent SEM.
The treatment with MOI 0.01 led to minimal LDH-release in both cell lines similar to the LDH-release in mock infected cells. A673 cells exhibited strong LDH-release at MOI 1 and to a lower extent at MOI 0.1. BRZ cells in contrast showed only little and paradoxical response to the treatment with the inserted 5-FC concentrations.

To confirm the data obtained from SRB assay, LDH-release assay was performed. Whereas SRB assay gives an overview of cell mass reduction, LDH assay measures LDH activity caused by cell death related LDH-release less background LDH activity.
Mock-infected A673 cells showed minimal LDH-release as a matter of basal cell death within 96 hours. Cells infected with MeV-SCD at MOI 0.01 showed no difference in LDH-release in comparison with mock-infected cells whereas cells infected with MOI 0.01 in combination with 5-FC showed a minimally increased LDH-release compared to mock-infected cells. Infection with MeV-SCD at MOI 0.1 led to an increase in LDH-release to nearly 20% and the addition of 5-FC

led to a LDH-release of nearly 40%. Infection with MOI 1 resulted in almost 55% LDH-release and could be increased to nearby 60% using 1 mM 5-FC additionally.

LDH-release in mock-infected and in BRZ cells infected with MOI 0.01 and 0.1 was almost the same extent. Infection with MeV-SCD at MOI 1 showed a paradox LDH-release response in all four independent experiments. With regard to SRB assay results we had expected increasing LDH-release following increasing MOI and 5-FC concentration. Contrary to our expectation, LDH-release actually increased with rising MOIs but decreased with rising 5-FC concentrations.

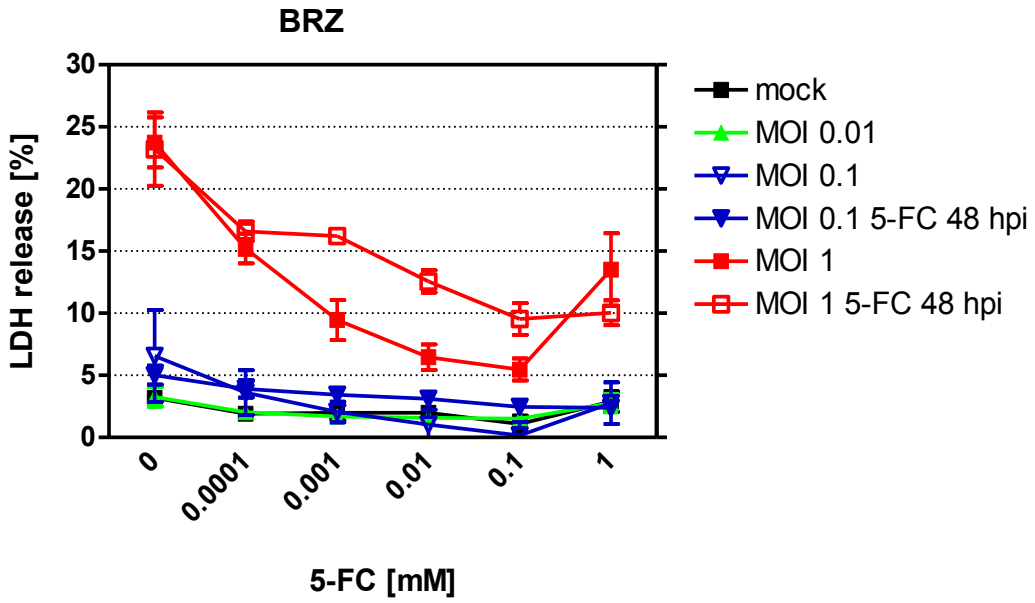

Figure 44. Alternative treatment of BRZ cells with 5-FC 48 hpi to enhance viral replication
To lengthen the process of viral replication in BRZ cells, 5-FC was added 48 hpi as an alternative to 5-FC treatment ab initio. There was no significant change in LDH-release compared to the previous experiments. One independent experiment is shown, error bars represent SD. The labelling of the Y-axis was shortened to 30% instead of 100% LDH-release.

As it has been shown that addition of prodrug immediately after infection can inhibit virus replication and thus lead to reduced cytotoxic effects (Ungerechts et al., 2007), an alternative protocol where 5-FC was added at 48 hpi was tested. But the results shown in **Figure 44** indicate that no significant change in LDH-release was detected. Infection with MeV-SCD at MOI 0.01 and 0.1 without prodrug and MOI 0.1 plus 5-FC 48 hpi only led to minimal LDH-release and

treatment with MOI 1 alone and MOI 1plus 5-FC 48 hpi amounted to the same. The addition of 5-FC 48 hpi did not lead to an improvement in terms of cytotoxicity.

3.5.1.3 SRH cells showed strong resistance phenomena to MeV-SCD treatment

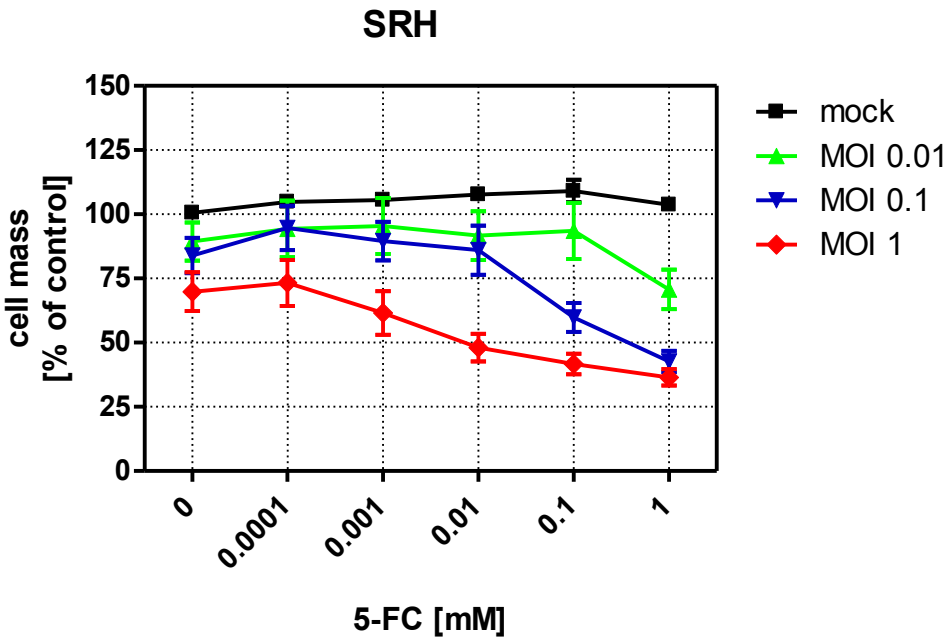

Figure 45. SRH cells survived MeV-SCD treatment with high MOI 1
SRH cells were infected with MeV-SCD at MOI 0.01, 0.1 and 1 or remained uninfected. Cell mass was measured using SRB assay. Data show the mean of three independent experiments, error bars represent SEM. The treatment with MeV ld-SCD alone (0 mM 5-FC) revealed primary resistance to MeV-SCD as more than 50% of the cells survived. The combination treatment of MeV ld-SCD with a maximum concentration of 1 mM 5-FC led to a cell mass reduction of about 30% at MOI 0.01, 55% at MOI 0.1 and of 60% at MOI 1.

Whereas A673 and BRZ cells died after MeV-SCD infection (

Figure 42), SRH cells which were clinically tested resistant to chemotherapy, showed a different reaction after infection with MeV-SCD. More than 50% of the SRH cells survived the infection with MeV-SCD at MOI 1 96 hpi. So SRH cells showed a primary resistance to MeV-SCD infection. The treatment with the increasing 5-FC concentrations of 0.0001 mM to 1 mM combined with MeV-SCD infection showed a reduction of cell mass to (i) 70% at MOI 0.01, (ii) 45% at MOI 0.1 and (iii) 40% at MOI 1. The remaining cell mass was too high to declare the treatment with MeV-SCD successful. So the use of an extremely

high MOI of 10 was considered to be the next step in searching for an effective instrument against SRH cells.

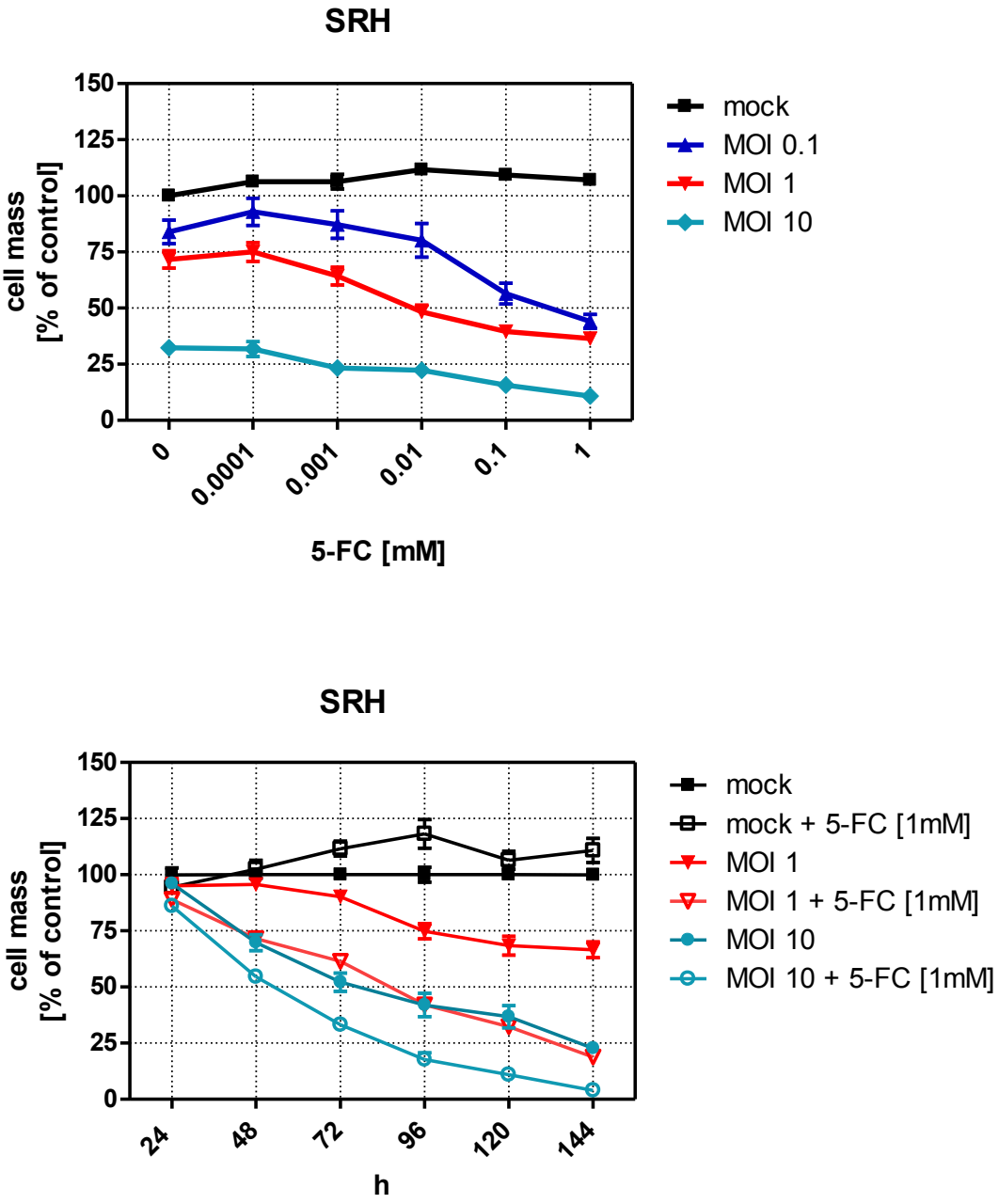

Figure 46. High MOI 10 combined with 1 mM 5-FC kills SRH cells 144 hpi
SRH cells were infected with MeV-SCD and were treated with 5-FC. The mean of three independent experiments is plotted, error bars show SEM. At the low MOI 0.1 and the high MOI 1, SRH cells showed primary resistance to MeV-SCD treatment. MeV ld-SCD at MOI 10 killed about 70% of the cells without addition of 5-FC. Increasing additional 5-FC concentrations led to decreasing cell mass. MeV-SCD at MOI 10 plus 1 mM 5-FC successfully reduced cell mass to 10% of control. The lengthened treatment up to 144 hpi led to a finally remaining cell mass of 5% of control.

In order to find a strategy to kill SRH cells with MeV-SCD, we tested another two different treatment options to find the best possible cell mass reduction. Firstly we increased the MOI to 10 and secondly we lengthened the process of incubation post infection to 144 hpi. We combined both strategies and incubated SRH cells after infection with MOI 10 for 144 hours. The treatment with MOI 1 without 5-FC showed little cell mass reduction to 75% cell mass 96 hpi and 65% cell mass 144 hpi. The combination treatment with MOI 1 and 1 mM 5-FC showed a clear decrease in cell mass to 40% cell mass 96 hpi and 20% cell mass 144 hpi. Infection with MOI 10 resulted in same results as in the trials with MOI 1 and 1 mM 5-FC 96 and 144 hpi. MOI 10 plus 5-FC led to a continuous decrease in cell mass over time to 20% of the control SRH cell mass 96 hpi and to 0% SRH cell mass 144 hpi.

3.5.1.4 SCOS cells resisted MeV-SCD treatment even at MOI 10

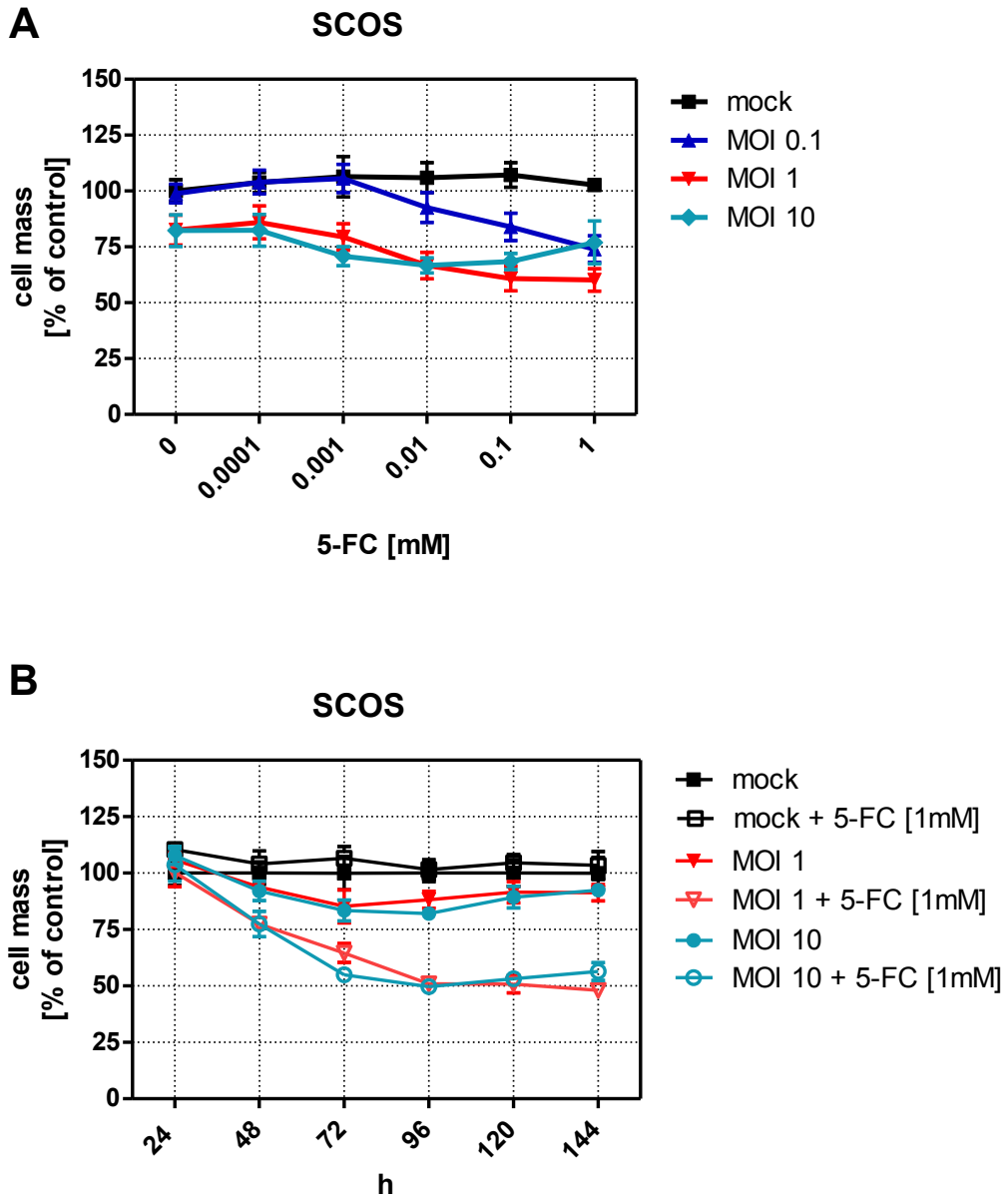

Figure 47. SCOS cells resisted combination treatment with MeV-SCD at MOI 10
SCOS cells were infected at MOI 0.1, 1 and 10 or remained mock-infected. 3 hpi cells were treated with different concentrations of 5-FC. Cell mass was determined 96 hpi (**A**) or daily until 144 hpi (**B**). Diagram **A** shows the mean of two independent experiments, diagram **B** shows one independent experiment, error bars represent SD.
96 hpi, cell mass of SCOS cells treated with MOI 1 and 1 mM 5-FC was reduced to 60% (**A**). The extension of incubation time to 144 hpi led to a further reduction of SCOS-cell mass to 50% in cells treated with MeV-SCD and 5-FC in combination. The infection with MeV-SCD at MOI 1 and 10 without addition of 5-FC only decreased cell mass to 90% of control 144 hpi.

SCOS cell line was derived from another sarcoma which showed therapy resistance in the clinical setting like SRH. In order to find a solution to this resistance phenomenon we used our MeV-SCD vector for SCOS infection. SCOS cells showed an even higher resistance towards MeV-SCD infection than SRH and were also declared primary resistant to MeV-SCD (according to the resistance definition specified by Tübingen virotherapy lab (AG Lauer)). The combination of MOI 1 with 1 mM 5-FC could enhance the cytotoxic effect in contrast to solely virus-treatment but cell mass was only reduced to 50% of control 144 hpi. MOI 10 and 1 mM 5-FC reduced cell mass to 55% of control.
Summing up, both SRH and SCOS tumor cells were found to be primary resistant to MeV ld-SCD treatment. So as to find an effective strategy to kill SRH and SCOS cells, alternative employment of the vaccinia vaccine virus GLV-1h68 treatment was the next step to try to overcome the resistance of SRH and SCOS tumor cells. We defined two aims for further treatment; firstly another vector system should be found to overcome resistance and secondly the high MOI 10 which according to current capabilities in vector production cannot be reached in human cancer patients should be reduced to a maximum of MOI 1.

3.5.2 GLV-1h68 shows a highly oncolytic potency

3.5.2.1 Cytotoxic effect of GLV-1h68 on SRH cells which survived MeV-SCD treatment with high MOIs

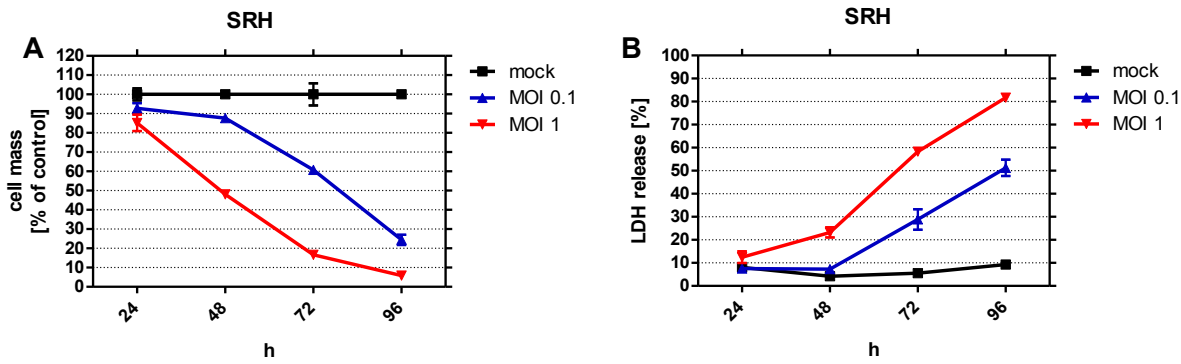

Figure 48. Cytotoxic effect of GLV-1h68 on SRH cells
SRH cells were infected with GLV-1h68 at MOI 0.1 and MOI 1 or remained uninfected. SRB-data (**A**) and LDH-data (**B**) show the mean of three independent experiments each, error bars represent SEM. GLV-1h68 effectively reduced cell mass to 25% of control at the low MOI of 0.1 and to less than 10% of control at MOI 1 96 hpi (**A**). In LDH-release assay cells showed proceeding increase in LDH-release over time resulting in 50% LDH-release at MOI 0.1 and 80% LDH-release at MOI 1 96 hpi.

SRH cells, which were classified as primary resistant to MeV-SCD, were treated with GLV-1h68 using MOI 0.1 and MOI 1. **Figure 48 A** shows the reduction of SRH cell mass to 25% of control at MOI 0.1 and to less than 10% at MOI 1 96 hpi. No resistance phenomenon was found when challenged. LDH-release assay (**B**) confirmed the findings in SRB-assay. LDH-release increased steadily over time to 50% in samples treated with MOI 0.1 and 80% in the samples treated with MOI 1 96 hpi. These experiments clearly demonstrated that the MeV-SCD resistant SRH cells reacted sensitive to GLV-1h68 at both MOIs and cell mass was reduced to less than 10% of control 96 hpi. Thereby, the necessity of “customized” approaches in virotherapeutic treatment of cancer patients is underlined in a most concrete way.

3.5.2.2 Cytotoxic effect of GLV-1h68 on PLC/PRF/5 cells

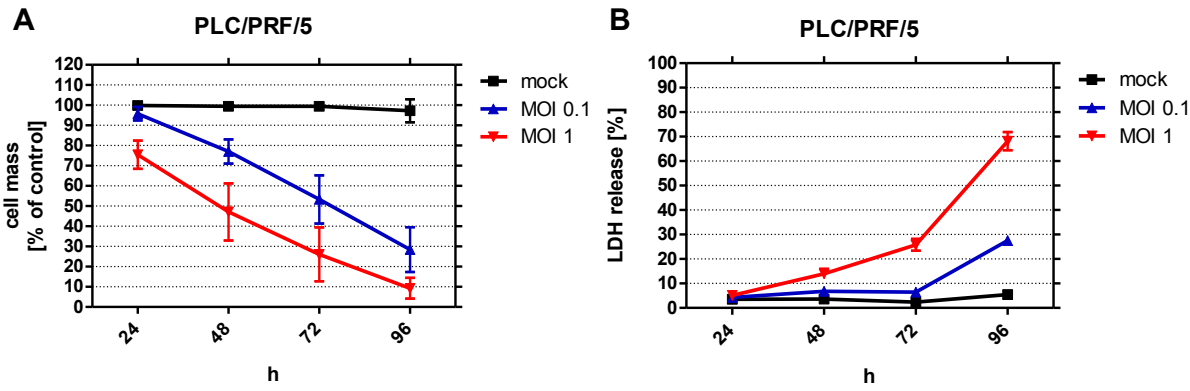

Figure 49. Cytotoxic effect of GLV-1h68 on PLC/PRF/5 cells
PLC/PRF/5 cells were infected with GLV-1h68 at MOI 0.1 and 1 or remained mock-infected. Cell death was measured in SRB and LDH assay, one representative experiment is shown in **A** and the mean of three independent experiments is shown in **B**. Error bars show SEM. GLV-1h68-treatment with MOI 0.1 led to a remaining cell mass of 30% 96 hpi. GLV-1h68 at MOI 1 led to a cell mass reduced to 10% 96 hpi (**A**). Increasing LDH-release (**B**) to 30% at MOI 0.1 and to 70% at MOI 1 96 hpi over time confirms increasing cell death with increasing time-span post infection and higher MOI as it was previously shown in **A**.

Besides the human sarcoma cell lines SRH and SCOS which were hard to treat in clinic, we also focused on tumor cell lines likely to cause peritoneal carcinosis, another cancer species which is currently not easy to treat.

We started with the evaluation of the PLC/PRF/5 human hepatoma cell line as hepatomas sometimes spread into the peritoneal cavity. PLC/PRF/5 cells were infected with GLV-1h68 at MOI 0.1 and 1 or remained uninfected. Cell mass in wells infected with MOI 0.1 decreased to nearly 30% of control and cell mass of cells treated with MOI 1 was reduced to 10% 96 hpi **Figure 49 A**. LDH-release assay showed marginal LDH-release in mock-infected cells, 25% LDH-release in cells treated with MOI 0.1 and the highest LDH-release up to 70% in cells infected with MOI 1 96 hpi (**B**). PLC/PRF/5 cells were successfully killed by GLV-1h68.

3.5.2.3 Cytotoxic effect of GLV-1h68 on CC531s cells

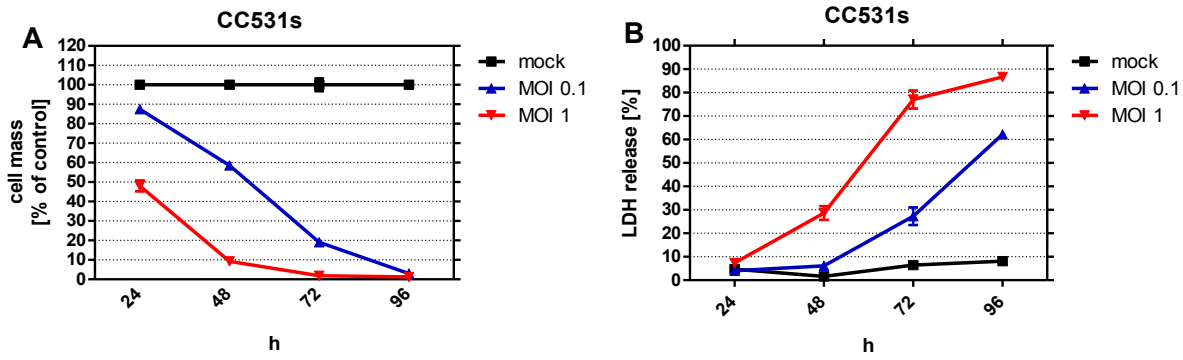

Figure 50. Eradication of CC531s cells by GLV-1h68
CC531s cells were infected with GLV-1h68 at MOI 0.1 and MOI 1 or remained mock-infected. Data represent the mean of three independent experiments, error bars show SEM. Cell mass of CC531s cells decreased continuously over time until there was 0% cell mass left 96 hpi with both MOI 0.1 and 1 (**A**). In LDH-release assay acknowledged this data showing high LDH-release under GLV-1h68 treatment of 60% at MOI 0.1 and 90% at MOI 1 96 hpi.

The colorectal carcinoma cell line CC531s of rat origin represents another cancer species likely to spread into the peritoneal cavity and is widely used in syngeneic animal models of peritoneal carcinosis. CC531s cells were infected with GLV-1h68 at MOI 0.1, 1 or remained uninfected. Cell mass of cultures treated with MOI 0.1 and MOI 1 was reduced to 0% of control 96 hpi (**A**). The high LDH-release rates of 60% at MOI 0.1 and 90% at MOI 1 were also indicators for the strong cytotoxic effect of GLV-1h68 on CC531s cells (**B**). CC531s cells were successfully killed by GLV-1h68.

3.5.2.4 Cytotoxic effect of GLV-1h68 on SKOV3ip.1 cells

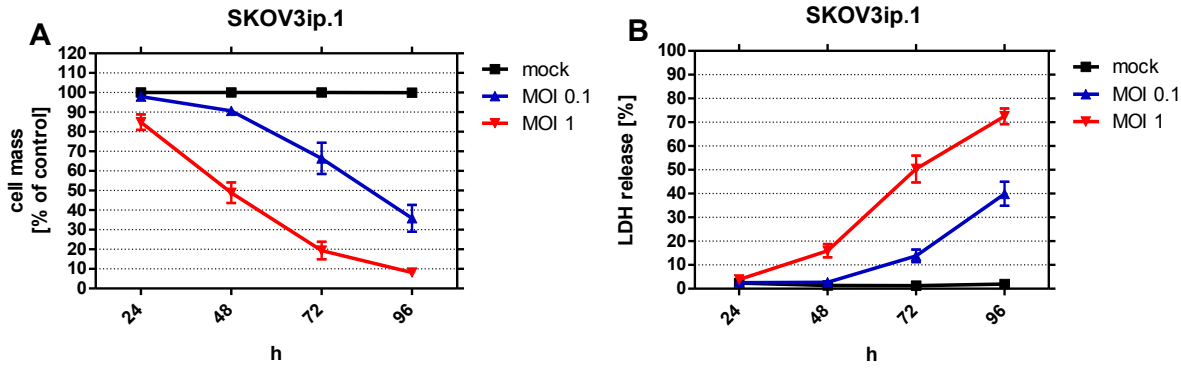

Figure 51. Cytotoxic effect of GLV-1h68 on SKOV3ip.1 cells
SKOV3ip.1 cells were infected with GLV-1h68 at MOI 0.1 and 1 or remained uninfected. Three independent experiments were performed and data show mean and SEM. The oncolytic potency of GLV-1h68 led to a decrease in cell mass of 70% at MOI 0.1 and of 90% at MOI 1 96 hpi. Data of LDH-release show the expected increase in LDH-release in conformity with decrease in cell mass. LDH release in cells infected with MOI 0.1 rose to 40% and cells infected with MOI 1 released about 70% of the available LDH in total 96 hpi.

Human SKOV3ip.1 cells displayed ovarian cancer as another tumor entity likely to spread into the peritoneal cavity and are also widely used in xenograft animal models of peritoneal carcinosis. SKOV3ip.1 cells were infected with GLV-1h68 at MOI 0.1 and MOI 1 or remained uninfected (**Figure 51**). SRB assay revealed a reduction of cell mass to 35% of control in cells infected with MOI 0.1 and a reduction to 10% of control in cells infected with MOI 1 96 hpi (**A**). Increasing LDH-release to 40% at MOI 0.1 and up to 70% at MOI 1 (**B**) confirmed the findings of the SRB assay.

Up to this point, there were no resistance phenomena towards the GLV-1h68-treatment observed and GLV-1h68 was able to overcome any problems observed in MeV-SCD-based oncolytic treatment of SRH cells. The next step was to evaluate the cytotoxic effect of GLV-1h68 in SCOS cells, which also were shown to be resistant to MeV-SCD infection as demonstrated in **3.5.1.4**.

3.6 The discovery of partially GLV-1h68-resistant cell-lines

3.6.1 Cytotoxic effect of GLV-1h68 on SCOS-cells

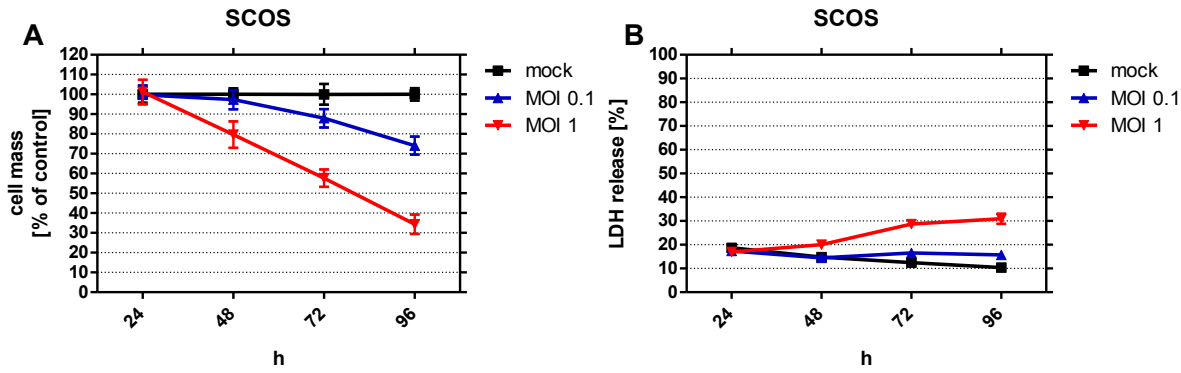

Figure 52. Cytotoxic effect of GLV-1h68 on SCOS cells
SCOS cells were infected with GLV-1h68 at MOI 0.1 and 1 or remained uninfected. SRB (**A**) and LDH assay (**B**) were performed. Data show the mean of three independent experiments each, error bars represent SEM. Cell mass of SCOS cells treated with MOI 0.1 was reduced to 75% of control and cell mass of SCOS cells treated with MOI 1 was reduced to 35% of control 96 hpi (**A**). LDH-release increased to 15% 96 hpi with MOI 0.1 and to 30% 96 hpi with MOI 1 (**B**).

SRB assay revealed that cell mass of SCOS cells was nearly reduced to 75% of control at MOI 0.1 and to almost 35% of control at MOI 1 96 hpi. So SCOS partially resisted the infection and oncolytic effects with GLV-1h68. LDH-release stayed minimal at MOI 0.1 throughout the duration of the experiment nearly according to the measured background LDH-release in the mock-infected cells. LDH-release in cells treated with MOI 1 reached an extent of 30% 96 hpi. These results in cell viability assays showed, that GLV-1h68-treatment alone was not sufficient to efficiently kill SCOS cancer cells.

3.7 Virotherapy using the armed GLV-1h95 led to a stronger cytotoxic effect than GLV-1h68-treatment alone

3.7.1 Cytotoxic effect of GLV-1h95 on SCOS cells

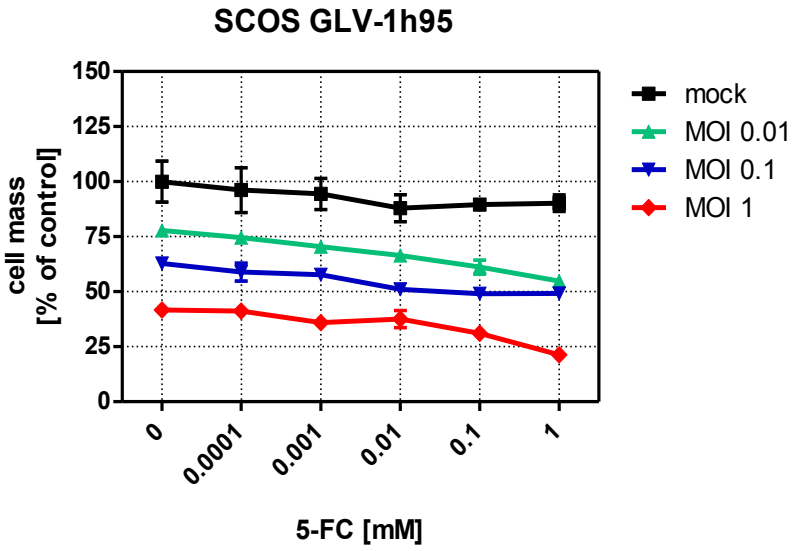

Figure 53. GLV-1h95 combined with 5-FC showed highly cytotoxic effect on SCOS cells
SCOS cells were infected with GLV-1h95 at MOI 0.01, 0.1 and 1 or remained uninfected. Cells were treated with increasing 5-FC-concentrations from 0.0001 to 1 mM to utilize the suicide gene function of armed virotherapeutic GLV-1h95. Cell mass was measured 96 hpi. Data show the results of one representative experiment, error bars represent SD. Cell mass of both cultures infected with MOI 0.01 and 0.1 plus 1 mM 5-FC was reduced to 50% of control 96 hpi. Cell mass of cells infected with MOI 1 plus 5-FC was reduced to nearly 20% at 96 hpi.

In order to find an efficient virotherapeutic against SCOS cells, the armed vaccinia vector GLV-1h95 was used for further examinations. GLV-1h95 was derived from its parental virotherapeutic GLV-1h68 and additionally encodes the suicide gene FCU1 in the A56R locus. FCU1 equates the suicide gene SCD in MeV-SCD and leads to the conversion of 5-FC into the toxic 5-FU when it is successfully expressed in tumor cells post infection.

SCOS cells were infected with GLV-1h95 and treated with the prodrug 5-FC which was metabolized into the toxic 5-FU by SCD expressed by GLV-1h95. The higher the MOI and the 5-FC-concentration, the higher was the reduction of the SCOS cell mass. MOI 0.01 and 0.1 combined with 1 mM 5-FC only reduced the SCOS cell mass to 50% of control. GLV-1h95 at MOI 1 and 1 mM 5-FC led to a remaining cell mass of about 25% of control. Compared to the results of the

GLV-1h68 effects on the SCOS cells where 35% of the cell mass remained 96 hpi, cell death could be enhanced, represented in a greater extent of cell mass reduction to 20% 96 hpi with GLV-1h95.

3.7.2 Comparison of GLV-1h68 and GLV-1h95 effects

In a next experiment designed to overcome primary resistances to virotherapeutics, the three tumor cell lines HT29 (colorectal carcinoma), SiHa (cervical squamous cell carcinoma) and NCI-H1299 (breast adenocarcinoma) which were defined as non-responders (**NR**) in xenograft models by Worschech et al. were infected with both GLV-1h68 and GLV-1h95. Infection efficacy using GFP expression by GLV-1h68 and cell mass behaviour post infection with GLV-1h68 and GLV-1h95 was monitored over 96 hours.

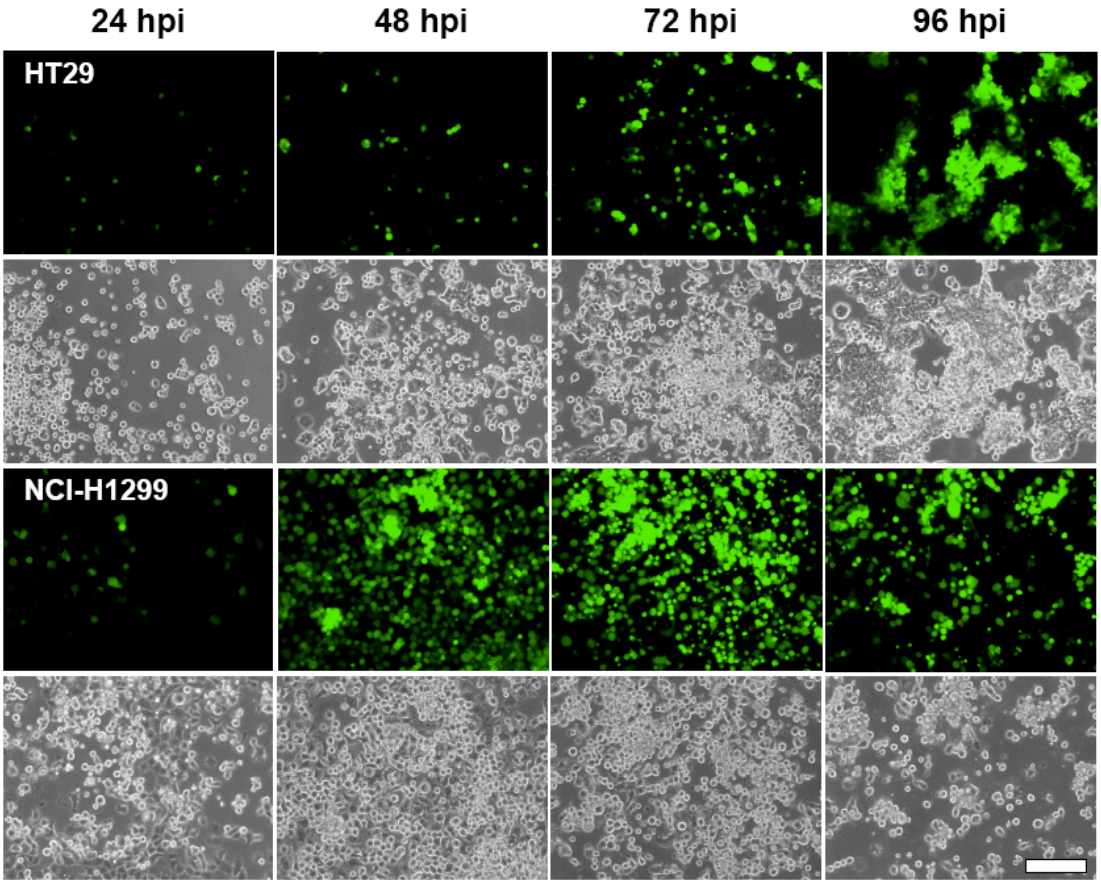

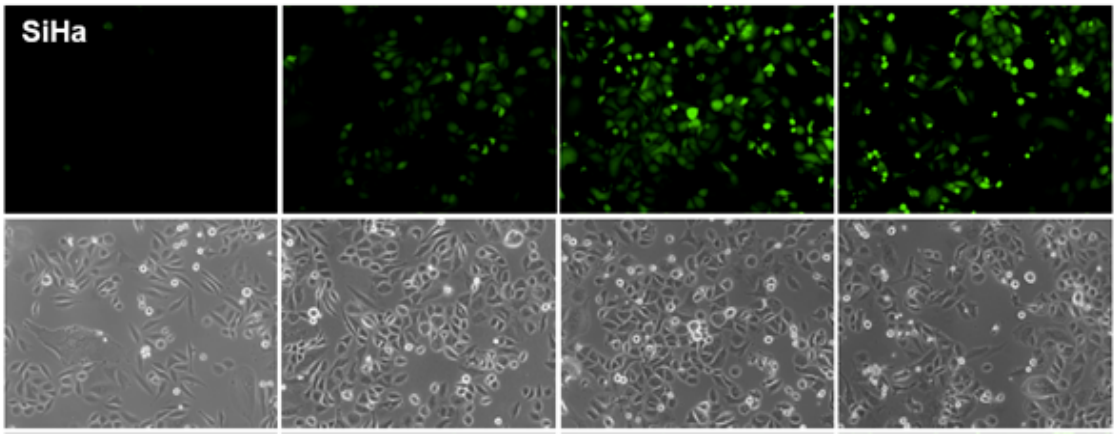

Figure 54. GFP expression after GLV-1h68-infection via GFP-fluorescence-monitoring and phase contrast microscopy
HT29, NCI-H1299 and SiHa tumor cells were infected with GLV-1h68 at MOI 0.1. Phase contrast and fluorescence photos were taken 24, 48, 72 and 96 hpi at the same magnification. Measuring carriage in the right lower corner represents 200 µm. Visible infection started 24 hpi in NCI-H1299 and HT29 cells, 48 hpi in SiHa and MDA-MB-231 cells. 75% of the HT29 cells, growing in adherent cell clusters, showed GFP expression 96 hpi. GFP-expression in NCI-H1299 cells increased strongly 48 hpi and 100% of the cells expressed GFP from 72 hpi. SiHa cells which have a low cell division rate also expressed GFP in nearly 90% of the cells from 72 hpi.

The three cell lines were infected with GLV-1h68 at MOI 0.1. 5% of the NCI-H1299 and HT29 cells were the first to express green fluorescent protein (GFP) 48 hpi. 50% of the SiHa expressed GFP from 48 hpi. HT-29, a cell line which grows in small adherent cell-clusters and not as a complete cell layer was totally infected 96 hpi but still exhibited adherence. 100% of the NCI-H1299 cells expressed GFP 72 hpi and the cells were already morphologically predominantly dead at this time point. 50% of the SiHa cells began to emit green fluorescence 48 hpi at low intensity. The infection was found to spread during the next 48 hours but most SiHa cells remained adherent under GLV-1h68-treatment at MOI 0.1. Taken these results together, all cell lines tested were successfully infected by GLV-1h68 although to different extents.

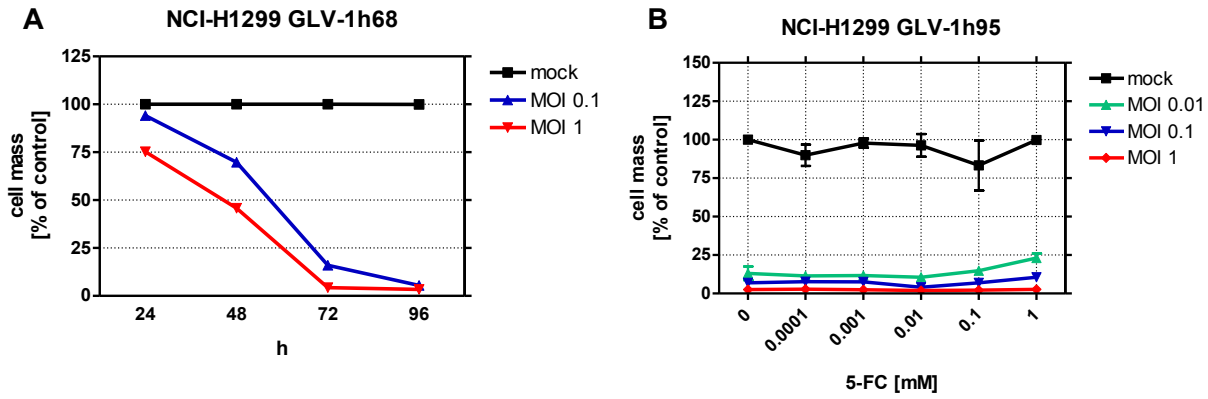

Figure 55. GLV-1h68 and GLV-1h95 minimize NCI-H1299 cell mass to the same extent
NCI-H1299 cells were infected with GLV-1h68 at MOI 0.1, 1 or remained mock-infected (**A**). In a second approach, cells were infected with GLV-1h95 at MOI 0.01, 0.1 and 1 or remained uninfected. 1 hpi, the cells were treated with increasing 5-FC-concentrations (**B**). SRB assay was performed at different time points (**A**) or 96 hpi alternatively (**B**). Data show one representative of three independent experiments done in quadruplicates. Error bars represent SD. Cell mass was reduced to 5% 96 hpi with GLV-1h68 at MOI 0.1 and 1 (**A**), and cell mass was reduced to 25% (MOI 0.01), 10% (MOI 0.1) and 5% (MOI 1) in combination with 1 mM 5-FC (**B**).

In order to compare cytotoxic potency of GLV-1h68 and GLV-1h95 SRB assay was performed **Figure 55.** NCI-H1299 cell mass was reduced to approximately 5% of control at 96 hpi with GLV-1h68 (**A**). Infection with the armed virus GLV-1h95 and the addition of 5-FC resulted in a remaining cell mass of 10% at MOI 0.1 and 5% at MOI 1 with all 5-FC-concentrations. The lower MOI 0.01 showed a minimally weaker effect of 25% remaining cell mass with the use of 1 mM 5-FC than MOI 0.1 and 1. GLV-1h95 infection without addition of 5-FC resulted in similar remaining cell masses of about 10% 96 hpi. Noticeably was the fact that cell mass infected with MOI 0.01 and 0.1 increased with increasing 5-FC concentrations which we did not expect but were able to reproduce in multiple other experiments (**B**).

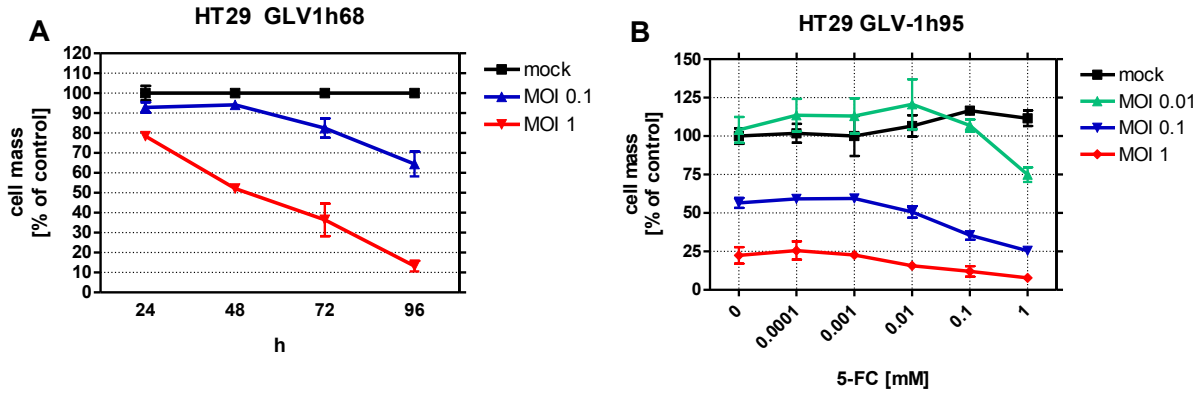

Figure 56. GLV-1h95 enhances the cytotoxic effect of GLV-1h68 on HT29 cells
HT29 cells were infected with GLV-1h68 at MOI 0.1 and 1 or remained mock-infected (**A**). In **B**, HT29 cells were mock-treated or infected with GLV-1h95 at MOI 0.01, 0.1 and 1 and were treated with different concentrations of 5-FC 1 hpi. Cell mass was measured 96 hpi (**B**). Data show one representative of three independent experiments respectively, error bars represent SD. Cell mass of HT29 cells was reduced to 80% (MOI 0.1) and 20% (MOI 1) with GLV-1h68 (**A**) and to 75% (MOI 0.01), 25% (MOI 0.1) and 10% (MOI 1) combined with 1 mM 5-FC 96 hpi (**B**).

GLV-1h68-treatment of HT29 cells at MOI 0.1 led to a resulting cell mass of still 80% of control at 96 hpi. The remaining cell mass of 60% 72 hpi at MOI 1 was only reduced to 20% 96 hpi. But the armed GLV-1h95 was able to enhance the cytotoxic effect of GLV-1h68. Cell mass was reduced to 25% of control after treatment with MOI 0.1 combined with 1 mM 5-FC and the cytotoxic effect was even enhanced by the use of MOI 1 and 1 mM 5-FC which led to a cell mass of nearly 10% of control. Thus, HT29 cells were nearly eradicated by GLV-1h95 at MOI 1 and 1 mM 5-FC at 96 hpi.

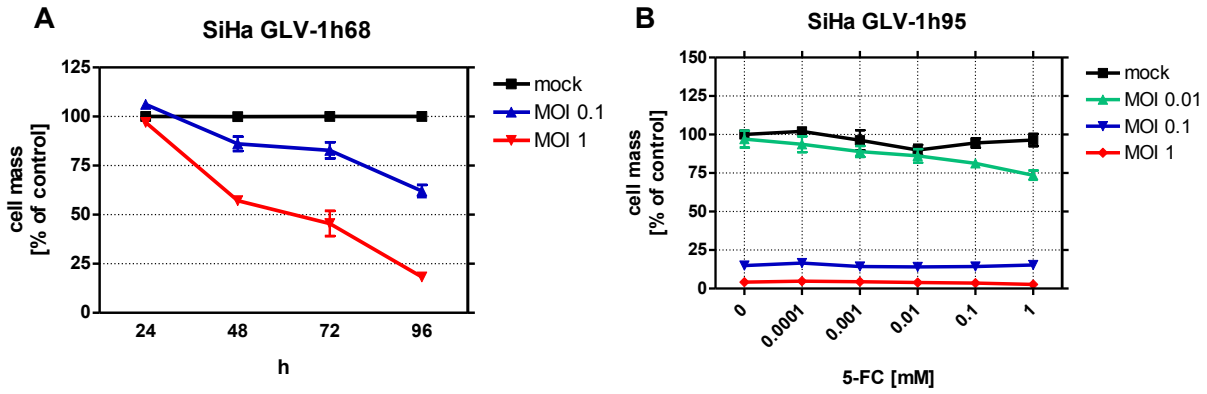

Figure 57. GLV-1h95 enhances the cytotoxic effect of GLV-1h68 on SiHa cells
SiHa cells were infected with GLV-1h68 at MOI 0.1 and 1 or remained mock-infected. In another approach, SiHa cells were infected with GLV-1h95 at MOI 0.01, 0.1, 1 or also remained uninfected. Increasing concentrations of 5-FC were added. Cell mass was measured at 96 hpi (**B**). Data show one representative of three experiments done in quadruplicates, error bars show SD. SiHa cell mass was reduced to 55% with MOI 0.1 and to 15% with MOI 1 96 hpi with GLV-1h68 (**A**), and cell mass was reduced to 75% (MOI 0.01), 20% (MOI 0.1) and nearly 0% (MOI 1) with GLV-1h95 and the addition of 1 mM 5-FC (**B**).

SiHa cells treated with GLV-1h68 at MOI 0.1 were reduced to 55% of control cell mass 96 hpi. The higher MOI 1 led to a remaining cell mass of 15% at 96 hpi. The treatment with GLV-1h95 showed a cell mass reduction up to 20% of control at MOI 0.1 and a reduction to nearly 0% remaining cell mass at MOI 1 and 1 mM 5-FC at 96 hpi. As it was shown in HT29 cells, GLV-1h95 could enhance the cytotoxic effect of GLV-1h68 in SiHa cells. GLV-1h95 alone at MOI 0.1 (MOI 1) reduced SiHa cell mass to 20% (15%) at 96 hpi whereas GLV-1h68 at MOI 0.1 (MOI 1) only reduced cell mass to 55% (5%) at 96 hpi. This shows the stronger cytotoxic effect of GLV-1h95 in contrast to GLV-1h68.

3.7.3 Replication behaviour of GLV-1h68 in non-responding tumor cell lines

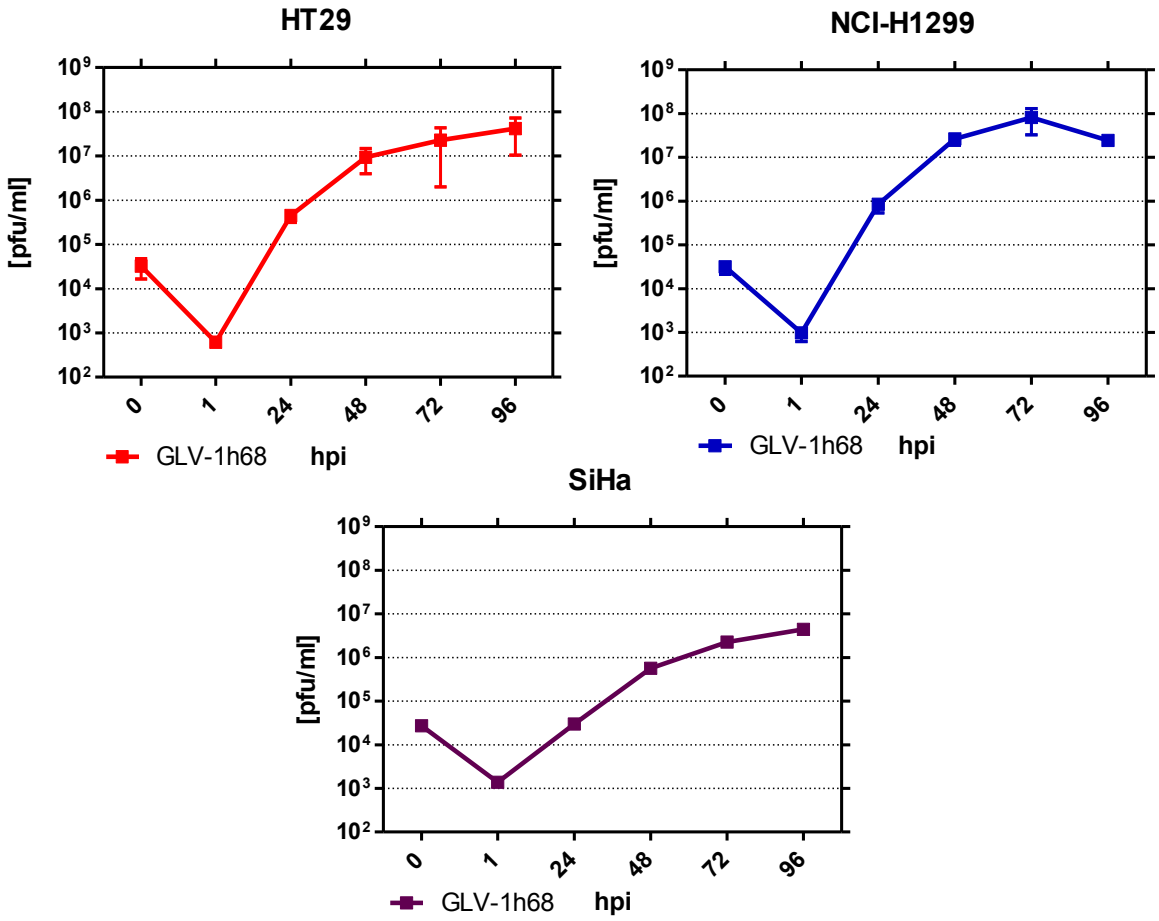

Figure 58. Replication behaviour of GLV-1h68 in HT29, NCI-H1299 and SiHa and cells
HT29, NCI-H1299 and SiHa cells were infected with GLV-1h68 at MOI 0.01. The inoculum (0 hpi) was frozen immediately and samples of 1, 24, 48, 72 and 96 hpi were frozen too. Plaque assay on CV-1 cells was performed in duplicates. Data show the mean of three independent experiments, error bars represent SEM. Viral replication yielded a massive titer increase up to 4.15E+07 pfu/ml (**HT29**), 2.44E+07 pfu/ml (**NCI-H1299**) and 4.4E+06 pfu/ml (**SiHa**) 96 hpi. Whereas viral titer increased over time to the highest titer 96 hpi in HT29 and SiHa whereas viral titer in NCI-H1299 cells decreased from 8.20E+07 pfu/ml 72 hpi to 2.44E+07 pfu/ml 96 hpi.

As HT29, NCI-H1299 and SiHa cells were designated as cell lines non-responding to GLV-1h68-based oncolysis by Worschech et al. and SiHa and NCI-H1299 were resistant to GLV-1h68-replication during the first 24 hpi, we independently re-evaluated these cell lines in order to confirm or refute these findings **(Figure 58)**. In our examinations GLV-1h68-replication was monitored over 96 hpi. Infection with GLV-1h68 resulted in a steady titer increase in all cell lines over time until 96 hpi except in NCH-H1299. Here, viral yield peaked at

8.20E+07 pfu/ml 72 hpi and decreased to 2.44E+07 pfu/ml 96 hpi. We observed no delay in viral replication behaviour as it was described by Worschech et al. GLV-1h68 replicated in all four cell lines and increased to viral titers of 4.15E+07 pfu/ml (HT29), 2.44E+07 pfu/ml (NCI-H1299) and 4.4E+06 pfu/ml (SiHa) 96 hpi. Differences in viral titer can be explained by slower cell division rate of SiHa cells which led to the lowest viral titer of 4.4E+06 pfu/ml (SiHa).

3.8 GLV-1h68 infection of primary human hepatocytes (PHH)

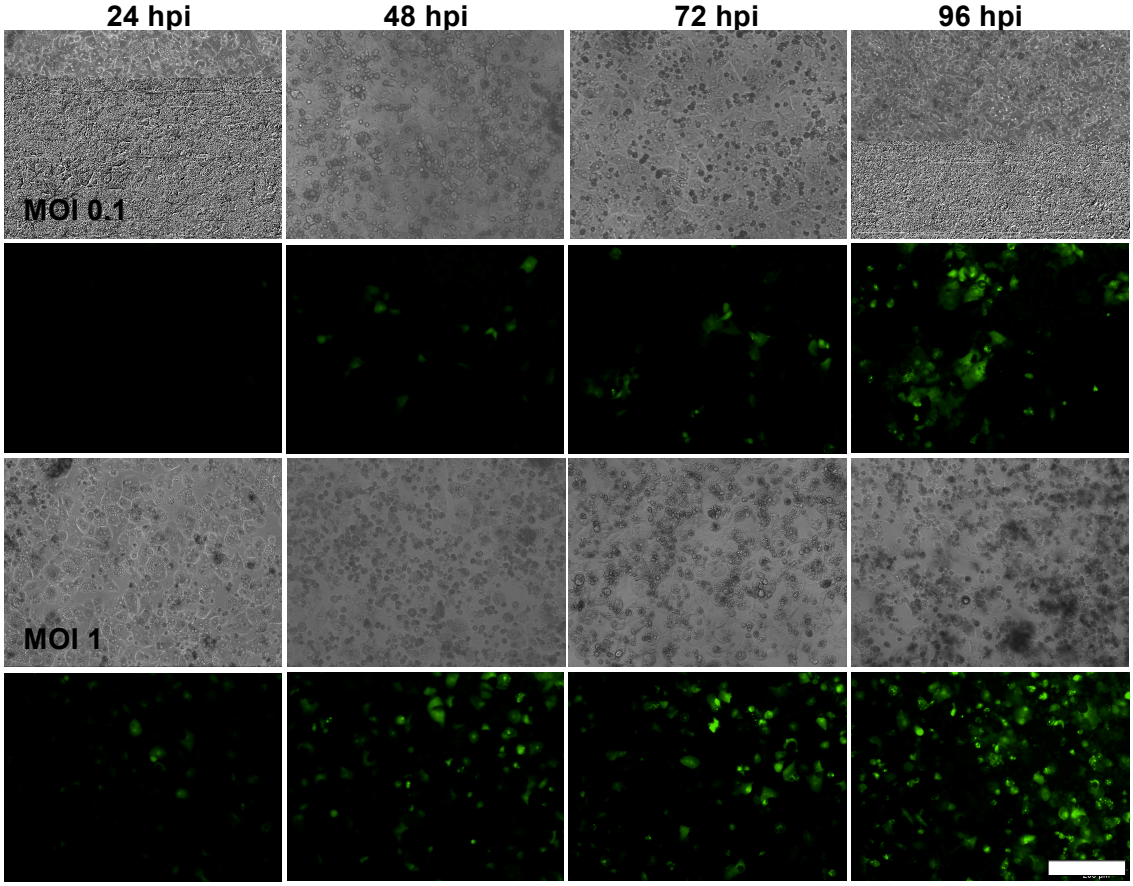

Figure 59. Infection of PHH with GLV-1h68
PHH were mock-infected or were infected with GLV-1h68 at MOI 0.1 and MOI 1. Phase contrast and fluorescence photos were taken at several time points post infection at the same magnification. Measuring carriage (white) in the right lower corner represents 200 µm. PHH infected with MOI 0.1 expressed GFP in 5% (48 hpi), 5% (72 hpi) and in 30% (96 hpi) of the cells. The corresponding phase contrast photos show, that PHH did not detach but grew despite viral infection. PHH infected with MOI 1 expressed GFP up from 24 hpi (10% of PHH) and 96 hpi 90% of PHH expressed GFP. 80% PHH had detached 72 hpi. PHH infected with MOI 1 predominantly detached but PHH infected with MOI 0.1 were still adherent 96 hpi which could be confirmed by SRB assay results (**Figure 60**).

In order to evaluate potential cytotoxic effects of GLV-1h68 on primary human tissues we performed infection experiments with primary human hepatocytes (PHH). PHH were infected with GLV-1h68 at MOI 0.1 and 1. Wells infected with MOI 0.1 expressed GFP in 5% (48 hpi, 72 hpi) and in 30% (96 hpi) of the cells. The corresponding phase contrast photos show, that PHH did not detach but grew despite viral infection. PHH infected with MOI 1 expressed GFP in 10% (24 hpi) and 90% (96 hpi) of the cells. 80% of the PHH infected with MOI 1 had detached 72 hpi. Both MOIs led to GFP expression in fluorescence microscopy; notably to a higher extent in PHH when infected with MOI 1. Phase contrast photos however revealed that PHH infected with MOI 0.1 grew over time and PHH infected with MOI 1 predominantly detached until 96 hpi (**Figure 59**).

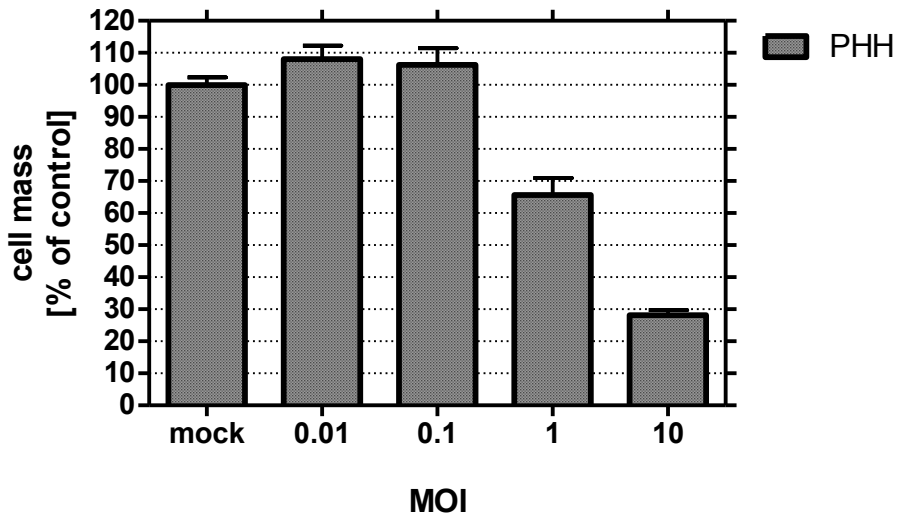

Figure 60. Infection of PHH with GLV-1h68
PHH cells were infected with GLV-1h68 at MOI 0.01, 0.1, 1 and the high MOI 10 or remained mock-infected. Cell mass in % of control was measured 96 hpi by SRB assay. Data show the result of one representative experiment, error bars represent SD. PHH cell mass infected with MOI 0.01 slightly increased to 105% and PHH mass infected with MOI 0.1 was 100% of control at 96 hpi. Cell mass of PHH infected with MOI 1 was reduced to 50% and cell mass infected with MOI 10 was reduced to 30% of control.

To get a clearer view of PHH cell mass change during the 96 hpi, SRB assay was performed. SRB-results indicated that PHH cell mass did not decrease under GLV-1h68-treatment at MOI 0.01 and 0.1. The higher MOI 1 (morphologic change in PHH is shown in **Figure 60**) led to a reduction in cell mass up to 50% of control and GLV-1h68 at very high MOI 10 killed nearly 75% of the non-transformed PHH. GLV-1h68 therefore does not exert cytotoxic effects to PHH at low MOIs such as 0.01 and 0.1 but kills half of the cells at MOI 1. Infection with MOI 10 showed highly cytotoxic effects and killed 75% of the PHHs. However, when “challenging” human hepatocytes in vitro with virotherapeutics it has to be taken into account that under in vivo conditions these primary cell lines are living in a three dimensional environment thereby being in contact with many other cell types, especially immune cells, which through diverse signalling activities efficiently inhibit replication of virotherapeutics in non-malignant cells. This perception is supported by our recent findings in our virotherapeutic clinical trial currently taking place at University Hospital Tübingen (ClinicalTrials.gov Identifier: NCT01443260).

4 Discussion

Cancer is one of the most frequent causes of death in the western world. After years of research in order to find novel curative therapy approaches, there is still no curative therapy option for many kinds of cancer. Therefore, the need for alternative cancer therapy options rises. Besides surgery, chemotherapy and radiotherapy which were made standard practice many years ago, novel therapy options like virotherapy are on the edge to enter the clinic. When Bluming and Ziegler et al. (1971) found out that a Burkitt's lymphoma in an African boy's face regressed and finally disappeared within weeks in association with a natural measles virus infection (Bluming et al., 1971), a proof-of-principle for oncolytic viruses as anti-cancer treatment option was given by nature. Measles virus (MeV) was shown to have an inherited oncolytic potency (Grote et al., 2001; Heinzerling et al., 2005; Peng et al., 2001; Phuong et al., 2003), which was also found for several other viruses like vaccinia virus (VACV) (Yu et al., 2004), or Newcastle Disease virus (NDV). To optimize the oncolytic efficacy of these viruses, therapeutic transgenes were inserted into the viral genome. The Super-CD (SCD) or FCU1 gene, encoding for the prodrug converting enzyme SCD (see paragraph 2.5) is one of the best characterized suicide genes which were inserted into several viruses like MeV or VACV to enhance the oncolytic efficacy of virotherapeutics against colorectal cancer (CRC) (Foloppe et al., 2008), breast cancer (Anderson et al., 2000), colorectal carcinoma and cholangiocarcinoma (Stackhouse et al., 2000) as well as prostate cancer (Freytag et al., 2003). SCD has also been integrated into the genome of adenoviruses which have been extensively studied in our lab and in many cooperating laboratories and showed significant enhancement of oncolytic effects in several studies (Graepler et al., 2005; Lemken et al., 2007; Warmann et al., 2006a; Warmann et al., 2006b; Warmann et al., 2009). Besides suicide genes which are able to toxify a primarily non-toxic prodrug, other therapeutic genes like anti-angiogenic transgenes (Frentzen et al., 2009; Guse et al., 2010; Thorne et al., 2006) or immune stimulatory genes (Parker et al., 2000; Wong et al., 2001) have already been inserted in viral genomes.

As there are still severe limitations in the treatment of chemotherapy-resistant human sarcomas and peritoneal carcinosis (Arnold et al., 2007), we here focused on the sarcoma cell lines A673 (extraosseus Ewing's sarcoma), BRZ (alveolar rhabdomyosarcoma), SRH (sclerosing rhabdomyosarcoma) and SCOS (osteosarcoma) and two cancer cell lines used in well characterized models of peritoneal carcinosis, CC531s (colorectal carcinoma) and SKOV3ip.1 (ovarian carcinoma), to investigate state-of-the-art MeV and VACV vector systems with regard to their infection and replication behaviour and oncolytic efficacies. Both vector systems were applied as a non-armed (MeV-eGFP/GLV-1h68) and an armed (MeV-SCD/GLV-1h95) version, respectively.

Similar infectability-patterns of cancer cells by MeV and VACV were observed monitoring marker gene expression

In a first step we analyzed the infection rate of both viral vector systems on the basis of marker gene expression. While MeV-eGFP contains the marker gene eGFP, infections with GLV-1h68 could be monitored using both GFP (*ruc-gfp)* and *β*-galactosidase (*lacZ*) expression.

The expression of GFP in MeV-eGFP infected sarcoma cell lines A673 and BRZ started to be detectable 24 hpi, maximizing between 48 and 72 hpi. GFP expression decreased 96 hpi due to the break-down of the biosynthesis machinery and the detachment of dead cells. It appeared surprising that cells infected with MOI 0.1 showed higher green fluorescence intensities than cells infected with MOI 1. However, this phenomenon can be explained easily by the fact that cell death occurs earlier under the treatment with MOI 1 leading to the detachment of the cells. Since GFP expression stops with cell death, fluorescence intensity decreased significantly earlier than in cells infected with MOI 0.1.

Green fluorescence intensity in GLV-1h68 infected cells overall appeared much weaker than in MeV-SCD infected cells but showed nearly the same behaviour concerning the period of GPF expression peaking at 48 to 72 hpi. Lower intensities of green fluorescence may be explained by the simple fact that GLV-1h68 expresses a non-enhanced form of GFP other than MeV-eGFP which

expresses an enhanced form of GFP (eGFP). When looking on the expression levels of all VACV-endoced marker genes it was found that the gene products of the *lacZ* and the *gusA* gene, *β*-galactosidase and *β*-glucoronidase, as well as the product of *ruc-gfp,* GFP, were expressed in 100% of the experiments. Thereby, evidence was provided that GLV-1h68 expresses all inserted marker genes on the same level. Results of our *XGal*-staining investigations, proving the expression of *β*-galactosidase within the infected cells, provided additional evidence of successful infection with GLV-1h68 in CC531s and SKOV3ip.1 cells. Taken together, infection of all cell lines (chemotherapy-resistant human sarcomas and peritoneal carcinosis cell lines) with both virotherapeutics MeV ld-eGFP and GLV-1h68 was successful.

Comparing the infection mechanisms of MeV and VACV, CD46 was identified as a receptor on cell surfaces for MeV Edmonston vaccine strains (Dorig et al., 1993; Naniche et al., 1993). In contrast to the well-known entry mechanism of MeV strains, there is no special entry molecule on cell surfaces known for the entry of VACV. A “problem” in understanding the entry mechanism of VACV are the two morphologically distinct infectious forms which are called IMV (intracellular mature virus) and EEV (extracellular enveloped virus) (Carter et al., 2005). G.C. Carter and M. Law described three envelope proteins of the IMVs which bind to glycosaminoglycans (GAGs) on the respective tumor cell surface and allow viral entry. But they discovered too that IMVs were also able to enter cells in a different way. The one conclusion they made of their investigations was that VACV IMVs enter cells via cell-membrane fusion. The viral core is subsequently released into the cytoplasm. Vanderplasschen et al. (1998) showed, that the entry mechanism of EEVs is dependent on a low-pH pathway in contrast to the IMV entry (Van Dorig et al., 2003). In conclusion neither IMVs nor EEVs enter tumor cells with the help of one distinct receptor (or it has not yet been discovered) making it impossible for us to provide a prediction of the GLV-1h68 infection rate by analysis of receptor expression on targeted tumor cells. Other than that, we could show that CD46 receptor density is closely associated with the level of MeV ld-SCD infection and cell death in the respective cell lines. As CD46 is known to be over-expressed on tumor cells in

comparison to non-malignant cells in the surrounding tissue, which was shown for HCC cells (Blechacz et al., 2006), multiple myeloma cells (Ong et al., 2006) and RCC cells (Meng et al., 2010), tumor cells display a favourable target for MeV. We determined the CD46 density on tumor cell surfaces using flow cytometry to calculate an arithmetic mean established by Anderson et al. (2004), which served as an approximate value of CD46 density. In accordance with Anderson et al., our experiments offered correlating results between the value of the calculated arithmetic mean of CD46 density and the extent of GFP expression and cell lysis in the four sarcoma cell lines. A673 cells, exhibiting the highest CD46 density, extensively expressed GFP all over the monolayer 48 and 72 hpi (at MOI 1) and so did the BRZ cells. Moreover, the BRZ cell layer presented syncytia formations consisting of multinucleated giant cells after cell-cell fusion which constitutes a typical CPE (cytopathic effect) for MeV infected tumor cells.

Summing up, our results showed that A673 and BRZ cells exhibited higher CD46 densities than SRH and SCOS cells with SCOS cells expressing least CD46. The CD46 density could be concordantly correlated to the level of GFP expression: the higher the CD46 density, the higher the GFP expression being a surrogate parameter for the extent of tumor cell infection.

Detailed analysis of infectability showed successful replication of both MeV and VACV

In Western Blot analysis, the presence of SCD after MeV-SCD infection of the cell lines A673 and BRZ was proven. A673 cells showed higher expression of SCD enzyme. This might be due to the higher CD46 density on A673 cell surface resulting in a higher viral load and consequently higher expression levels of the virotherapeutic-encoded SCD transgene. The higher concentration of SCD (and 5-FU) in the infected cells might have been responsible for the rapid cell death of A673 and BRZ cells after additional treatment with 5-FC: the more SCD is expressed, the higher the conversation rate of 5-FC into 5-FU is elevated. 5-FU as a “classical” cytotoxic compound triggers cell death. As we only analyzed the *total amount* of intracellular SCD when we performed

Western Blot analysis we could not say anything about the functionality of SCD. To gain knowledge about the *functionality* of SCD, a HPLC (high performance liquid chromatography) could have been additionally performed to detect the conversation rate of 5-FC into 5-FU demonstrating the functionality of the converting enzyme SCD. Dr. J. Lampe in our laboratory determined the conversion of 5-FC into 5-FU by HPLC in hepatoma cell lines after infection with MeV-SCD and addition of 5-FC. In these cells, up to 100% of 5-FC was converted into 5-FU (Lampe et al., manuscript submitted).

The replication of both viral vectors was monitored *in vitro* by growth curve assays. Titration of MeV-SCD in A673 and BRZ cells was performed on Vero cells showing increasing viral titres over a period of 96 h in both supernatant and cell lysate resulting in viral titres of 10^7 pfu/ml in case of A673 cells and approximately $2x10^5$ pfu/ml in BRZ cells. Replication of GLV-1h68 in CC531s and SKOV3ip.1 cells was shown in standard plaque assay titrated on CV-1 cells. Viral yield peaked at $7.58x10^6$ pfu/ml in CC531s cells and $1.59x10^7$ pfu/ml in SKOV3ip.1 cells 96 hpi. The process of both MeV-SCD and GLV-1h68 replication was also monitored in electron microscopy for the first time (*in cooperation with the University Clinic of Dermatology Tübingen, Prof. Dr. med. Schaller, Mrs. B. Fehrenbacher*). Viral fabrics, pre-stages, completed intra- and extracellular brick-shaped viral particles and even budding viruses could be fixed giving a 100% morphologic evidence of viral reproduction within the tumor cells. Besides focusing on viral replication and cell destruction, two different morphological forms of apoptotic mitochondria were detected in SKOV3ip.1 cells 72 hpi with GLV-1h68 pointing to an apoptotic cell death following VACV infection as it has already been shown by Seubert C.M. et al. (2011) who observed activation of the intrinsic apoptotic pathway after the combination treatment of breast cancer cell lines with a *β*-galactosidase-activatable prodrug and GLV-1h68 (Seubert et al., 2011). However, VACV kills cells not only by initiating apoptotic pathways but also by other mechanisms e.g. taking over the cellular biosynthesis machinery and suppressing the cell's RNA-, DNA- and protein synthesis.

GLV-1h68 replication was also monitored in tumor cell lines of different origins which were characterized as non-responders to GLV-1h68 by Worschech et al. (2009). Worschech et al. described poor replication of GLV-1h68 in the cell lines SiHa (cervical squamous cell carcinoma) and NCI-H1299 (breast cancer) 24 hpi with GLV-1h68 in vitro and non-responding of HT29 (colorectal carcinoma) tumors in a xenograft mouse model after intravenous injection of GLV-1h68 (Worschech et al., 2009). Other than expected we found a quite obvious increase in viral yield 24 hpi in our experiments, increasing further until viral replication stagnated 72 hpi in NCI-H1299 cells and 96 hpi in SiHa and HT29 cells. This discrepancy might result from differences in cell culture conditions or preparation of the virus stocks used in here. In order to come to a common understanding of which tumor cell lines indeed exhibit a primary resistance to GLV-1h68-based oncolysis a repetition of the xenograft animal experiments has to be undertaken. However, animal experimentation was beyond the scope of this doctoral thesis and has to be done in separate work.

Oncolytic efficacy of MeV and VACV differed a lot regarding cell killing efficiencies

The most important step of our investigations was to monitor and compare the oncolytic efficacy of MeV-SCD and GLV-1h68. Therefore, we performed two well established cytotoxicity assays, the SRB and the LDH assay. In SRB assay, cell death was measured as cell mass reduction in percent compared to mock-infected control. In LDH assay, increase in LDH compared to mock-infected cells was a marker for cell lysis. To classify tumor cells which were resistant to virotherapeutic treatment we developed a resistance definition for both MeV and VACV. A tumor cell line was declared to be primary resistant to MeV-SCD/ GLV-1h68 oncolysis when the remaining cell mass was above 50% of the control at MOI 1 (MeV-SCD)/ MOI 0.1 (GLV-1h68) at 96 hpi.

As a result, A673 and BRZ cells were completely eradicated 96 hpi with MeV-SCD. SRH cells reacted resistant (more than 50% remaining cell mass at 96 hpi) and SCOS cells strongly resisted treatment (more than 75% remaining cell mass at 96 hpi) with MeV-SCD. LDH release in BRZ cells *decreased* with

addition of higher 5-FC concentrations which we had expected to be exactly the other way round. As 5-FC is suspected to negatively interact with viral replication, the addition of 5-FC was postponed to 48 hpi (instead of 3 hpi) to extend the process of “unaffected” viral replication. Several authors found out that the success of suicide gene therapy is grossly dependent on the right timing of prodrug addition (Seo et al., 2005; Ungerechts et al., 2007; Ungerechts et al., 2010; Wildner et al., 1999). Thus, Ungerechts et al. (2007/2010) suggested the time point of maximal viral replication as being the best for the prodrug addition. Despite non-specific results in LDH assay, the syncytial morphology, a typical cytopathic effect (CPE) post MeV infection (Blechacz et al., 2006; Peng et al., 2001; Phuong et al., 2003) followed by apoptotic or non-apoptotic cell death, morphological aspects in phase contrast microscopy and SRB data of both A673 and BRZ cells were evidence of successful tumor cell killing *in vitro*.

In order to enhance the oncolytic effect of MeV-SCD in SRH and SCOS cells, our experiment was stretched to 144 hpi to allow effective replication of MeV-SCD. The maximal dose of MOI 1 was increased to MOI 10 plus the highest concentration of 1 mM 5-FC to raise the number of viral particles per cell. As a result, SRH cells were totally eradicated 144 hpi with MeV-SCD at MOI 10 plus 1 mM 5-FC. SCOS cells still were found to be resistant, despite this extensive virotherapeutic treatment including usage of the vector-encoded suicide gene function. More than 50% of the SCOS cell mass stayed attached at the end of the experiment. Yet we had to consider the possible damage after administration of MeV-SCD at MOI 10 to healthy tissue *in vivo*. Such a high level of viral load could cause serious side effects in healthy tissues as there could be too few tumor cells as a target for the viral particles. Instead of killing cancer cells, viruses might also attack healthy cells. Avoiding high MOIs, GLV-1h68 was chosen to overcome SCOS resistance to MeV-SCD. Of note, SCOS could not be completely eradicated by GLV-1h68 but were reduced to 35% of control 96 hpi at MOI 1.

Human sarcomas had already been successfully treated with virotherapy (He et al.; 2012) but there have also been unsuccessful investigations (Cripe et al.,

2001). He S. et al. (2012) lately published their research on human sarcoma cell lines treated with GLV-1h68 *in vitro* and *in vivo* (single intratumoral injection of GLV-1h68 into HT-1080 fibrosarcoma xenografts) which showed transgene expression in all tumor cell lines and cytotoxicity to three of four tested cell lines. There was no evidence of viral spread to healthy tissue in the xenograft model and near-complete reduction of the tumors at 28 days post infection (dpi) (He et al., 2012).

Therefore, in this work the resistant sarcoma cell lines and the before mentioned non-responding tumor cell lines (Worschech et al., 2009) were treated with an armed VACV. Thereby, we set out to come to a more comprehensive picture on the effectiveness of virotherapeutic approaches (including employment of suicide gene armed vector variants) in the treatment of chemotherapy-resistant sarcomas. Different armed VACV encoding Cytosine Deaminase (CD) have already been applied *in vitro* and *in vivo* (Gnant et al., 1999; McCart et al., 2000). Moreover Mc Cart et al. (2000) could show that the oncolytic efficacy of VACV alone was improved by the insertion of CD and the addition of 5-FC. As 5-FU is known to reduce the protein-, DNA- and RNA-production of the host cell to a minimum and additionally provides the advantageous “bystander effect”, it makes GLV-1h95 a promising cytotoxic tool. Moreover, 5-FC addition would allow to reduce the MOI, potentially decreasing therapy limiting viral side effects to a minimum. When GLV-1h95 was applied at MOI 1 plus 1 mM 5-FC this could not improve cell mass reduction 96 hpi in comparison with GLV-1h68 because cell mass had already been reduced to a minimum with GLV-1h68, but could definitely reduce cell mass to a higher extent than GLV-1h68 at the lower MOI 0.1 plus 1mM 5-FC. GLV-1h95 even reduced cell mass of the resistant sarcoma cell line SCOS to less than 25% of control at MOI 1 and 1 mM 5-FC. Thus, the suicide gene VACV-based virotherapeutic GLV-1h95 was demonstrated to be most effective in the challenging context of highly chemotherapy-resistant human sarcomas.

Regarding the *in vivo* application of GLV-1h68 in previous studies, the ability of GLV-1h68 to lyse tumor cells and cause regression of human xenograft tumors has already been shown and led to a significant reduction of primary tumors

induced by PC-3 and DU-145-cells in nude mice, regression of human prostate tumors (Gentschev et al., 2010), solid breast tumors (Zhang et al., 2007), HCC (hepatocellular carcinoma) (Gentschev et al., 2011), malignant pleural mesothelioma (Kelly et al., 2008), anaplastic thyroid carcinoma (Lin et al., 2007), canine mammary carcinoma (Gentschev et al., 2009; Gentschev et al., 2010) and human pancreatic tumors (Yu et al., 2009). Furthermore, Worschech et al. (2009) achieved to reduce several species of xenograft tumors after GLV-1h68 infection which they called *in vivo* responders (Worschech et al., 2009). Beyond these findings, Gentschev et al. and Kelly et al. (2009) showed that GLV-1h68 was able to reduce metastatic lymph nodes in a tumor xenograft model caused by a PC-3 induced prostate carcinoma (Kuriyama et al., 1998) and in an immunocompetent animal model of a metastatic melanoma (Kelly et al., 2009). In the phase I trial of Park et al. (2008) the poxvirus JX-594 was found to spread throughout the body to distant metastases (Park et al., 2008).

As there have not been yet any evaluations of GLV-1h95 *in vivo* like it was done already with GLV-1h68, we suggest further investigation of GLV-1h95 *in vitro* and *in vivo* to precisely evaluate its oncolytic efficacy and possible superiority in comparison to non-armed virotherapeutic vector generations.

Safety investigation in PHHs revealed an excellent safety profile at low MOIs

Regarding the safety of virotherapeutics, we wanted to investigate if our oncolytic viruses exert any toxicity on healthy/non-malignant cells. Therefore, we infected primary human hepatocytes (PHHs) with increasing concentrations of GLV-1h68 from MOI 0.01 to MOI 10. Fluorescence microscopy showed few infected cells at MOI 0.1 96 hpi and widespread GFP expression at MOI 1 at 72 - 96 hpi indicating that most of the cells were infected with GLV-1h68 at MOI 1 but only few cells were infected after treatment with MOI 0.1. Confirming this data, cell mass infected with MOI 1 was reduced to 50% of control whereas cell mass infected with MOI 0.1 was not reduced in our cytotoxicity testing. When we had a closer look on the infected cell layers at MOI 1 using phase contrast microscopy, we got the impression that most of the cells indeed were infected

and expressed GFP but they were still well attached to the bottom of the plates. So the question was how to differentiate between simply infected and dead cells. The problem is that the SRB assay only displays cell mass reduction but no cell death mechanisms not leading to cell lysis or cell mass reduction. The *in vitro* finding of virus infection in healthy cells could also be shown by Zhang et al. (2009), who detected very low GLV-1h68 concentrations in healthy liver, kidney and heart tissue and higher concentrations in the lung tissue of nude mice after injection of GLV-1h68 (Zhang et al., 2009). Contrary to this, Shu-Fu et al. (2007) showed that GLV-1h68 could replicate within tumor cells but not in non-malignant healthy cells (Shu-Fu et al., 2007) and Lin et al. (2008) showed that GLV-1h68, injected into healthy tissue, could not be retraced at 10 dpi and no toxic side effects could be detected *in vivo* (Lin et al., 2008).

JX-594, another engineered oncolytic poxvirus, has also been tested with regard to its safety profile and gives an idea of possible virus-related side effects on normals tissues. In a phase I study in patients with HCC, grade 1 and 2 flu-like symptoms were observed, dose-related hypotension, hyperbilirubinaemia, increase in monocytes and eosinophils, thrombocytopenia and neutropenia also occurred. None of the patients died treatment related and some cases of stable disease and even objective tumor response were observed (Park et al., 2008). Park et al. (2008) called the safety of JX-594 “acceptable”. A clinical phase I trial currently taking place at the Royal Marsden Hospital, Surrey, UK (EudraCT-Nr. 2007-004228-18), so far revealed no dose limiting cytotoxicity and especially no singificant elevation of transaminases was detected after intravenous application of GLV-1h68. Moreover, VACV has already demonstrated an acceptable safety profile in humans, since it was given to millions of people as a smallpox vaccine.

The outstanding safety profile of MeV has also been confirmed many times before (Blechacz et al., 2006; Springfeld et al., 2006). In this line, investigation of MeV-hCEA only displayed minimal cytopathic effects on healthy cells (Peng et al., 2002).

In summary we detected significant GFP expression and cell mass reduction in our *in vitro* trials in PHH only at high MOI 1. One explanation for our results of PHH cell damage at high MOI might be the lack of an integrated immune system in the *in vitro* cell cultures in contrast to clinical and preclinical *in vivo* testing of GLV-1h68. The immune system especially in healthy tissues is normally able to get rid of the viruses attacking healthy cells. Our *in vitro* results on PHH thereby do reflect the “artifical” conditions being quite often associated with cell culture research. Accordingly, it is not surprising that our *in vitro* findings could not be confirmed by current clinical research in which elevated transaminases are observed quite rarely and are not clearly related to a direct virotherapeutic effect (our unpublished results).

As the ultimate goal in virotherapy should be complete cytoreduction, the higher cytotoxic effect of GLV-1h95 compared to GLV-1h68, even though it was only a moderate difference, is stimulating to investigate also GLV-1h95 in further clinical trials. In addition, further investigations using a combination of different virotherapeutics e.g. VACV and MeV should be considered to enhance MeV cytotoxicity and to find synergistic effects, especially in cancer patients exhibiting primary resistance to virotherapeutic treatment of either viro-therapeutic. This approach already has been successfully tested preclinically by Le Boef et al. (2010) concurrently using a VACV and a vesicular stomatitis virus (VSV) and is now being tested also in our laboratory. Furthermore, the combination of oncolytic viruses and radiotherapy has been successfully tested preclinically (Hanna et al., 1997; Kievit et al., 1999; Pederson et al., 1997; Pederson et al., 1998; Stackhouse et al., 2000; Xing et al., 2009; Zhang et al., 2003) as it has also been done with oncolytic viruses and chemotherapy, which is known to lead to a better tumor regression in contrast to only using one of them (Mahoney et al., 2010; Yu et al., 2009). In order to enhance oncolytic efficacy, these approaches also should be expedited. Indeed, there is an actively recruiting clinical trial (Phase I Trial Of Attenuated Vaccinia Virus (GL-ONC1) Delivered Intravenously With Concurrent Cisplatin and Radiotherapy in Patients With Locoregionally Advanced Head and Neck Carcinoma;

ClinicalTrials.gov Identifier: NCT01584284) in which the GMP-produced version of GLV-1h68 (called GL-ONC1) is tested in conjunction with radiotherapy.

For further investigations we propose to evaluate the oncolytic potential of GLV-1h68 in a preclinical syngeneic animal model of peritoneal carcinosis. The well-established WAG/Rij rat animal model of the peritoneal carcinosis (Pelz et al., 2005; Pelz et al., 2006; Zedeck et al., 1974;) is available for the treatment of syngeneic CC531s induced peritoneal carcinosis (Pelz et al., 2005; Pelz et al., 2006; Zedeck et al., 1974;). Intraperitoneally injected CC531s cells causing a peritoneal tumor mass will afterwards be treated with both peritonectomy (state-of-the-art surgical intervention) and intraperitoneal instillation of GLV-1h68 ideally leading to a complete cytoreduction which significantly would improve prognosis and overall survival. Debulking surgery combined with HIPEC already lengthened survival of peritoneal carcinosis patients (Königsrainer et al., 2008; Verwaal et al., 2003). Another well characterized xenograft model of the peritoneal carcinosis in athymic mice (Hasegawa et al., 2006; Peng et al., 2002; Yoneda et al., 1998) caused by intraperitoneal application of SKOV3ip.1 cells (Yoneda et al., 1998) constitutes an alternative preclinical model which also could be useful for preclinical *in vivo* trials. Tumor volume could be monitored using micro-PET-MRT-monitoring or immune-scintigraphy at different time points throughout the trial as it has already been done by several other authors (Pichler et al., 2008; Pross et al., 2001).

Bridging the gap between animal *in vivo* trials and phase I studies in humans, the concept of using human *Precision Cut Tumor Tissue Slices (PCTTS)* which was established by Zimmermann et al. (2009) in our laboratory has already been successfully tested in terms of infection, replication and tumor cell killing with human HCC/liver tissues and might be a helpful tool for the preclinical selection of a potentially effective virotherapeutic in a “customized” setting. Last but not least, *Single Cell Suspensions (SCS)* of human tumor material display another effective method to pre-evaluate oncolytic viral vectors before applying them *in vivo*. In 2012, Prof. U.M. Lauer et al. started a phase I/II trial “*A Study of GL-ONC1, an Oncolytic Vaccinia Virus, in Patients With Advanced Peritoneal Carcinomatosis*” (ClinicalTrials.gov Identifier: NCT01443260), treating

peritoneal carcinosis by virotherapy at the Medical University Hospital Tübingen with the hope to find an effective therapeutic against this deleterious form of cancer.

Summing up our findings, MeV-SCD, GLV-1h68 and GLV-1h95 were investigated *in vitro* with regard to their ability of infection, replication behaviour and oncolysis as potential virotherapeutics in the fight against cancer. We found out that MeV-SCD was able to kill primarily therapy-resistant sarcoma cell lines expressing high levels of CD46 but failed to efficiently kill the latter expressing low levels of CD46. GLV-1h68 however was able to kill primarily therapy-resistant sarcoma cell lines, the peritoneal carcinosis causing cell lines CC531s and SKOV3ip.1 and all the cell lines denominated as '*in vivo* non-responders' in prior work by Worschech et al. (2009). The SCOS cells, which were found to be highly resistant to MeV-SCD oncolysis, also resisted GLV-1h68 treatment albeit to a lower extent. The armed vector GLV-1h95 finally led to massive cell mass reduction also of SCOS cells. The additional effect of the suicide gene therapy with GLV-1h95 and 5-FC especially became obvious in trials with low MOI 0.1. Healthy PHHs were demonstrated to be infected by GLV-1h68 but stayed alive and mostly unaffected at low MOI 0.1.

Therefore, our virotherapeutic approaches should be short-listed to fight especially against highly chemotherapy-resistant cancer entities, such as peritoneal carcinosis and sarcomas, in order to overcome current severe therapy resistances.

5 Summary/Zusammenfassung

Resistances to common therapy approaches in cancer therapy are a worldwide problem today. Virotherapy is one of the novel anti-cancer strategies currently being investigated in preclinical experiments and clinical trials. Virotherapy is based on attenuated, replication-competent oncolytic viruses which selectively infect, replicate in and kill tumor cells without significantly harming healthy tissue. To advance the inherited oncolytic effect of viruses, transgenes like anti-angiogenic, immuno-stimulatory or suicide genes were inserted into the viral genome.

For our examinations we chose two genetically modified viral vector systems, MeV (MeV-SCD) and VACV (GLV-1h68/GLV-1h95), which hold an outstanding safety profile and recently have entered extensive clinical testing as state-of-the-art virotherapeutics. Both vector systems encode for marker genes and were armed with the suicide gene SCD which converts the non-toxic prodrug 5-FC into the common chemotherapeutic 5-FU.

MeV-SCD, GLV-1h68 and GLV-1h95 were investigated with regard to their ability of infection, replication behaviour and oncolysis *in vitro* as potential virotherapeutics in the fight against cancer. Summing up our findings we could demonstrate that MeV-SCD was able to kill primarily therapy-resistant sarcoma cell lines expressing high levels of CD46 but failed to kill the latter expressing low levels of CD46. CD46 is known to be the entrance molecule for MeV on tumor cells. GLV-1h68 however was able to kill primarily therapy-resistant sarcoma cell lines, the peritoneal carcinosis causing cell lines CC531s and SKOV3ip.1 and also all the cell lines called '*in vivo* non-responders' by Worschech et al. (2009). The SCOS cells, which were highly resistant to MeV-SCD, also resisted GLV-1h68 treatment to a lower extent. The armed vector GLV-1h95 finally led to massive cell mass reduction of SCOS cells. The additional effect of the suicide gene therapy with GLV-1h95 and 5-FC especially became obvious in our experiments with low MOI 0.1. Healthy PHHs were infected by GLV-1h68 but stayed mostly unaffected at MOI 0.1. Therefore, our

virotherapeutics should be short-listed to fight against peritoneal carcinosis and sarcomas in order to overcome current therapy resistances.

We suppose that future preclinical investigations should take place in the well-established WAG/Rij rat animal model of the peritoneal carcinosis (Zedeck et al., 1974; Pelz et al., 2005; Pelz et al., 2006) and further studies should be done using primary human tumor material like *Single Cell Suspensions* (SCS) or *Precision Cut Tumor Tissue Slices (PCTS)* to confirm our findings *in vivo.*

In der Krebstherapie auftretende primäre Therapie-Resistenzen stellen weltweit ein schwerwiegendes Problem dar. Bei der Virotherapie handelt es sich um eine neuartige Therapie-Strategie, die momentan präklinisch und klinisch erprobt wird. Diese Methode basiert auf attenuierten replikationskompetenten onkolytischen Viren, die selektiv Tumorzellen infizieren, intrazellulär replizieren und die Tumorzellen abtöten, ohne umliegendes gesundes Gewebe zu schädigen. Um die intrinsische onkolytische Aktivität der eingesetzten Viren weiter zu verbessern, wurden Transgene wie Antiangiogenese-, Immunstimulations- und Suizid-Gene in das Genom verschiedener Viren eingefügt.

In dieser Dissertation wurden zwei genetisch modifizierte virale Vektorsysteme, MeV (MeV-SCD) und VACV (GLV-1h68/GLV-1h95) verwendet, die ein hervorragendes Sicherheitsprofil aufweisen und derzeit in verschiedenen Phase I/II Studien extensiv gestetet werden. Die Genome von VACV und MeV wurden dahingehend rekombinant modifiziert, dass diese Markergene und das Suizidgen SCD enthalten. SCD hat die Funktion, den primär nicht-toxischen Wikrstoff 5-FC in das gut bekannte Chemotherapeutikum 5-FU umzuwandeln, welches dann zusätzlich zur Zelltötung beiträgt. Somit kann in der Umgebung erfolgreich infizierter Tumorzellen eine SCD-basierte lokale Chemotherapie erfolgen.

MeV-SCD, GLV-1h68 und GLV-1h95 als potentielle Virotherapeutika wurden im Hinblick auf ihre Fähigkeit Tumorzellen zu infizieren, unter Inanspruchnahme des zellulären Biosyntheseapparates zu replizieren und die Tumorzellen letztlich zu töten, untersucht.

Unsere Ergebnisse zeigen, dass MeV-SCD primär Therapie-resistente Sarkomzelllinien in Abhängigkeit von deren CD46 Rezeptor-Expression töten können, wobei CD46 den Eintrittsmechanismus von MeV in Tumorzellen darstellt. Jene Sarkomzelllinien, die eine hohe CD46 Expression aufweisen, wurden besonders gut abgetötet, während Zelllinien mit niedrigerer CD46 Expression durch die virotherapeutische Behandlung mit MeV-SCD weniger geschädigt wurden. Das VACV-basierte Virotherapeutikum GLV-1h68 hingegen konnte alle primär Therapie-resistenten Sarkomzelllinien abtöten und war darüber hinaus fähig, die beiden Peritonealkarzinose-verursachenden Zelllinien CC531s und SKOV3ip.1 abzutöten. Auch die zuvor als „*in vivo* non-responder“ bezeichneten Zelllinien von Worschech et al. (2009) konnten im Rahmen dieser Arbeit unter *in vitro* Bedingungen erfolgreich abgetötet werden. Lediglich die am stärksten resistente Sarkomzelllinie SCOS konnte nur in der Kombination aus GLV-1h95 und gleichzeitig verabreichter prodrug 5-FC hinreichend abgetötet werden. Die zusätzliche Suizidgenfunktion des VACV GLV-1h95 konnte in unseren Experimenten nur bei der niedrigen MOI 0.1 eine onkolytische Effektivitätssteigerung bewirken, da bei höheren MOIs der direkte onkolytische Effekt zu dominant war als dass noch ein zusätzlicher Suizidgeneffekt hätte zum Tragen kommen können. Gesunde primäre humane Hepatozyten überlebten die Behandlung mit GLV-1h68 bei niedriger „Viruslast“ (MOI 0.1), bei höherer Viruslast (MOI 1) zeigten sich ebenfalls ausgeprägte zytotoxische Effekte, was allerdings weitestgehend auf die artifiziellen Verhältnisse der *in vitro* Primärzellkultur zurückgeführt werden muss, da sich in den bisherigen Klinischen Versuchen keine Korrelate für eine signifikante Leberzellschädigung finden lassen.

Aufgrund unserer vielversprechenden Ergebnisse postulieren wir, dass die von uns präklinisch getesteten Virotherapeutika sowohl in dem etablierten WAG/Rij

Ratten Model der Peritonealkarzinose als auch an primärem humanen Tumormaterial in Form von Zellvereinzelungen und primären humanen Gewebekulturschnitten getestet werden sollen, um die weitere klinische Entwicklung dieser beiden Virotherapeutika-Familien weiter voranzutreiben.

6 Abbreviations

APS	ammonium persulfate
ATCC	American Type Culture Collection
BSA	bovine serum albumin
CD46	cluster of differentiation 46 receptor
CD150	cluster of differentiation 150 receptor
CMC	Carboxymethylcellulose sodium salt
CPE	cytopathic effect
ctrl.	control
ddH_2O	double-distilled water
DMEM	Dulbecco`s modified Eagle medium
DMEM-2	DMEM supplemented with 2% FBS
DMEM-10	DMEM supplemented with 10% FBS
DMSO	Dimethylsulfoxide
DNA	desoxyribonucleic acid
dpi	days post infection
dUMP	deoxyuridine monophosphate
ECL	ECL detection reagent 1+2
EDTA	Ethylenediaminetetraacetic acid
eGFP	enhanced green fluorescent protein
FACS	**f**luorescence **a**ctivated **c**ell **s**orting
FBS	fetal bovine serum
GFP	green fluorescent protein
GLV-1h68	vaccinia vaccine virus
gusA	gene which encodes for *β*-glucoronidase
HA	hemagglutinin
HEPES	4-(2-hydroxyethyl)-1-piperazineethanesulfonic acid
HIPEC	Hypertherme intraperitoneale Chemoperfusion
hpi	hours post infection
HPLC	high performance liquid chromatography
HRP	horseradish peroxidase

i.p.	intraperitoneal
kb	kilo base
kDa	kilo Dalton
lacZ	gene which encodes for *β*-galactosidase
ld	leader
LDH	lactate dehydrogenase
LIVP	Lister strain from the Institute for Research on Viral Preparations
MeV	measles virus
MeV-GFP	measles virus including the leader sequence green fluorescence protein
MeV-SCD	measles virus including the leader sequence Super Cytosine Deaminase
MOI	multiplicity of infection
NAD^+	Nicotinadenindinukleotide $_{ox}$
NADH	Nicotinadenindinukleotide $_{red}$
NEAA	non-essential amino acids
NP40	Nonidet P-40, nonionic detergent
NR	non-responder
OD	optical density
PBS	phosphate buffered saline
PCTTS	Precision Cut Tumor Tissue Slices
PFA	paraformaldehyde
PFU	plaque forming unit
PHH	primary human hepatocytes
pos.	positive
PVDF	polyvinylidene difluoride
RNA	ribonucleic acid
RNAP	RNA polymerase
rpm	rounds per minute
RT	room temperature
RUC-GFP	Renilla Luciferase green fluorescent protein fusion gene
SCD	Super Cytosine Deaminase

SCS	Single Cell Suspension
SD	standard deviation
SDS	Sodiumdodecylsulfate
SEM	standard error of the mean
SLAM	Human **s**ignalling **l**ymphocyte **a**ctivation **m**olecule
SRB	sulforhodamine B
TBS	Tris-buffered saline
TBS-T	TBS-Triton = TBS+ 0.02% Triton X-100
TBS-Tween	Tris.buffered saline containing Tween 20
TCA	trichloracetic acid
TCID50	50% end point dilution assay
TEMED	tetramethylenediamine ($C_6H_{12}N_2$)
Tris	trishydroxymethylaminomethane
Triton X-100	nonionic detergent, Octylphenol ethylene oxide condensate
TS	thymidylate synthetase
UPRT	uracil phosphoribosyltransferase
UV	ultra violet
X-Gal	5-bromo-4-chloro-3-indolyl-*β*-D-galactopyranoside
YCD	yeast (Saccharomyces cerevisiae) Cytosine Deaminase
YUPRT	yeast (Saccharomyces cerevisiae) uracil phosphoribosyltransferase
5-FC	5-fluorocytosine
5-FU	5-fluorouracil
5-FdUMP	5-fluoro-deoxyuridine monophosphate
5-FUMP	5-fluorouridine monophosphate
5-FUTP	5-fluorouridine triphosphate

7 List of figures

FIGURE 1. ONCOLYTIC MECHANISM OF A VIRAL AGENT/VIROTHERAPEUTIC (LIU ET AL., 2004) 2
FIGURE 2. SCHEMATIC REPRESENTATION OF VACV 5
FIGURE 3. REPLICATION CYCLE OF VACV 6
FIGURE 4. GENOME OF THE GLV-1H68 VIRUS DERIVED FROM LIVP (ZHANGET AL., 2007) 7
FIGURE 5. GENOME OF THE GLV-1H95 VARIANT DERIVED FROM GLV-1H68 8
FIGURE 6. MEASLES VIRUS (MEV) INCLUDING SIX STRUCTURAL PROTEINS AND THE NEGATIVE STRAND RNA (GUY UNGERECHTS, NCT HEIDELBERG) 8
FIGURE 7. WILD TYPE MEV GENOME (LIGHT BLUE) AND MEV-SCD/GFP GENOME (ORANGE) 10
FIGURE 8. YEAST FCY1/FUR1 (FCU1) FUSION GENE (ERBS ET AL., 2000) 11
FIGURE 9. SUICIDE GENE THERAPY USING THE SUPER-CD/ 5-FC SYSTEM 12
FIGURE 10. NEUBAUER HAEMOCYTOMETER 19
FIGURE 11. 5-FC CONCENTRATIONS IN A 24-WELL PLATE 21
FIGURE 12. GREEN FLUORESCENCE INTENSITY MEASUREMENT 23
FIGURE 13. THE CORRECT ORDER OF THE BLOTTING MEMBRANES FROM BACK TO FRONT 30
FIGURE 14. THE OXIDATION OF NADH TO NAD^+ IS CATALYZED BY THE ENZYME LACTATE DEHYDROGENASE 34
FIGURE 15. SAMPLE DILUTION FOR VIRUS TITRATION IN DMEM-5 37
FIGURE 16. $TCID_{50}$-TITRATION FOR VIRAL GROWTH CURVE OF MEV LD-TRK 38
FIGURE 17. $TCID_{50}$-FORMULA BY SPEARMAN (1908) AND KÄRBER (1931) 38
FIGURE 18. 24-WELL PLATE AFTER CRYSTAL VIOLET STAINING SHOWING VARYING NUMBERS OF PLAQUES 42
FIGURE 19. LABELLING OF A $CD46^+$ CELL WITH ANTI-CD46-ANTIBODY AND PHYCOERYTHRIN (PE) 44
FIGURE 20. ELECTRON MICROSCOPY OF MEV-SCD INFECTED A673 CELLS 45
FIGURE 21. MEV-SCD INFECTION IN BRZ CELLS 46
FIGURE 22. MEV-SCD INFECTION IN BRZ CELLS 47
FIGURE 23. ELECTRON MICROSCOPY PHOTOS OF A SKOV3IP.1 CANCER CELL 48
FIGURE 24. GLV-1H68 INFECTED SKOV3IP.1 CELL 24 HPI 49
FIGURE 25. VIRAL REPLICATION IN A SKOV3IP.1 CELL 48 HPI WITH GLV-1H68 AT MOI 0.1 50
FIGURE 26. VIRUS-PRODUCTION IN A GLV-1H68 INFECTED SKOV3IP.1 CELL AT MOI 0.1 72 HPI 51
FIGURE 27. APOPTOTIC SKOV3IP.1 CELLS AFTER VIRUS PRODUCTION 52
FIGURE 28. APOPTOSIS IN VIRUS INFECTED SKOV3IP.1 CELLS 52
FIGURE 29. VIRUS PRODUCTION IN CC531S CELLS INFECTED WITH GLV-1H68 AT MOI 0.1 53
FIGURE 30. VIRUS-PRODUCTION IN CC531S CELLS INFECTED WITH GLV-1H68 AT MOI 0.1 24 HPI 54
FIGURE 31. FLOW-CYTOMETRIC QUANTIFICATION OF CD46 DENSITY ON TUMOR CELL SURFACES 56
FIGURE 32. MONITORING OF MEV-GFP-INFECTION BY FLUORESCENCE MICROSCOPY 58
FIGURE 33. LARGE SYNCYTIA-FORMATION OF BRZ CELLS AFTER MEV-SCD-INFECTION 59
FIGURE 34. WESTERN BLOT ANALYSIS OF SCD EXPRESSION IN A673 AND BRZ CELL LYSATES 60
FIGURE 35. GFP-MONITORING OF FLUORESCENCE INTENSITY IN GLV-1H68 INFECTED CELL LINES 61
FIGURE 36. MEASUREMENT OF INFECTION KINETICS IN GLV-1H68 INFECTED SKOV3IP.1 CELLS 62
FIGURE 37. X-GAL-STAINING OF GLV-1H68 INFECTED CELLS 63
FIGURE 38. *B*-GALACTOSIDASE EXPRESSION OF GLV-1H68-INFECTED CC531S CELLS 64
FIGURE 39. MEV-SCD REPLICATION IN A673 AND BRZ CELLS 65
FIGURE 40. REPLICATION BEHAVIOUR OF GLV-1H68 IN CC531S AND SKOV3IP.1 CELLS 67
FIGURE 41. 5-FU TREATMENT OF TUMOR CELL LINES TO ENSURE SUSCEPTIBILITY 69
FIGURE 42. MEASUREMENT OF A673 AND BRZ CELL MASS DECREASE AFTER MEV-SCD INFECTION 70
FIGURE 43. CYTOTOXIC EFFECT OF MEV-SCD AND 5-FC ON A673 AND BRZ CELLS IN VITRO 71
FIGURE 44. ALTERNATIVE TREATMENT OF BRZ CELLS WITH 5-FC 48 HPI TO ENHANCE VIRAL REPLICATION 72
FIGURE 45. SRH CELLS SURVIVED MEV-SCD TREATMENT WITH HIGH MOI 1 73
FIGURE 46. HIGH MOI 10 COMBINED WITH 1 MM 5-FC KILLS SRH CELLS 144 HPI 74
FIGURE 47. SCOS CELLS RESISTED COMBINATION TREATMENT WITH MEV-SCD AT MOI 10 76
FIGURE 48. CYTOTOXIC EFFECT OF GLV-1H68 ON SRH CELLS 78
FIGURE 49. CYTOTOXIC EFFECT OF GLV-1H68 ON PLC/PRF/5 CELLS 79
FIGURE 50. ERADICATION OF CC531S CELLS BY GLV-1H68 80
FIGURE 51. CYTOTOXIC EFFECT OF GLV-1H68 ON SKOV3IP.1 CELLS 81

FIGURE 52. CYTOTOXIC EFFECT OF GLV-1H68 ON SCOS CELLS 82
FIGURE 53. GLV-1H95 COMBINED WITH 5-FC SHOWED HIGHLY CYTOTOXIC EFFECT ON SCOS CELLS 83
FIGURE 54. GFP EXPRESSION AFTER GLV-1H68-INFECTION VIA GFP-FLUORESCENCE-MONITORING AND PHASE CONTRAST MICROSCOPY 85
FIGURE 55. GLV-1H68 AND GLV-1H95 MINIMIZE NCI-H1299 CELL MASS TO THE SAME EXTENT 86
FIGURE 56. GLV-1H95 ENHANCES THE CYTOTOXIC EFFECT OF GLV-1H68 ON HT29 CELLS 87
FIGURE 57. GLV-1H95 ENHANCES THE CYTOTOXIC EFFECT OF GLV-1H68 ON SIHA CELLS 88
FIGURE 58. REPLICATION BEHAVIOUR OF GLV-1H68 IN HT29, NCI-H1299 AND SIHA AND CELLS 89
FIGURE 59. INFECTION OF PHH WITH GLV-1H68 90
FIGURE 60. INFECTION OF PHH WITH GLV-1H68 91

8 List of tables

TABLE 1. GROWTH AREA AND VOLUMES USED IN VARIOUS CULTURE VESSELS 18
TABLE 2. VOLUMES USED FOR CULTURE MEDIUM AND INOCULUM IN DIFFERENT CELL CULTURES 20
TABLE 3. FIXATION AND STAINING SOLUTION FOR *B*-GALACTOSIDASE-STAINING USING X-GAL 25
TABLE 4. CHEMICALS FOR WESTERN BLOT ANALYSIS 26
TABLE 5. PRIMARY ANTIBODIES FOR WESTERN BLOT 26
TABLE 6. SECONDARY ANTIBODIES FOR WESTERN BLOT ANALYSIS 27
TABLE 7. COMPOSITION OF THE STACKING AND THE SEPARATING GEL 29
TABLE 8. MATERIALS FOR SRB ASSAY 32
TABLE 9. MATERIALS FOR LDH-RELEASE ASSAY 33
TABLE 10. MATERIALS FOR THE ESTABLISHMENT OF A MEASLES VIRUS GROWTH CURVE 36
TABLE 11. MATERIALS FOR THE PREPARATION OF VIRUS PLAQUING OVERLAY MEDIUM CMC 39
TABLE 12. MATERIALS FOR CRYSTAL VIOLET STAIN 39
TABLE 13. VIRAL DILUTION SERIES FOR VIRUS TITRATION ON CV-1 CELLS 41
TABLE 14. FROM PLAQUE ASSAY COUNT TO VIRAL TITER 42
TABLE 15. MATERIALS FOR FLOW CYTOMETRY 43

9 References

Akbulut H, Zhang L, Tang Y, Deisseroth A. (2003). "Cytotoxic effect of replication-competent adenoviral vectors carrying L-plastin promoter regulated E1A and cytosine deaminase genes in cancers of the breast, ovary and colon." Cancer Gene Ther **10**(5): 388-395.

Al'tshteĭn AD, Zakharova LG, Loparev VN, Pashvykina GV, Gorodetskiĭ SI (1985). "Isolation of a recombinant vaccinia virus based on the LIVP strain inducing the surface antigen of the hepatitis B virus." Dokl Akad Nauk SSSR **285**(3): 696-9.

American Cancer Society (2011). Global Cancer Facts & Figures 2nd Edition, No. 861811.

Anderson LM, Krotz S, Weitzman SA, and Thimmapaya B (2000). "Breast cancer-specific expression of the Candida albicans cytosine deaminase gene using a transcriptional targeting approach." Cancer Gene Ther *7*, 845-852.

Anderson BD, Nakamura T, Russell SJ, Peng KW. (2004). "High CD46 Receptor Density Determines Preferential Killing of Tumor Cells by Oncolytic Measles Virus." Cancer Research 64, 4919–4926

Arakawa S Jr, Hamami G, Umezu K, Kamidono S, Ishigami J, Arakawa S. (1987). "Clinical trial of attenuated vaccinia virus AS strain in the treatment of advanced adenocarcinoma. Report on two cases." J Cancer Res Clin Oncol **113**(1): 95-98.

Arnold D, Lordick, F (2007). "Systemic treatment of peritoneal metastases." Chirurg; 78:1117-22.

Blechacz B, Splinter PL, Greiner S, Myers R, Peng KW, Federspiel MJ, Russell SJ, LaRusso NF. (2006), "Engineered measles virus as a novel oncolytic viral therapy system for hepatocellular carcinoma." Hepatology **44**(6): 1465-77.

Bluming AZ, Ziegler JL. (1971). "Regression of Burkitt's lymphoma in association with measles infection." Lancet **2**(7715): 105-106.

Buller RM, Smith GL, Cremer K, Notkins AL, Moss B. (1985) "Decreased virulence of recombinant vaccinia virus expression vectors is associated with a thymidine kinase-negative phenotype." Nature Oct 31-Nov 6; **317**(6040):813-5.

Carter GC, Law M, Hollinshead M, Smith GL. (2005). "Entry of the vaccinia virus intracellular mature virion and its interactions with glycosaminoglycans." J Gen Virol **86**(Pt 5): 1279-1290.

Chen N, Zhang Q, Yu YA, Stritzker J, Brader P, Schirbel A, Samnick S, Serganova I, Blasberg R, Fong Y, Szalay AA. (2009). "A novel recombinant vaccinia virus expressing the human norepinephrine transporter retains oncolytic potential and facilitates deep-tissue imaging." Mol Med. 2009 May-Jun;15(5-6):144-51. Epub 2009 Feb 25.

Chung-Faye GA, Chen MJ, Green NK, Burton A, Anderson D, Mautner V, Searle PF, Kerr DJ. (2001). "In vivo gene therapy for colon cancer using adenovirus-mediated,

transfer of the fusion gene cytosine deaminase and uracil phosphoribosyltransferase." Gene Ther **8**(20): 1547-1554.

Coffey MC, Strong JE, Forsyth PA, Lee PW. (1998). "Reovirus therapy of tumors with activated Ras pathway." Science **282**(5392): 1332-1334.

Cono J, Casey CG, Bell DM; Centers for Disease Control and Prevention. (2003). "Smallpox vaccination and adverse reactions. Guidance for clinicians." MMWR Recomm Rep **52**(RR-4): 1-28.

Cripe TP, Dunphy EJ, Holub AD, Saini A, Vasi NH, Mahller YY, Collins MH, Snyder JD, Krasnykh V, Curiel DT, Wickham TJ, DeGregori J, Bergelson JM, Currier MA. (2001). "Fiber knob modifications overcome low, heterogeneous expression of the coxsackievirus-adenovirus receptor that limits adenovirus gene transfer and oncolysis for human rhabdomyosarcoma cells." Cancer Res **61**(7): 2953-2960.

Dörig RE, Marcil A, Chopra A, Richardson CD. (1993). "The human CD46 molecule is a receptor for measles virus (Edmonston strain)." Cell **75**, 295-305.

Enders JF, Peebles TC. (1954). "Propagation in tissue cultures of cytopathogenic agents from patients with measles." Proc Soc Exp Biol Med **86**(2): 277-286.

Erbs P, Exinger F, Jund R. (1997). "Characterization of the Saccharomyces cerevisiae FCY1 gene encoding cytosine deaminase and its homologue FCA1 of Candida albicans." Curr Genet **31**(1): 1-6.

Erbs P, Regulier E, Kintz J, Leroy P, Poitevin Y, Exinger F, Jund R, Mehtali M. (2000). "In vivo cancer gene therapy by adenovirus-mediated transfer of a bifunctional yeast cytosine deaminase/uracil phosphoribosyltransferase fusion gene" Cancer Res. **60**(14): 3813-22

Esquivel J, Vidal-Jove J, Steves MA, Sugarbaker PH. (1993). "Morbidity and mortality of cytoreductive surgery and intraperitoneal chemotherapy." Surgery **113**(6): 631-636.

Fenner F. (1993). "Smallpox: emergence, global spread, and eradication." Hist Philos Life Sci **15**(3): 397-420.

Ferlay J, Shin HR, Bray F, Forman D, Mathers CD, Parkin D. GLOBO-CAN 2008, Cancer Incidence and Mortality Worldwide: IARC Cancer-Base No.10 [Internet]. Lyon, France: International Agency for Research on Cancer.2010; Available from: http://globocan.iarc.fr

Fogar P, Navaglia F, Basso D, Greco E, Zambon CF, Fadi E, Falda A, Stranges A, Vannozzi F, Danesi R, Pedrazzoli S, Plebani M. (2007). "Suicide gene therapy with the yeast fusion gene cytosine deaminase/uracil phosphoribosyltransferase is not enough for pancreatic cancer." Pancreas **35**(3): 224-31.

Foloppe J, Kintz J, Futin N, Findeli A, Cordier P, Schlesinger Y, Hoffmann C, Tosch C, Balloul JM, Erbs P. (2008) "Targeted delivery of a suicide gene to human colorectal tumors by a conditionally replicating vaccinia virus." Gene Ther. **15**(20): 1361-71.

Frentzen A, Yu YA, Chen N, Zhang Q, Weibel S, Raab V, Szalay AA. (2009), "Anti-VEGF single-chain antibody GLAF-1 encoded by oncolytic vaccinia virus significantly enhances antitumor therapy." Proc Natl Acad Sci U S A **106**, 12915-12920

Freytag SO, Stricker H, Pegg J, Paielli D, Pradhan DG, Peabody J, DePeralta-Venturina M, Xia X, Brown S, Lu M, Kim JH. (2003), „Phase I study of replication-competent adenovirus-mediated double-suicide gene therapy in combination with conventional-dose three-dimensional conformal radiation therapy for the treatment of newly diagnosed, intermediate- to high-risk prostate cancer." Cancer Res **63**(21): 7497-506.

Gentschev I, Müller M, Adelfinger M, Weibel S, Grummt F, Zimmermann M, Bitzer M, Heisig M, Zhang Q, Yu YA, Chen NG, Stritzker J, Lauer UM, Szalay AA. (2011). "Efficient colonization and therapy of human hepatocellular carcinoma (HCC) using the oncolytic vaccinia virus strain GLV-1h68." *PLoS One* **6**, e22069.

Gentschev I, Ehrig K, Donat U, Hess M, Rudolph S, Chen N, Yu YA, Zhang Q, Bullerdiek J, Nolte I, Stritzker J, Szalay AA. (2010). "Significant Growth Inhibition of Canine Mammary Carcinoma Xenografts following Treatment with Oncolytic Vaccinia Virus GLV-1h68." J Oncol **2010**: 736907.

Gentschev I, Stritzker J, Hofmann E, Weibel S, Yu YA, Chen N, Zhang Q, Bullerdiek J, Nolte I, Szalay AA. (2009). "Use of an oncolytic vaccinia virus for the treatment of canine breast cancer in nude mice: preclinical development of a therapeutic agent." Cancer Gene Ther **16**(4): 320-328.

Gentschev I, Donat U, Hofmann E, Weibel S, Adelfinger M, Raab V, Heisig M, Chen N, Yu YA, Stritzker J, Szalay AA. (2010). "Regression of Human Prostate Tumors and Metastases in Nude Mice following Treatment with the Recombinant Oncolytic Vaccinia Virus GLV-1h68." J Biomed Biotechnol, 489759 Epub.

Glehen O, Cotte E, Schreiber V, Sayag-Beaujard AC, Vignal J, Gilly FN. (2004). "Intraperitoneal chemohyperthermia and attempted cytoreductive surgery in patients with peritoneal carcinomatosis of colorectal origin." Br J Surg **91**(6): 747-754.

Glockzin G, Ghali N, Lang SA, Agha A, Schlitt HJ, Piso P**.** (2007). "Peritoneal carcinomatosis. Surgical treatment, including hyperthermal intraperitoneal chemotherapy." Chirurg **78**(12): 1100, 1102-1106, 1108-1110.

Gnant MF, Puhlmann M, Bartlett DL, Alexander HR Jr. (1999). "Regional versus systemic delivery of recombinant vaccinia virus as suicide gene therapy for murine liver metastases." Ann Surg **230**(3): 352-360; discussion 360-351.

Gnant MF, Puhlmann M, Alexander HR Jr, Bartlett DL. (1999). "Systemic administration of a recombinant vaccinia virus expressing the cytosine deaminase gene and subsequent treatment with 5-fluorocytosine leads to tumor-specific gene expression and prolongation of survival in mice." Cancer Res **59**(14): 3396-3403.

Graepler F, Lemken ML, Wybranietz WA, Schmidt U, Smirnow I, Gross CD, Spiegel M, Schenk A, Graf H, Lauer UA, Vonthein R, Gregor M, Armeanu S, Bitzer M, Lauer UM. (2005), "Bifunctional chimeric SuperCD suicide gene -YCD: YUPRT fusion is highly effective in a rat hepatoma model." World J Gastroenterol **11**(44): 6910-9.

Greentree LB. (1983). "Hodgkin's disease: therapeutic role of measles vaccine." Am J Med **75**(6): 928
Griffin, D., and Bellini, W. Measles virus. In: Fields, D. Knipe, and P. Howley (eds.), Fields Virology, Vol. 3, pp. 1267-1312. New York: Lippincott-Raven Publishers, 1996.

Grote D, Russell SJ, Cornu TI, Cattaneo R, Vile R, Poland GA, Fielding AK. (2001). "Live attenuated measles virus induces regression of human lymphoma xenografts in immunodeficient mice." Blood **97**(12): 3746-3754.

Guse K, Sloniecka M, Diaconu I, Ottolino-Perry K, Tang N, Ng C, Le Boeuf F, Bell JC, McCart JA, Ristimäki A, Pesonen S, Cerullo V, Hemminki A. (2010). "Antiangiogenic arming of an oncolytic vaccinia virus enhances antitumor efficacy in renal cell cancer models." J Virol **84**(2): 856-866.

de Haan PG, Felix HS, Peters R. (1972). "Mapping of the gene for cytosine deaminase on the Escherichia coli chromosome." Antonie Van Leeuwenhoek **38**(3): 257-263.

Hamid O, Varterasian ML, Wadler S, Hecht JR, Benson A 3rd, Galanis E, Uprichard M, Omer C, Bycott P, Hackman RC, Shields AF. (2003). "Phase II trial of intravenous CI-1042 in patients with metastatic colorectal cancer." J Clin Oncol **21**(8): 1498-1504.

Hamstra DA, Rice DJ, Fahmy S, Ross BD, Rehemtulla A. (1999). "Enzyme/prodrug therapy for head and neck cancer using a catalytically superior cytosine deaminase." Hum Gene Ther **10**(12): 1993-2003.

Hanna NN, Mauceri HJ, Wayne JD, Hallahan DE, Kufe DW, Weichselbaum RR. (1997). “Virally directed cytosine deaminase/5-fluorocytosine gene therapy enhances radiation response in human cancer xenografts.” Cancer Res *57*, 4205-4209.

Hansen RM, Libnoch JA. (1978). "Remission of chronic lymphocytic leukemia after smallpox vaccination." Arch Intern Med **138**(7): 1137-1138.

Hasegawa K, Pham L, O'Connor MK, Federspiel MJ, Russell SJ, Peng KW. (2006). “Dual therapy of ovarian cancer using measles viruses expressing carcinoembryonic antigen and sodium iodide symporter.” Clin Cancer Res. **12**(6): 1868-75.

He S, Li P, Chen CH, Bakst RL, Chernichenko N, Yu YA, Chen N, Szalay AA, Yu Z, Fong Y, Wong RJ. (2012). “Effective oncolytic vaccinia therapy for human sarcomas.” J Surg Res **175**(2): 53-60.

Heinzerling L, Künzi V, Oberholzer PA, Kündig T, Naim H, Dummer R. (2005). „Oncolytic measles virus in cutaneous T-cell lymphomas mounts antitumor immune responses in vivo and targets interferon-resistant tumor cells.” Blood 7: 2287-94.

Hofer S., Herrmann R. (1998). "40 years of 5-fluorouracil--still an attractive cytostatic." Schweiz Med Wochenschr. **128**(34): 1253-1260.

Kanai R, Wakimoto H, Cheema T, Rabkin SD. (2010). "Oncolytic herpes simplex virus vectors and chemotherapy: are combinatorial strategies more effective for cancer?" Future Oncol **6**(4): 619-634.

Kelly KJ, Brader P, Woo Y, Li S, Chen N, Yu YA, Szalay AA, Fong Y. (2009). "Real-time intraoperative detection of melanoma lymph node metastases using recombinant

vaccinia virus GLV-1h68 in an immunocompetent animal model." Int J Cancer **124**(4): 911-918.

Kelly KJ, Woo Y, Brader P, Yu Z, Riedl C, Lin SF, Chen N, Yu YA, Rusch VW, Szalay AA, Fong Y. (2008). "Novel oncolytic agent GLV-1h68 is effective against malignant pleural mesothelioma." Hum Gene Ther **19**(8): 774-782.

Khuri FR, Nemunaitis J, Ganly I, Arseneau J, Tannock IF, Romel L, Gore M, Ironside J, MacDougall RH, Heise C, Randlev B, Gillenwater AM, Bruso P, Kaye SB, Hong WK, Kirn DH. (2000). "A controlled trial of intratumoral ONYX-015, a selectively-replicating adenovirus, in combination with cisplatin and 5-fluorouracil in patients with recurrent head and neck cancer." Nat Med **6**(8): 879-885.

Kievit E, Bershad E, Ng E, Sethna P, Dev I, Lawrence TS, Rehemtulla A. (1999). "Superiority of yeast over bacterial cytosine deaminase for enzyme/prodrug gene therapy in colon cancer xenografts." Cancer Res **59**, 1417-1421.

Kim JH, Oh JY, Park BH, Lee DE, Kim JS, Park HE, Roh MS, Je JE, Yoon JH, Thorne SH, Kirn D, Hwang TH. (2006). "Systemic armed oncolytic and immunologic therapy for cancer with JX-594, a targeted poxvirus expressing GM-CSF." Mol Ther **14**(3): 361-370.

Kirn DH, Thorne SH. (2009). "Targeted and armed oncolytic poxviruses: a novel multi-mechanistic therapeutic class for cancer." Nat Rev Cancer **9**(1): 64-71.

Klinikum der Universität München LMU, "Interner Klinikleitfaden, Kolorektales Karzinom"
http://www.klinikum.uni-muenchen.de/Medizinische-Klinik-und-Poliklinik-II/de/downloads/klinikleitfaden/index.html

Königsrainer I, Aschoff P, Zieker D, Beckert S, Glatzle J, Pfannenberg C, Miller S, Hartmann JT, Schroeder TH, Brücher BL, Königsrainer A. (2008) "Selection criteria for peritonectomy with hyperthermic intraoperative chemotherapy (HIPEC) in peritoneal carcinomatosis." Zentralbl Chir. Sep;133:468-72.

Kuriyama S, Mitoro A, Yamazaki M, Tsujinoue H, Nakatani T, Akahane T, Toyokawa Y, Kojima H, Okamoto S, Fukui H. (1999). "Comparison of gene therapy with the herpes simplex virus thymidine kinase gene and the bacterial cytosine deaminase gene for the treatment of hepatocellular carcinoma." Scand J Gastroenterol **34**(10): 1033-1041.

Kuriyama S, Masui K, Sakamoto T, Nakatani T, Kikukawa M, Tsujinoue H, Mitoro A, Yamazaki M, Yoshiji H, Fukui H, Ikenaka K, Mullen CA, Tsujii T. (1998). "Bystander effect caused by cytosine deaminase gene and 5-fluorocytosine in vitro is substantially mediated by generated 5-fluorouracil, Anticancer Res. **18** (5A): 3399-406.

Lampe J. (2012). "Armed oncolytic measles vaccine virus for the treatment of hepatocellular carcinoma." (Dissertation)

Lemken ML, Graepler F, Wolf C, Wybranietz WA, Smirnow I, Schmidt U, Gregor M, Bitzer M, Lauer UM. (2007). „Fusion of HSV-1 VP22 to a bifunctional chimeric SuperCD suicide gene compensates for low suicide gene transduction efficiencies." Int J Oncol **30**(5): 1153-61

Lin SF, Yu Z, Riedl C, Woo Y, Zhang Q, Yu YA, Timiryasova T, Chen N, Shah JP, Szalay AA, Fong Y, Wong RJ. (2007). "Treatment of anaplastic thyroid carcinoma in vitro with a mutant vaccinia virus." Surgery **142**(6): 976-983; discussion 976-983.

Lin SF, Price DL, Chen CH, Brader P, Li S, Gonzalez L, Zhang Q, Yu YA, Chen N, Szalay AA, Fong Y, Wong RJ. (2008). "Oncolytic vaccinia virotherapy of anaplastic thyroid cancer in vivo." J Clin Endocrinol Metab **93**(11): 4403-4407.

Liu TC, Galanis E, Kirn D. (2007). "Clinical trial results with oncolytic virotherapy: a century of promise, a decade of progress." Nat Clin Pract Oncol **4**(2): 101-117.

Lorence RM, Rood PA, Kelley KW. (1988). "Newcastle disease virus as an antineoplastic agent: induction of tumor necrosis factor-alpha and augmentation of its cytotoxicity." J Natl Cancer Inst **80**(16): 1305-1312.

Mahoney DJ, Stojdl DF. (2010), "Potentiating oncolytic viruses by targeted drug intervention." Curr Opin Mol Ther **12**, 394-402.

Mastrangelo MJ, Eisenlohr LC, Gomella L, Lattime EC. (2000). "Poxvirus vectors: orphaned and underappreciated." J Clin Invest **105**(8): 1031-1034.

McCart, J. A., Puhlmann, M. et al. (2000). "Complex interactions between the replicating oncolytic effect and the enzyme/prodrug effect of vaccinia-mediated tumor regression." Gene Ther **7**(14): 1217-1223.

Meng X, Nakamura T, Okazaki T, Inoue H, Takahashi A, Miyamoto S, Sakaguchi G, Eto M, Naito S, Takeda M, Yanagi Y, Tani K. (2010). "Enhanced antitumor effects of an engineered measles virus Edmonston strain expressing the wild-type N, P, L genes on human renal cell carcinoma." Mol Ther **18**(3): 544-551.

Moss B. (2006). "Poxvirus entry and membrane fusion." Virology **344**(1): 48-54.

Moss B, Earl, PL. (1998). "*Expression of proteins in mammalian cells using vaccinia viral vectors*." Current protocols in Molecular Biology 16.15.1-16.15.5.

Naniche D, Varior-Krishnan G, Cervoni F, Wild TF, Rossi B, Rabourdin-Combe C, Gerlier D. (1993). "Human membrane cofactor protein (CD46) acts as a cellular receptor for measles virus." J Virol **67**, 6025-6032.

Nemunaitis J, Khuri F, Ganly I, Arseneau J, Posner M, Vokes E, Kuhn J, McCarty T, Landers S, Blackburn A, Romel L, Randlev B, Kaye S, Kirn D. (2001). "Phase II trial of intratumoral administration of ONYX-015, a replication-selective adenovirus, in patients with refractory head and neck cancer." J Clin Oncol **19**(2): 289-298.

Nishiyama T, Kawamura Y, Kawamoto K, Matsumura H, Yamamoto N, Ito T, Ohyama A, Katsuragi T, Sakai T. (1982). "[Antineoplastic effect of 5-fluorocytosine and cytosine deaminase on brain tumor (author's transl)]." Neurol Med Chir (Tokyo) **22**(5): 344-352.

Ong HT, Timm MM, Greipp PR, Witzig TE, Dispenzieri A, Russell SJ, Peng KW. (2006). "Oncolytic measles virus targets high CD46 expression on multiple myeloma cells." Exp Hematol **34**(6): 713-720.

Ottolino-Perry K, Diallo JS, Lichty BD, Bell JC, McCart JA. (2010). "Intelligent design: combination therapy with oncolytic viruses." Mol Ther **18**(2): 251-263.
Park BH, Hwang T, Liu TC, Sze DY, Kim JS, Kwon HC, Oh SY, Han SY, Yoon JH, Hong SH, Moon A, Speth K, Park C, Ahn YJ, Daneshmand M, Rhee BG, Pinedo HM, Bell JC, Kirn DH. (2008). "Use of a targeted oncolytic poxvirus, JX-594, in patients with refractory primary or metastatic liver cancer: a phase I trial." Lancet Oncol **9**(6): 533-542.

Parker JN, Gillespie GY, Love CE, Randall S, Whitley RJ, Markert JM. (2000), "Engineered herpes simplex virus expressing IL-12 in the treatment of experimental murine brain tumors." Proc Natl Acad Sci U S A **97**, 2208-2213.

Pasquinucci G. (1971). "Possible effect of measles on leukaemia." Lancet **1**(7690): 136.

Pederson LC, Buchsbaum DJ, Vickers SM, Kancharla SR, Mayo MS, Curiel DT, Stackhouse MA. (1997). "Molecular chemotherapy combined with radiation therapy enhances killing of cholangiocarcinoma cells in vitro and in vivo." Cancer Res **57**: 4325-4332.

Pederson LC, Vickers SM, Buchsbaum DJ, Kancharla SR, Mayo MS, Curiel DT, Stackhouse MA. (1998). "Combined cytosine deaminase expression, 5-fluorocytosine exposure, and radiotherapy increases cytotoxicity to cholangiocarcinoma cells." J Gastrointest Surg **2**: 283-291.

Pelz JO, Doerfer J, Hohenberger W, Meyer T. (2005). "A new survival model for hyperthermic intraperitoneal chemotherapy (HIPEC) in tumor-bearing rats in the treatment of peritoneal carcinomatosis." BMC Cancer **30**;5:56.

Pelz JO, Doerfer J, Dimmler A, Hohenberger W, Meyer T. (2006). "Histological response of peritoneal carcinomatosis after hyperthermic intraperitoneal chemoperfusion (HIPEC) in experimental investigations." BMC Cancer **22**;6:162.

Pelz JO, Doerfer J, Hohenberger W, Meyer T. (2005). "A new survival model for hyperthermic intraperitoneal chemotherapy (HIPEC) in tumor-bearing rats in the treatment of peritoneal carcinomatosis." BMC Cancer **30**;5:56.

Peng KW, TenEyck CJ, Galanis E, Kalli KR, Hartmann LC, Russell SJ. (2002). "Intraperitoneal therapy of ovarian cancer using an engineered measles virus." Cancer Res. **62**(16): 4656-62.

Peng KW, Ahmann GJ, Pham L, Greipp PR, Cattaneo R, Russell SJ. (2001). „Systemic therapy of myeloma xenografts by an attenuated measles virus." Blood **98**(7): 2002-2007.

Phuong LK, Allen C, Peng KW, Giannini C, Greiner S, TenEyck CJ, Mishra PK, Macura SI, Russell SJ, Galanis EC. (2003). "Use of a vaccine strain of measles virus genetically engineered to produce carcinoembryonic antigen as a novel therapeutic agent against glioblastoma multiforme." Cancer Res **63**(10): 2462-2469.

Pichler BJ, Wehrl HF, Judenhofer MS. (2008) „Latest advances in molecular imaging instrumentation." J Nucl Med.49 Suppl 2:5S-23S. Review.

Pross M, Schulz HU, Günther T, Hönl K, Mantke R, Koch A, Halangk W, Reymond MA, Lippert H. (2001). “Real-time assessment of intraperitoneal tumor growth in a rat model using CEA immunoscintigraphy. Surgery **129**(6): 745-8.

Rabenau und Schwebke, 2005.

Roizman B, Joklik W, Fields B, Moss B, (1994). “The destruction of smallpox virus stocks in national repositories: a grave mistake and a bad precedent.” Infect Agents Dis. **3**(5): 215-7.

Sadeghi B, Arvieux C, Glehen O, Beaujard AC, Rivoire M, Baulieux J, Fontaumard E, Brachet A, Caillot JL, Faure JL, Porcheron J, Peix JL, François Y, Vignal J, Gilly FN. (2000). "Peritoneal carcinomatosis from non-gynecologic malignancies: results of the EVOCAPE 1 multicentric prospective study." Cancer **88**(2): 358-363.

Seo E, Abei M, Wakayama M, Fukuda K, Ugai H, Murata T, Todoroki T, Matsuzaki Y, Tanaka N, Hamada H, Yokoyama KK. (2005). “Effective gene therapy of biliary tract cancers by a conditionally replicative adenovirus expressing uracil phosphoribosyltransferase: significance of timing of 5-fluorouracil administration.” Cancer Res **65**, 546-552.

Seubert CM, Stritzker J, Hess M, Donat U, Sturm JB, Chen N, von Hof JM, Krewer B, Tietze LF, Gentschev I, Szalay AA. (2011). "Enhanced tumor therapy using vaccinia virus strain GLV-1h68 in combination with a beta-galactosidase-activatable prodrug seco-analog of duocarmycin SA." Cancer Gene Ther **18**(1): 42-52.

Shu-Fu L, Yu Z, Riedl C, Woo Y, Zhang Q, Yu YA, Timiryasova T, Chen N, Shah JP, Szalay AA, Fong Y, Wong RJ. (2007). “Treatment of anaplastic thyroid carcinoma in vitro with a mutant vaccinia virus.” Surgery **14**(6): 976-983.

Skehan P, Storeng R, Scudiero D, Monks A, McMahon J, Vistica D, Warren JT, Bokesch H, Kennedy S, Boyd MR. (1990). “New colorimetric cytotoxicity assay for anticancer-drug screening.” J Natl Cancer Inst **82**: 1107-1112.

Springfeld C, von Messling V, Frenzke M, Ungerechts G, Buchholz CJ, Cattaneo R. (2006) “Oncolytic efficacy and enhanced safety of measles virus activated by tumor-secreted matrix metalloproteinases.” Cancer Res. **66**(15):7694-700.

Stackhouse MA, Pederson LC, Grizzle WE, Curiel DT, Gebert J, Haack K, Vickers SM, Mayo MS, Buchsbaum DJ. (2000). “Fractionated radiation therapy in combination with adenoviral delivery of the cytosine deaminase gene and 5-fluorocytosine enhances cytotoxic and antitumor effects in human colorectal and cholangiocarcinoma models.“ Gene Ther **7**(12): 1019-26.

Stojdl DF, Lichty B, Knowles S, Marius R, Atkins H, Sonenberg N, Bell JC. (2000). "Exploiting tumor-specific defects in the interferon pathway with a previously unknown oncolytic virus." Nat Med **6**(7): 821-825.

Sugarbaker PH. (2007). "Peritonectomy procedures." Cancer Treat Res **134**: 247-264.

Taqi AM, Abdurrahman MB, Yakubu AM, Fleming AF. (1981). "Regression of Hodgkin's disease after measles." Lancet **1**(8229): 1112.

Tassel D, Madoff MA. (1968). "Treatment of Candida sepsis and Cryptococcus meningitis with 5-fluorocytosine. A new antifungal agent." JAMA **206**(4): 830-832.

Thorne SH, Tam BY, Kirn DH, Contag CH, Kuo CJ. (2006). "Selective intratumoral amplification of an antiangiogenic vector by an oncolytic virus produces enhanced antivascular and anti-tumor efficacy." Mol Ther **13**(5): 938-946.

Toth K, Kuppuswamy M, Shashkova EV, Spencer JF, Wold WS. (2010). "A fully replication-competent adenovirus vector with enhanced oncolytic properties." Cancer Gene Ther **17**(11): 761-770.

Ungerechts G, Springfeld C, Frenzke ME, Lampe J, Johnston PB, Parker WB, Sorscher EJ, Cattaneo R. (2007). "Lymphoma chemovirotherapy: CD20-targeted and convertase-armed measles virus can synergize with fludarabine." Cancer Res. **67**(22): 10939-47.

Ungerechts, G., Frenzke, M.E., Yaiw, K.C., Miest, T., Johnston, P.B., and Cattaneo, R. (2010). "Mantle cell lymphoma salvage regimen: synergy between a reprogrammed oncolytic virus and two chemotherapeutics." Gene Ther. **17**(12):1506-16.

Vanderplasschen A, Hollinshead M, Smith GL. (1998). "Intracellular and extracellular vaccinia virions enter cells by different mechanisms." J Gen Virol **79 (Pt 4)**: 877-887.

Vanderplasschen A, Mathew E, Hollinshead M, Sim RB, Smith GL. (1998). "Extracellular enveloped vaccinia virus is resistant to complement because of incorporation of host complement control proteins into its envelope." Proc Natl Acad Sci U S A **95**(13): 7544-7549.

Verwaal VJ, van Ruth S, de Bree E, van Sloothen GW, van Tinteren H, Boot H, Zoetmulder FA. (2003). "Randomized trial of cytoreduction and hyperthermic intraperitoneal chemotherapy versus systemic chemotherapy and palliative surgery in patients with peritoneal carcinomatosis of colorectal cancer." J Clin Oncol **21**(20): 3737-3743.

Warmann SW, Armeanu S, Heigoldt H, Ruck P, Vonthein R, Heitmann H, Seitz G, Lemken ML, Bitzer M, Fuchs J, Lauer UM. (2009), "Adenovirus-mediated cytosine deaminase/5-fluorocytosine suicide gene therapy of human hepatoblastoma in vitro." Pediatr Blood Cancer **53**(2): 145-51.

Warmann SW, Armeanu S, Frank H, Buck H, Graepler F, Lemken ML, Heitmann H, Seitz G, Lauer UM, Bitzer M, Fuchs J. (2006a), "In vitro gene targeting in human hepatoblastoma" Pediatr Surg Int **22**(1): 16-23.

Warmann SW, Armeanu S, Heitmann H, Ruck P, Seitz G, Wessels JT, Lemken ML, Lauer UM, Fuchs J, Bitzer M. (2006b), "Optimizing vector application for gene transfer into human hepatoblastoma cells." Pediatr Surg Int **22**(9): 733-42.

Wildner O. (1999). "In situ use of suicide genes for therapy of brain tumours." Ann Med **31**(6): 421-9.

Wong RJ, Patel SG, Kim S, DeMatteo RP, Malhotra S, Bennett JJ, St-Louis M, Shah JP, Johnson PA, Fong Y. (2001), "Cytokine gene transfer enhances herpes oncolytic therapy in murine squamous cell carcinoma." Hum Gene Ther **12**, 253-265

Worschech A. (2010) : “Oncolytic therapy with Vaccinia virus GLV-1h68, comparative microarray analysis of infected xenografts and infected human tumor cell lines.” (Dissertation)

Worschech A, Chen N, Yu YA, Zhang Q, Pos Z, Weibel S, Raab V, Sabatino M, Monaco A, Liu H, Monsurró V, Buller RM, Stroncek DF, Wang E, Szalay AA, Marincola FM. (2009). "Systemic treatment of xenografts with vaccinia virus GLV-1h68 reveals the immunologic facet of oncolytic therapy." BMC Genomics **10**: 301.

Xing L, Sun X, Deng X, Kotedia K, Urano M, Koutcher JA, Ling CC, Li GC**.** (2009). “Expression of the bifunctional suicide gene CDUPRT increases radiosensitization and bystander effect of 5-FC in prostate cancer cells.” Radiother Oncol. **92**: 345-352.

Yoneda J, Kuniyasu H, Crispens MA, Price JE, Bucana CD, Fidler IJ. **(**1998). “Expression of angiogenesis-related genes and progression of human ovarian carcinomas in nude mice.” J. Natl. Cancer Inst. **90**: 447-454.

Yoon SS, Nakamura H, Carroll NM, Bode BP, Chiocca EA, Tanabe KK. (2000). "An oncolytic herpes simplex virus type 1 selectively destroys diffuse liver metastases from colon carcinoma." FASEB J **14**(2): 301-311.

Yu YA, Shabahang S, Timiryasova TM, Zhang Q, Beltz R, Gentschev I, Goebel W, Szalay AA. (2004). “Visualization of tumors and metastases in live animals with bacteria and vaccinia virus encoding light-emitting proteins.” Nat Biotechnol **22**: 313.

Yu YA, Galanis C, Woo Y, Chen N, Zhang Q, Fong Y, Szalay AA. (2009). "Regression of human pancreatic tumor xenografts in mice after a single systemic injection of recombinant vaccinia virus GLV-1h68." Mol Cancer Ther **8**(1): 141-151.

Zedeck MS, Sternberg SS. (1974) “A model system for studies of colon carcinogenesis: tumour induction by a single injection of methylazoxymethanol acetate.” J Natl Cancer Inst. **53**: 1419-21.

Zhang Q, Yu YA, Wang E, Chen N, Danner RL, Munson PJ, Marincola FM, Szalay AA. (2007). “Eradication of solid human breast tumors in nude mice with an intravenously injected light-emitting oncolytic vaccinia virus.” Cancer Res. **67**(20):10038-46.

Zhang Q, Liang C, Yu YA, Chen N, Dandekar T, Szalay AA. (2009). "The highly attenuated oncolytic recombinant vaccinia virus GLV-1h68: comparative genomic features and the contribution of F14.5L inactivation." Mol Genet Genomics **282**(4): 417-435.

Zhang Z, Shirakawa T, Hinata N, Matsumoto A, Fujisawa M, Okada H, Kamidono S, Matsuo M, Gotoh A. (2003). Combination with CD/5-FC gene therapy enhances killing of human bladder-cancer cells by radiation. J Gene Med **5**, 860-867.

Zimmermann M, Armeanu S, Smirnow I, Kupka S, Wagner S, Wehrmann M, Rots MG, Groothuis GM, Weiss TS, Königsrainer A, Gregor M, Bitzer M, Lauer UM. (2009). "Human precision-cut liver tumor slices as a tumor patient-individual predictive test system for oncolytic measles vaccine viruses." Int J Oncol **34**(5): 1247-1256.

10 Danksagung

An erster Stelle möchte ich mich herzlich bei meinem Doktorvater Prof. Dr. Ulrich M. Lauer für seine große Unterstützung bedanken. Er hat mir die Möglichkeit gegeben, Einblicke in die Welt der Virotherapie zu bekommen und dort meine Kenntnisse zu vertiefen. Sein anhaltendes Interesse an meiner Arbeit, sein stets unglaublich schnelles Antworten auf Emails zu jeglichen Tag- und Nachtzeiten und sein immer offenes Ohr für Zwischenberichte und Lagebesprechungen war vorbildlich und für mich von unschätzbarem Wert.
Die Aufforderung zur und Unterstützung bei der Erweiterung meiner wissenschaftlichen Kompetenzen durch die Erstellung von Postern und Vorträgen für Kongresse und Labor-Seminare und seine bereitwillige Durchsicht dieser Dokumente, kann ich ihm nicht hoch genug anrechnen. Ich kann mir keinen besseren Doktorvater vorstellen.
Lieber Ulli, ganz besonders möchte ich mich bei Dir für Deinen Einsatz beim Erwerb meines einjährigen Promotionsstipendiums des Interdisziplinären Zentrums für Klinische Forschung Tübingen (IZKF) bedanken. Darüber hinaus danke ich Dir für die Unterstützung bei der Bewerbung an der Brown University, der Organisation meines Auslandsaufenthaltes in Australien und den Vorschlag für die Studienstiftung des Deutschen Volkes, mit denen Du mich auch außerhalb der Promotion sehr unterstützt hast.

Herrn Prof. Dr. Ulrich M. Lauer und Herrn Prof. Dr. M. Bitzer gilt mein Dank für die Bereitstellung sämtlicher Laborgeräte und -materialien. Der gesamten AG Lauer/Bitzer danke ich für die wunderschöne Zeit in einem sehr harmonischen und humorvollen Laborteam, das stets bedingungslose Hilfsbereitschaft und Unterstützung bot.

Prof. Dr. M. Schaller und Frau B. Fehrenbacher aus der Universitäts-Hautklinik Tübingen danke ich für die elektronenmikroskopischen Aufnahmen der von mir verwendeten Zelllinien und Viren. Ihre Bilder geben meiner Doktorarbeit eine ganz individuelle und anschauliche Note.

Prof. Dr. R. Handgretinger und S. Schleicher aus der Universitäts-Kinderklinik Tübingen danke ich für die zur Verfügung gestellten primären Zelllinien aus Therapie-resistenten Tumoren, die zur Erkenntnisgewinnung bei der Überwindung primärer Resistenzen sehr viel beigetragen haben.

Besonderer Dank gilt meiner Betreuerin Dr. Susanne Berchtold, die mich mit viel Geduld und Zeitaufwand in die Welt des Masern-Impfvirus MeV-SCD eingeführt hat und damit den Grundstein zu meinem eigenständigen wissenschaftlichen Arbeiten gelegt hat. Liebe Susanne, ich danke Dir vor allem für Deine selbstlose Pflege meiner Zellen an so manchem Wochenende, für Deine mehrmalige gründliche Durchsicht sämtlicher Paper, Poster, Präsentationen und Doktorarbeitskapitel, für Deine ständige Hilfsbereitschaft und höchst motivierte Betreuung deiner Doktoranden/Innen als auch für Dein ungemein beruhigendes „Omm“ in aussichtslosen Situationen.

Dr. Martina Zimmermann möchte ich für ein stets offenes Ohr in VACV-Fragen, für diverse Protokolle und die äußerst gründliche Durchsicht meiner Doktorarbeit danken. Liebe Martina, jetzt hast Du mich mit der Abgabe der Doktorarbeit doch unerwartet deutlich geschlagen, Glückwunsch!

Irina Smirnow gebührt mein Dank für das große Labor-Einmaleins zum Umgang mit VACV. Liebe Irina, danke für die stets angebrachte Strenge und die äußerst effektive Anleitung in der Arbeit mit VACV.

Dr. Johanna Lampe möchte ich für die kritische Durchsicht meiner Arbeit und die fachlich höchst wertvollen Inputs danken. Vielen Dank für Deine ehrliche Art und die Zeit, die Du meiner Doktorarbeit gewidmet hast.

Danke an Timo Schips, der maßgeblich an der Formatierung meiner Doktorarbeit beteiligt war, mich aus der einen oder anderen Doktorarbeitskrise gerettet hat und mir im äußersten Notfall sogar seinen Laptop überließ, um den Abschluss meiner Promotion nicht zu gefährden.

Abschließend danke ich meinen Eltern, Geschwistern und Großeltern, die während des Studiums und vor allem während der Doktorarbeit immer für mich da waren, wenn ich sie brauchte.